This paper reports on a study of differences in soil potassium concentration and stable carbon isotope ratio across a savanna–forest ecotone in the neotropics. Thus, this paper addresses relevant scientific questions within the scope of BG. The paper presents novel data and analysis, and the description of the experiments and calculations are sufficiently complete and precise to allow reproduction. The results are consistent with what is known of neotropical plant ecology and substantial conclusions are reached. The title clearly reflects the contents of the paper, and the abstract provides a concise and complete summary. However, there are three areas that should be improved before reconsideration for publication in BG: 1) clarification of the significant results and reduction of null results; 2) reduction of speculation beyond the scope of study; and 3) interpretation of statistical results.

There were many measurements made of the soil and vegetation. Amongst the many measures, only a few were found to show significant and meaningful differences; these were [K] in the soil, leaf A_{max}, canopy area index, tree height and leaf $\delta^{13}C$, which is a proxy for water-use efficiency (Leffler and Evans 1999 *Oecologia*, Zolfaghar et al. 2014 *Australian Journal of Botany*). Particularly, the physiological mechanisms relating soil [K], tolerance of water deficits, A_{max} and stomatal conductance should be clarified. Thus, as [K] increased, A_{max} decreased with an associated increase in $\delta^{13}C$, and stomatal conductance (and E) were consequently reduced to a larger extent than A to support the rise in water-use efficiency (and $\delta^{13}C$). The basis for the relationship between [K], photosynthetic capacity, stomatal conductance, canopy area index and canopy height should be specified. Simultaneously, the large amount of detail describing the comparisons that were not significant (e.g., Figs. 6, 7, 10) could be removed to the supplementary information. The information that is removed to the Supplement could be replaced by illustrations from Tables S1, S2 and S3, which were cited in support of the soil results.

The scientific methods and assumptions are valid and clearly outlined, although the methods and results are not sufficient to support the global scope of the scientific questions, interpretations and conclusions. In the Introduction, the study intends to address the question of different systematic patterns (i.e., "alternative steady states") across savanna ecosystems. As Lehmann et al. (2014) demonstrated, local fire and vegetation history is essential for explaining the different vegetation-fire-climate trajectory across continents of the Southern Hemisphere. With fire occupying such a pivotal role in the savanna dynamics of Africa and Australia (Lehman et al. 2014), failure to address fire in this ecotone limits the applicability of results to address questions about systematic control of savanna ecotones worldwide. However, this paper could offer an important contribution to BG by taking a more local approach in the Introduction, Discussion and Conclusions. It would be additionally useful to clarify how this ecotone is in a novel and unusual situation (as stated in the first sentence of each of the first two paragraphs of the Discussion).

The statistical rigour did not appear to be constant throughout the text. In some cases, significance seems to be stated at very large p-values (e.g., "but with the best fit line for savanna plots only significant at $p = 0.183$," page 7889, line 6). In another case (page 7901, lines 12 and 15), $p = 0.098$ is not significant in one test, whilst $p = 0.090$ is significant in another test. Caution should be used in describing statistical summaries of functions that are not significant. For example, if a slope is not significantly different from zero, differences in positive *versus* negative slopes is not meaningful (page 7903, lines 22–23).

Specific comments:

Fig. 4c and page 7889, line 13: considering the sample size and small slope, it does not seem correct that the savanna MAP–B_u line should have a coefficient of determination that is significantly different from zero. Even if the stats were correct, however, the small slope restricts the noteworthiness of this relationship.

Fig. 7 and page 7901, lines 24–29: The trend lines are not convincing due to the very large amounts of variability shown at each level of P_A.

Page 7907, line 23 to page 7908, line 2: Clarify the meaning of the colour and size patterns.

Page 7908, line 21: how do the modelled values of $[K]_{sa}$ compare to measured values?

Page 7912, lines 17–18: explain N lixiviation and denitrification (e.g., through urease) as these topics were not introduced before this point of the discussion.

Technical corrections:

I had some difficulty following the meaning of some of the text. The writing could be simplified in certain long sentences to clarify the meaning (e.g., page 7886, 15–20; page 7905, lines 17–19; page 7912, lines 1–10; page 7913, lines 5–29; page 7915, lines 5–9). In general, the text could be substantially shortened and focused, especially in the Discussion section. Also see suggested corrections applied to the following pages.

Biogeosciences Discuss., 12, 7879–7977, 2015
www.biogeosciences-discuss.net/12/7879/2015/
doi:10.5194/bgd-12-7879-2015

Biogeosciences
Discussions
Open Access

Edaphic, structural and physiological contrasts across Amazon Basin forest-savanna ecotones suggest a role for potassium as a key modulator of tropical woody vegetation structure and function

J. Lloyd[1,2], T. F. Domingues[3], F. Schrodt[4,5], F. Y. Ishida[2], T. R. Feldpausch[6], G. Saiz[7], C. A. Quesada[8], M. Schwarz[9], M. Torello-Raventos[10], M. Gilpin[11], B. S. Marimon[12], B. H. Marimon-Junior[12], J. A. Ratter[13], J. Grace[14], G. B. Nardoto[15], E. Veenendaal[16], L. Arroyo[17], D. Villarroel[18], T.J Killeen[19], M. Steininger[20], and O. L. Phillips[11]

[1]Department of Life Sciences, Imperial College London, Silwood Park Campus, Buckhurst Road, Ascot, Berkshire SL5 7PY, UK
[2]Centre for Tropical Environment and Sustainability Sciences (TESS) and College of Marine and Environmental Sciences, James Cook University, Cairns, 4870, Qld, Australia

[3]Universidade de São Paulo, Faculdade de Filosofia Ciências e Letras de Ribeirão Preto, Av Bandeirantes, 3900, CEP 14040-901, Bairro Monte Alegre, Ribeirão Preto, SP, Brazil
[4]Max Planck Institute for Biogeochemistry, Postfach 10 0164, 07701 Jena, Germany
[5]iDiv, German Centre for Integrative Biodiversity Research, Halle-Jena-Leipzig, Deutscher Platz 5e, 04103 Leipzig, Germany
[6]Geography, College of Life and Environmental Sciences, University of Exeter, EX4 4RJ, UK
[7]Karlsruhe Institute of Technology, Institute of Meteorology and Climate Research, 82467, Garmisch-Partenkirchen, Germany
[8]Instituto Nacional de Pesquisas da Amazonia, Manaus, Cx Postal 2223 – CEP 69080-971, Brazil
[9]Fieldwork Assistance, PSF 101022, 07710, Jena, Germany
[10]Centre for Tropical Environment and Sustainability Sciences (TESS) and College of Science Technology and Engineering, James Cook University, Cairns, Qld, Australia
[11]School of Geography, University of Leeds, LS2 9JT, UK
[12]Universidade do Estado de Mato Grosso, Br 158, Km 655, Antiga FAB, Nova Xavantina, MT. CEP 78690-00, Brazil
[13]Royal Botanic Garden, Edinburgh, EH3 5NZ, Scotland, UK
[14]School of Geosciences, University of Edinburgh, EH8 9XP, Scotland, UK
[15]Campus Darcy Ribeiro – Prédio da FACE Brasília, Distrito Federal, 70910-900, Brazil
[16]Centre for Ecosystem Studies, University of Wageningen, P.O. Box 47, 6700AA, Wageningen, the Netherlands
[17]Universidad Autonoma Gabriel Rene Moreno, Avenidas Centenario, Venezuela y Av. 26 de Febrero 56 Santa Cruz de la Sierra, Bolivia
[18]Museo Noel Kempff Mercado, Av. Irala no 565 – casilla 2489, Santa Cruz, Bolivia
[19]Agrotecnologica Amazonica, Santa Cruz, Bolivia
[20]Conservation International, Washington DC, USA

Received: 25 March 2015 – Accepted: 26 March 2015 – Published: 26 May 2015

Correspondence to: J. Lloyd (jonathan.lloyd@imperial.ac.uk)

Published by Copernicus Publications on behalf of the European Geosciences Union.

Abstract

Sampling along a precipitation gradient in tropical America extending from *ca.* 0.8 to 2.0 m a^{-1}, savanna soils had consistently lower exchangeable cation concentrations and higher C / N ratios than nearby forest plots. These soil differences were also reflected in canopy averaged leaf traits with savanna trees typically having higher leaf mass per unit area but lower mass-based nitrogen (N_m) and potassium (K_m). Both N_m and K_m also increased with declining mean annual precipitation (P_A), but most area-based leaf traits such as leaf photosynthetic capacity showed no systematic variation with P_A or vegetation type. Despite this invariance, when taken in conjunction with other measures such mean canopy height, area-based soil exchangeable potassium content, $[K]_{sa}$, proved to be an excellent predictor of several photosynthetic properties (including ^{13}C isotope discrimination). Moreover, when considered in a multivariate context with P_A and soil plant available water storage capacity (θ_P) as covariates, $[K]_{sa}$ also proved to be an excellent predictor of stand-level canopy area, providing drastically improved fits as compared to models considering just P_A and/or θ_P. Neither calcium, magnesium nor soil pH could substitute for potassium when tested as alternative model predictors (ΔAIC > 10). Nor for any model could simple soil texture metrics such as sand or clay content substitute for either $[K]_{sa}$ or θ_P. Taken in conjunction with recent work in Africa and the forests of the Amazon Basin this suggests – in combination with some newly conceptualised interacting effects of P_A and θ_P also presented here – a critical role for potassium as a modulator of tropical vegetation structure and function.

1 Introduction

Forests and savannas dominate the tropical vegetated regions of the Earth covering around 0.2 of the Earth's surface (Torello-Raventos et al., 2013). At a broad scale, it has been long recognised that the distribution of these two biomes, each with its own structural characteristics and species composition, is principally governed by precipita-

tion and its seasonality (Schmimper, 1903), but with soil chemical characteristics also important (Lloyd et al., 2008; Lehmann et al., 2011; Veenendaal et al., 2015). Edaphic conditions are especially influential in regions where the two biomes intersect – often referred to as "ecotones" or "Zones of (Ecological) Transition" (ZOT) – both forest and savanna existing as discrete "patches" under similar climatic conditions (Murdoch et al., 1976; Furley and Ratter, 1988; Cochrane, 1989; Ratter, 1992; Thompson et al., 1992; Lehmann et al., 2011; Saiz et al., 2012; Schrodt et al., 2014; Veenendaal et al., 2015).

The role of soils in influencing vegetation distribution patterns within ZOT is, however, still equivocal with some authors arguing that fire-mediated feedbacks determine the nature of alternative vegetation types within this region through a mechanism related to the maintenance of alternative stable states (Warman and Moles, 2009; Hirota et al., 2011; Staver et al., 2011; Hoffmann et al., 2012; Murphy and Bowman, 2012). It has also been argued that large scale differences in fire-mediated feedbacks are required to account for apparent inter-continental differences in savanna–precipitation relationships (Lehmann et al., 2014).

One key argument of the fire-mediated feedback/alternative stable state community has been that in many cases woody vegetation formation types can be found where they would not be expected on the basis of climate and/or soils alone (Staver et al., 2011; Murphy and Bowman, 2012; Lehmann et al., 2014). Yet, – other concerns aside (Hanan et al., 2013; Veenendaal et al., 2015) – we perhaps should ask ourselves if at present we really do know exactly what climatic and/or edaphic factors are likely to be important. Here, of particular note is the importance of physical as well as chemical soil properties in influencing tropical vegetation structure and with a range of physical factors such as soil texture, depth to water table and the presence/absence of impermeable layers all potentially important (Cole, 1960; Avenard and Tricart, 1972; Ratter, 1992; Thompson et al., 1992; Williams et al., 1996; Mills et al., 2006; Lloyd et al., 2008, 2009).

Tropical South America provides a particularly interesting "living laboratory" for an investigation into the importance of climate/soil interactions as drivers of variations in tropical vegetation structure and function, with “Seasonally Dry Tropical Forests” extending into rainfall areas with mean annual precipitation rates (P_A) of less than $0.9\,\mathrm{m\,a^{-1}}$ (Prado and Gibbs, 1993; Killeen et al., 2006; Pennington et al., 2006) and, most importantly often occurring in close proximity to a structurally and floristically distinct savanna-like cerrado formations (Daly and Mitchell, 2000). This occurs not only at relatively low precipitations of $< 1.0\,\mathrm{m\,a^{-1}}$ (Villarroel et al., 2010) but also – with both vegetation types found more or less in a continuum – across a range of differing precipitation regimes extending to the southern Amazon forest boundary for which P_A is typically around $1.6\,\mathrm{m\,a^{-1}}$ (Ratter, 1992; Killeen et al., 1998; Durigan and Ratter, 2006; Marimon et al., 2006; Mews et al., 2012; Torello-Raventos et al., 2013; Veenendaal et al., 2015). Moreover, within the Amazon Basin itself savanna “inliers” are sometimes found growing in close proximity to the dominant forest vegetation at rainfall up to $2.0\,\mathrm{m\,a^{-1}}$ ~~and beyond~~ (Cole, 1960; Eiten, 1978; Thompson et al., 1992; Cochrane and Cochrane, 2010; Torello-Raventos et al., 2013; Rossatto, 2014). It is thus possible to find paired savanna and forest sites across a precipitation gradient extending from less than $1.0\,\mathrm{m\,a^{-1}}$ to more than $2.0\,\mathrm{m\,a^{-1}}$.This provides a ready means for quantifying the relative importance of soils vs. climate as modulators of forest/savanna structure and function.

In terms of measurement and modelling strategies appropriate to quantify the relative importance of soils vs. climate as modulators of tropical vegetation structure and function, some guidance can be obtained from the production orientated forestry literature for which there are many examples of empirical models integrating both edaphic and climatic factors with the overall aim of predicting site-to-site differences in stand productivity. For example Grigal (2009) found a soil site index measure incorporating water availability (depth to water and drainage), nutrients (base saturation and organic matter) and site (bulk density and stone volume) to provide good predictions of the growth of aspen trees in Minnesota. Male (1981) found soil depth (to rock) to be a good predictor for a range of coniferous species in sub-tropical Queensland (Australia). Turner et al. (1990) found a wide range of attributes such as parent rock type, texture profile,

depth to and nature of any impeding layer and condition of the uppermost 0.1 m soil combining together as factors contributing to variations in the productivity of *Pinus radiata* forest in Australia. Briggs (1994) used soil rooting depth and drainage class to delineate forest productivity classes in Maine and Ritchie and Hamann (2008) found that water capacity of the soil (depth, texture and type of bedrock) was effective at characterizing the productivity of Douglas Fir saplings (Weiskittel et al., 2011).

Most of the above studies have not focussed on specific soil chemical parameters – and indeed deliberately so: this being to facilitate the ready scaling up of these productivity measurements on the basis of limited spatial soils information. But with, at least in some cases, soil chemical status indirectly included as a predictor variable through the inclusion of a parent material term. Soil physical and chemical properties are inevitably correlated to at least some degree due to their mutual associations during pedogenesis (Quesada et al., 2010). Thus, some “hidden soil fertility effects” are probably present in many of the above metrics based on soil physical properties.

It is reasonable to anticipate that soil nutrient status should affect tropical vegetation structure and dynamics as there are numerous studies both correlative (Askew et al., 1970; Goodland and Pollard, 1973; Lopes and Cox, 1977; Furley and Ratter, 1988, 1992; Oliveira-Filho and Ratter, 2002; Quesada et al., 2012; Schrodt et al., 2014) and experimental (Wright et al., 2011; Santiago et al., 2012; Sayer et al., 2012; Alvarez-Clare et al., 2013) showing specific nutrient effects on a range of ecosystem properties. Conceptually at least three mechanisms by which nutrients could affect vegetation structure and function can be envisioned. First, especially as may be relevant to high biomass vegetation types, there may simply not be enough nutrients available to sustain a higher biomass. This is as implicitly assumed by Bond (2010) and Silva et al. (2013) in their analyses of savanna and nutrient stocks. Second, a shortage of photosynthetically relevant nutrients such as nitrogen could potentially be associated with reduced rates of carbon acquisition as is implicitly assumed in many process-based models of forest productivity in the temperate zone (Weiskittel et al., 2011) – for example Comins and McMurtrie (1993): and has also been suggested for soil phosphorus and Amazon forest wood production rates (Mercado et al., 2011). Thirdly, given the many roles played by both macro-and micro-nutrients in plants (Hänsch and Mendel, 2009; Maathuis, 2009) it is quite conceivable that growth or mortality ~~processes~~ not directly related to photosynthetic carbon acquisition be affected. As illustration, there are clear and important roles for both potassium and calcium in wood cambial growth ~~processes~~ (Fromm, 2010) and with the many reports of positive effects of potassium fertilization on crop productivity mostly accounting for its effects in terms of improved plant water relations rather than photosynthetic carbon acquisition per se (Römheld and Kirkby, 2010; Wang et al., 2013; Ahmad and Maathuis, 2014; Anschütz et al., 2014; Hafsi et al., 2014; Shabala and Pottosin, 2014; Zörb et al., 2014). This is thought to be due to the role of potassium as a key osmoticum in plants, as well as with important roles in long-distance water transport (El-Mesbahi et al., 2012; Wang et al., 2013; Anschütz et al., 2014).

Indeed, these observations, taken along with the many positive reports of woody plant growth responses to improved soil potassium status (Tripler et al., 2006), numerous demonstrations that potassium can – at least to some extent – ameliorate adverse effects of soil water~~,~~ deficits on plant growth (Egilla et al., 2005; Umar, 2006) and the clear tendency for savanna species to have a lower potassium requirement than forest species (Rossatto et al., 2013; Schrodt et al., 2014; Viani et al., 2014) all suggest that potassium availability could potentially be important in accounting for any edaphic effects across the wide precipitation range for which forests and savanna both occur.

It is also possible that other cations could be involved in any other observed soil-associated modulations of tropical vegetation physiognomy. For example, Cochrane (1989) found very low Ca/Mg ratios in Brazilian savanna subsoils and hypothesised that these might be limiting for new root growth. High concentrations of toxic ions might also be important with Priess et al. (1999), for example, attributing very high fine-root turnover rates in Venezuelan sub-montane forests to high exchangeable aluminium concentrations in the soil.

Nevertheless, as already noted, some authors have suggested that tropical vegetation structure and function across the 1.0 to $2.0\,\mathrm{m\,a^{-1}}$ precipitation range are mostly determined by fire-mediated feedbacks and the existence of alternative stable states (Warman and Moles, 2009; Hirota et al., 2011; Staver et al., 2011; Hoffmann et al., 2012). In which case it would reasonably ~~be~~ expected that no systematic pattern of vegetation structure in relation to climate and/or soils should emerge (Sankaran et al., 2005; Hoffmann et al., 2012; Murphy and Bowman, 2012; Lehmann et al., 2014). Soil–climate–vegetation interactions along "long" ecological gradients are, however, likely to be complex and with significant multiple interactions. For example, a number of studies have shown that the optimum vegetation rooting depth should (and does) increase with precipitation as long as potential evaporation continues to exceeds rainfall (as a rule of thumb this is for $P_\mathrm{A} < 2.2\,\mathrm{m\,a^{-1}}$) (Schenk and Jackson, 2002; Collins and Bras, 2007; Guswa, 2010). This means that any adverse effect of a restricted root zone on annual rates of plant water uptake is likely to be considerably less at lower ~~of,~~ higher P_A.

Moreover, impermeable layers such as laterite which are common in all but the most severely weathered soils groups typically found across the tropical lands (Thomas, 1974) could potentially even have a positive effect on soil water balances and hence vegetation structure at low P_A if reductions in large precipitation event drainage losses associated with such layers were not to be fully offset by increased runoff rates. This has been suggested, for example, by Dye and Walker (1980), as one potential causative factor for the existence of a very high biomass *Colophospermum mopane* stands as are sometimes found at $P_\mathrm{A} < 0.7\,\mathrm{m\,a^{-1}}$ in Southern Africa (Mapaure, 1994).

In addition to measurements of soil and climate, leaf trait characterisations can also help disentangle causes for regional scale variations in canopy structure. For example, where a nutrient is limiting it might reasonably be expected that foliar concentrations would be more closely correlated with the appropriate measures of soil availability than when a nutrient is available in excess (Quesada and Lloyd, 2015). Likewise, measurements of photosynthetic capacity in relation to foliar nitrogen and/or phosphorus concentrations can also yield information as to the extent to which these elements may be influencing rates of carbon acquisition (Domingues et al., 2010, 2014; Bloomfield et al., 2014). Leaf-level measurements on their own do, however, only provide part of the story. For example, in high-light and water-limited environments optimal whole-plant photosynthetic carbon gain should be attained through the construction of relatively few leaves but with higher photosynthetic capacities as compared to moister lower-insolation climates (Buckley et al., 2002; Farquhar et al., 2002). This photosynthetic capacity – leaf area trade-off means that sensible interpretation of any leaf–level photosynthetic trait data also requires some knowledge on canopy leaf areas for any sort of meaningful interpretation (Cernusak et al., 2011).

Analysis of the δ^{13}C of leaf dry matter further provides a convenient method for investigating leaf physiology because it relates to the ratio of intercellular to ambient CO_2 mole fractions (C_i/C_a) during photosynthesis (Farquhar et al., 1989). Thus, foliar δ^{13}C provides a time-integrated proxy measurement of important leaf gas exchange characteristics, especially in terms of changes in photosynthetic capacity relative to those of stomatal conductance, hence providing some indication of the extent to which leaf-level carbon acquisition might be "compromised" as a consequence of stomatal closure in relation to high soil and/or atmospheric water deficits (Lloyd and Farquhar, 1994; Schulze et al., 1998; Miller et al., 2001). In term of cations, a role for potassium in the adjustment of savanna trees to more severe soil water deficits has already been suggested by ~~(~~Schrodt et al.~~,~~ 2014) as an explanation for high foliar concentrations in the leaves of African savanna species at lower P_A.

The current study reports on the climate, soil, leaf and canopy structural characteristics of nine forest and eleven savanna stands of the Amazon Basin sampled along a precipitation gradient extending from 0.82 to 2.12 m a^{-1}. Specific questions addressed are:

1. Are there consistent differences in the physical and/or chemical properties of forest vs. savanna soils across a range of sites differing in precipitation?

2. If so, how are these differences reflected in differences in leaf-level measures of foliar nutrient content, δ^{13}C and photosynthetic capacity?

3. How do associated canopy structural characteristics such as leaf area, average and upper canopy tree heights and stand-level biomass vary with precipitation for forest vs. savanna vegetation formation types? And once variations in soil physical and chemical properties have been taken into account – noting the likely importance of interactions with precipitation regimes – can we then account for variations in tropical forest and savanna structure using simple statistical models such as are applied in the forestry production literature? Or do variations in canopy structure in relation to climate remain so enigmatic that an invocation of "alternative stable states" becomes necessary?

2 Materials and methods

2.1 Study area

Data presented here come from twenty plots sampled in the southern and eastern areas of the Amazon Basin, located in regions where both forest and savanna vegetation formation types were known to occur (Figs. 1 and 2). Most of these plots were specifically sampled as part of the Tropical Biomes in Transition project (Torello-Raventos et al., 2013), though with both plant and soil data for two forest plots (viz. TAP-123 and TAP-04) coming from previous measurements made as part of the RAINFOR project (Fyllas et al., 2009; Quesada et al., 2010, 2011). Additional photosynthesis and foliar N and P data for the forest plot TAP-04 come from Domingues et al. (2005). A list of all plots sampled along with selected climate and soil properties can be found in Supplement Table S1).

Measurements from the TROBIT program were made in two field campaigns, each over a period of ca. two months. First, sampling in Bolivia from February to April 2007 of 9 plots across a rainfall gradient from 0.82 m a^{-1} at TUC-01 to 1.45 m a^{-1} at LFB-01 (Noel Kempff Mercado National Park). Second, a sampling of 10 plots in Brazil from April to June 2008 with a range of P_A from 1.51 m a^{-1} at NXV-01 to 2.02 m a^{-1} at ALC-02. All sampling campaigns had been timed to coincide with the end of the wet season and the timing of expected maximum plant physiological activity and standing herbaceous biomass.

2.2 Stand structure and species identification

Full details of canopy cover, tree height (H) and stand biomass estimates are provided in Torello-Raventos et al. (2013) and Veenendaal et al. (2015), and are thus only summarised briefly here. In short, we inventoried all trees and shrubs with a diameter (D) at breast height (1.3 m) of greater than 0.1 m with transect measurements being used for the estimation of size and abundance of smaller saplings, shrubs and seedlings ($D > 25$ mm and $H > 1.5$ m). Selected trees and shrubs in each plot were then used for determinations of site-specific allometric equations relating either H or estimated projected canopy areas (C_A) to D. These equations were then used to estimate mean and 0.95 quantile heights (from here on denoted as $\langle H_U \rangle$, and H^* respectively) as well as stand level crown area index, C_W – defined as the sum of all woody individuals canopy projected area (including the skylight transmitted component) divided by the ground area. Allometric equations employing some combination of D and/or H and/or C_A taken from a range of previously published sources or specifically developed as part of the TROBIT project were then used to estimate stand level biomass (Veenendaal et al., 2015). Height and biomass estimates for the non-TROBIT forest plot TAP-123 comes from Feldpausch et al. (2011) with C_W for TAP-123 and the nearby TAP-4 calculated from leaf area index measurements of these stands (Fyllas et al., 2014) using relationships given in Veenendaal et al. (2015). Woody and herbaceous species were usually identified in the field by local botanists, but where necessary specimens were collected and verified against herbarium collections.

2.3 Soil physical and chemical properties

Soil sampling methods are described in detail in Quesada et al. (2010, 2011) and are thus only briefly summarized here. In brief, for each one hectare plot, five soil cores were collected and soil retained over the depths 0–0.05, 0.05–0.10, 0.10–0.20, 0.20–0.30, 0.30–0.50, 0.50–1.00, 1.00–1.50 and 1.50–2.00 m using an undisturbed soil sampler (Eijkelkamp Agrisearch Equipment BV, Giesbeek, The Netherlands). In addition, each plot usually had one soil pit dug to a depth of 2.0 m with samples collected from the pit walls at the same depths as above. Where possible, coring from the bottom of the soil pit for a further 2.0 m was also undertaken, giving a total maximum depth sampled of 4.0 m. All sampling was done following a standard protocol of RAINFOR network (http://www.geog.leeds.ac.uk/projects/rainfor/pages/manualstodownload.html) in such a way to best account for spatial variability within the plot.

Soil samples were air dried, usually in the field, and then once back in the laboratory had roots, detritus, small rocks and particles over 2 mm removed.

2.3.1 Soil bulk density

Samples for bulk density determinations were taken from pit wall samples using specially designed container rings of known volume (Eijkelkamp Agrisearch Equipment BV, Giesbeek, The Netherlands) and subsequently oven dried at 105 °C until constant weight, cooled to room temperature in a sealed desiccant before final weight determinations were made. Three bulk density samples were collected at each sampling depth.

2.3.2 Soil texture and plant available soil water

Particle size analysis was performed using the pipette method (Gee and Bauder, 1986) with plant available soil water (θ_P) obtained through an estimation of soil water retention characteristics based on the particle size pedotransfer functions for tropical soils given by Hodnett and Tomasella (2002) for each sampled layer. Individual layer values (−0.01 to −1.5 MPa) were then integrated to the maximum rooting depth for each profile or integrated to four meters for the case of roots not having been observed to be constrained in any way.

2.3.3 Soil chemical properties

As described in detail by Quesada et al. (2010, 2011) samples were analysed for: pH in water at 1 : 2.5, with exchangeable cations determined by the silver-thiourea method (Pleysier and Juo, 1980). Phosphorus pools were obtained from standard fractionation procedures as modified from Hedley et al. (1982). Soil carbon and nitrogen was determined using an automated analyser (Pella, 1990; Nelson and Sommers, 1996). Samples from Bolivia were analysed in the School of Geography, University of Leeds with those from Brazil at *Instituto Nacional de Pesquisas da Amazonia* in Manaus.

2.3.4 Plant available nutrients

As in Quesada and Lloyd (2014) the amount of nutrient available per unit ground area ($[\Theta]_{\mathrm{S,a}}$) was estimated according to

$$[\Theta]_{\mathrm{S,a}} = \int_{z=0}^{z=d} \rho_{\mathrm{b}} [\Theta]_{\mathrm{ex,m}} \mathrm{d}z \tag{1}$$

where $[\Theta]_{\mathrm{S,a}}$ is the soil nutrient content (expressed as $\mathrm{g\,m^{-2}}$ or $\mathrm{mol\,m^{-2}}$), ρ_{b} is the soil bulk density (typically in $\mathrm{kg\,m^{-3}}$), $[\Theta]_{\mathrm{ex,m}}$ is the plant available soil nutrient on mass basis (typically $\mathrm{g\,g^{-1}}$ or $\mathrm{mmol\,g^{-1}}$), z is the soil depth (below the soil surface) and d is the depth of soil nutrient availability considered; here – so as to be consistent with Quesada et al. (2012), taken to be 0.3 m.

2.4 Leaf traits

Traits were assessed on an individual basis for at least 10 individuals with a diameter at breast height (1.3 m) greater than 0.1 m within each 1 ha plot. Trees were further selected on the basis that climbing the tree or cutting the branch from the ground could retrieve sun-exposed top-canopy branches. For each tree, a branch was harvested from the top canopy as described in Lloyd et al. (2010). A list of the species sampled is given in Table S2 along with details of the species' assumed affinity ("forest" vs. "savanna") and leaf habit – both these characteristics being mostly based on local botanical knowledge. In terms of leaf habit, trees were categorised as being deciduous (trees remain bare until leaf flush is induced by re-hydration), brevi-deciduous (short bare period in the dry season followed by leaf flush), semi-deciduous (trees losing old foliage as growth of new leaves starts) or evergreen (trees are never leafless but flush or shed leaves in regular periods or continuously throughout the year).

2.4.1 Leaf mass per unit area (M_{a})

The ratio of fresh, one-sided area of a leaf to its dry weight was obtained by separating at least 10 healthy adult leaves from the bulk leaf sampled from each branch. Each leaf was then scanned using a flatbed scanner attached to a laptop as ~~fast~~ as possible after harvesting in the field. Where scanning on the day of collection was impossible due to logistical reasons, leaves were stored in tightly sealed plastic bags under cool and dark conditions for a maximum of two days to avoid changes in the leaf area. The surface area of the leaf-scans was subsequently analysed on an individual basis using WinFOLIA™ (Regent Instruments Inc. Ottawa, Canada). The scanned leaves were then oven dried to constant weight at 70 °C for about 24 h to prevent enzymatic decomposition, and their dry mass determined after cooling in a desiccator. Where this was not possible due to logistic reasons, leaves were air dried in the field and oven dried as soon as possible.

2.4.2 Sample preparation

Bolivian leaf sample preparation and analyses were undertaken at the University of Leeds (UoL) with Brazilian samples processed and analysed at the *Instituto Nacional de Pesquisas da Amazonia*, (INPA) in Manaus with the exception of carbon and nitrogen determinations which were undertaken at the *Centro de Energia Nuclear na Agricultura*, CENA in Piracicaba, Brazil. Leaf material not used for the determination of M_a were dried as described above. About 20 g dry weight subsamples were then taken for the determination of foliar nutrients and isotopes. ~~In order to~~ prepare the leaf samples for these analyses, the main vein and petiole of each leaf were removed and the dried subsample ground through a 1.0 mm (20 mesh) sieve.

2.4.3 Carbon and nitrogen determinations

~~At UoL and CENA~~ foliar nitrogen $[N]_m$ and carbon $[C]_m$ in the bulk leaf samples were determined on 15–30 mg of the ground plant material using elemental analysis (EURO EA CHNSO Analyser, HEKAtech GbhB, Wegberg, Germany in UoL and with a CARLO ERBA EA 1110 CHN, Thermo Fisher Scientific, GmbH, Germany at CENA).

2.4.4 Cation and phosphorus determinations

At UoL foliar cations (calcium, potassium and magnesium) and phosphorus in the ground samples were determined by inductively coupled plasma optical emissions spectrometry (ICP-OES) (PerkinElmer Optima 5300DV, PerkinElmer, Shelton, CT, USA) following acid digestion (Lloyd et al., 2010). In the INPA laboratory samples were digested using a nitric/perchloric acid mixture, with concentrations of Ca, Mg and K determined using an Atomic Absorption Spectrophotometer (Model 1100b, Perking Elmer, Norwalk, CT, USA) as described by Anderson and Ingram (1993) and with phosphorus determined by Colorimetry (Olsen and Sommers, 1982) using a UV visible spectrophotometer (model 1240, Shimadzu, Kyoto, Japan). Sample dilutions for

AAS determinations were made with a 0.55 % lanthanum suppressant solution for Ca and Mg, and with a 0.2 % CsCl solution for K. Details of solutions and standard series preparation can be obtained from (Van Reeuwijk, 2002).

2.4.5 Leaf construction costs

The cost of leaf construction (expressed as g glucose g^{-1} DW) was estimated as in Poorter and de Jong (1999) viz.

$$K = (-1.041 + 5.077\mathrm{C_m})(1 - \phi_\mathrm{m}) + 5.325\mathrm{N_{org}}, \tag{2}$$

where K is the construction cost, $\mathrm{C_m}$ is the leaf carbon concentration, where ϕ_m is the leaf mineral content and $\mathrm{N_{org}}$ is the leaf organic N concentration (all in $\mathrm{g\,g^{-1}}$ DW). For the purposes of calculation we assumed that all N present in the leaves was in the organic form (i.e. free nitrate levels were minimal as seems to be the case at least for Amazon forest species, Bloomfield, 2012), and with leaf mineral content being approximated as the sum of the measured cations (Sect. 2.4.4).

2.4.6 Estimation of canopy nutrient concentrations

The total amount of each nutrient contained in the foliage Θ_C was estimated as (Quesada and Lloyd, 2015);

$$\Theta_\mathrm{C} = L\langle\Theta_\mathrm{m}\rangle\langle M_\mathrm{a}\rangle, \tag{3}$$

where L is the stand leaf area index ($D > 0.1$ m) taken from Veenendaal et al. (2015) – and $\langle\Theta_\mathrm{m}\rangle$ and $\langle M_\mathrm{a}\rangle$ are the species-abundance-weighted mass-based leaf nutrient estimates and leaf mass per unit area respectively (see Sect. 2.6.2). Eq. (3) is by necessity an approximation – ignoring within canopy gradients for example – and also assuming a species' abundance is a good indication of its relative leaf area. But, especially for comparison of canopy and soil available nutrient stocks it does have advantages as compared more simplistic approaches such as in Cleveland et al. (2011) where variations in leaf area or M_a are not even taken into account. Moreover, taken in conjunction with the "soil equivalent" Eq. (1) (Sect. 2.3.3) Eq. (3) allows both plant and soil nutrient stocks to be expressed on a per unit ground area basis (e.g., $\mathrm{mol\,m^{-2}}$) this then providing a ready means for quantitative comparisons.

2.5 Climatological data

Precipitation climatologies for all sites were obtained from the interpolated WorldClim dataset (Hijmans et al., 2005).

2.6 Statistical analyses

2.6.1 Variance partitioning

As in Fyllas et al. (2009) the relative proportions of the total variance within the dataset was apportioned to genetic, environmental and "residual" components for each trait (Θ). Taking into account that the majority of species sampled could be assigned as being affiliated with either the forest ($\mathbb{F}$) or savanna ($\mathbb{S}$) biomes the model fitted here was

$$\Theta = \mathbb{A}/S + p + \varepsilon, \tag{4}$$

where $\mathbb{A}$ represents the affiliation of species S (either forest or savanna) located within plot p and with ε being the residual variance: the nesting of S within $\mathbb{A}$ allows a splitting of the total between species variance into an intra- and inter-biome component. As noted by Fyllas et al. (2009), the residual variance component includes any intraspecies variability as well as any measurement error. These calculations were done using the lme4 package (Bates et al., 2014) available within the R statistical platform (R-Development-Core-Team, 2014), treating all terms as random effects.

2.6.2 Variations in plot-level means in relation to vegetation type and precipitation

For each leaf trait Θ (including the area based light and CO_2 saturated photosynthetic capacity, A_{max}) plot-level community-weighted means $\langle\Theta\rangle$ and standard deviation (SD) were estimated using standard formulas (Bevington and Robinson, 1969) and weighting each observation according to the ratio n_s/n_p where n_s = the number of individuals of that species sampled in the plot (Lopez-Gonzalez et al., 2011) and with n_p being the total numbers of that species in the plot as determined through floristic inventory (Torello-Raventos et al., 2013). These calculations were done using the wt.mean function within the SDMTools package (VanDerWal et al., 2014) available within the R statistical platform (R-Development-Core-Team, 2014). Estimates of $\langle\Theta\rangle$ and associated weights so obtained were then investigated in relation to variations in mean annual precipitation according to

$$\langle\Theta\rangle = \mu + \alpha\mathbb{S} + s_1(P_A) + \mathbb{S}s_2(P_A), \tag{5}$$

where μ represents the dataset mean for trees located within the forest ($\mathbb{F}$) vegetation type (i.e. $\mathbb{V} = \mathbb{F}$), $\mathbb{S}$ is an indicator variable taking a value of one for all trees located within savanna formations (for which by definition $\mathbb{V} \neq \mathbb{F}$) and zero otherwise, s_1 is a non-parametric smoother, fitted to the dataset as a whole, P_A is the mean annual precipitation as estimated for the plot in question and s_2 is a non-parametric smoother defining the difference between forest and savanna vegetation formation types. Equation (5) thus allows for differences in overall average trait values as well as for differing interactions with precipitation for forest vs. savanna vegetation formation types: with these two aspects of variation tested through a simple t test on the (fixed) α term with $s_2(P_A) = 0$ (i.e. an imposition of the same precipitation response on both $\mathbb{V}$) and a simple F test evaluating the effect of inclusion of the $s_2(P_A)$ term in Eq. (5) (Zuur et al., 2009). For the fitting of Eq. (5) we used the gam mgcv function (Wood, 2006, 2011) as available within the R statistical package (R-Development-Core-Team, 2014).

Equation (5) was also used (without weights) in analyses of variations in bulked stand levels soil and canopy properties.

2.6.3 Soil–climate–vegetation associations

A variety of regression/correlation techniques were applied depending on the nature of the data and questions posed. These included ordinary least squares (OLS) regression, Kendall's distribution free test for independence (Hollander and Wolfe, 1999) and non-parametric (robust) regression (McKean et al., 2009). All were undertaken using the R statistical platform (R-Development-Core-Team, 2014) using the stats or Rfit package (Kloke and McKean, 2013). For multivariate OLS regressions variance inflation factors (VIF) were also calculated and are presented in the relevant tables along with the associated "tolerance" (= 1/VIF). OLS regression coefficients are presented in both original and standardised form. The latter are presented as standardised values, this giving the relative change in the dependent variable per unit SD of each independent variable. Though potentially open to misinterpretation (Grace and Bollen, 2005) this provides a simple measure of the relative importance of the various factors accounting for the variation in stand structure or physiological variables investigated, the standardising factor being the variability (after transformation where appropriate) of the various candidate independent variables along the precipitation transect as measured by our dataset.

3 Results

3.1 Soil properties

Across the precipitation (P_A) gradient, forest soils had an exchangeable base cation content (usually referred to as the "sum of bases" = $[\mathrm{Ca}]_{\mathrm{ex}} + [\mathrm{K}]_{\mathrm{ex}} + [\mathrm{Mg}]_{\mathrm{ex}} + [\mathrm{Na}]_{\mathrm{ex}} = \Sigma_{\mathrm{B}}$) significantly greater than the savanna soils (Fig. 3a) as also reflected by an estimated $\alpha = -9.1 \pm 3.1\,\mathrm{mmol\,kg^{-1}}$ for the model fit of Eq. (5) ($p = 0.010$). That analysis also

showed a difference between the two $\mathbb{V}$ in their overall precipitation dependencies with the Eq. (5) "s_2" term being significant at $p = 0.005$. That is to say, the forest ($\mathbb{F}$) and savanna ($\mathbb{S}$) soils differed both in their overall average Σ_{B} and in the way that Σ_{B} varied with precipitation. For both $\mathbb{V}$, Σ_{B} were clearly higher at low P_A. Across the precipitation gradient individual cation concentrations were typically $[\mathrm{Ca}]_{\mathrm{ex}} \geqslant [\mathrm{Mg}]_{\mathrm{ex}} \gg [\mathrm{K}]_{\mathrm{ex}}$ for any individual plot: with $[\mathrm{Ca}]_{\mathrm{ex}}$ and $[\mathrm{Mg}]_{\mathrm{ex}}$ increasing more markedly with declining P_A than was the case for $[\mathrm{K}]_{\mathrm{ex}}$ (see Table S1 for actual values).

Soil C/N ratios ($\mathrm{CN_s}$) also varied with both $\mathbb{V}$ and P_A (Fig. 3b) with $\mathbb{S}$ soil being on average $2.3 \pm 0.6\,\mathrm{g\,g^{-1}}$ higher than for $\mathbb{F}$ soils ($p \le 0.001$). In both cases $\mathrm{CN_s}$ declined with decreasing P_A and with the difference between the two fitted curves (after accounting for intercept differences) not significant ($p = 0.155$).

Extractable soil phosphorus concentrations, $[\mathrm{P}]_{\mathrm{extr}}$, also showed a dependence upon both $\mathbb{V}$ and P_A (Fig. 3c) with markedly lower values in savanna sites as reflected in the fitted value of α in Eq. (5) being $-143 \pm 44\,\mathrm{mg\,kg^{-1}}$ ($p = 0.005$). There was also a clear difference between $\mathbb{F}$ and $\mathbb{S}$ in the way $[\mathrm{P}]_{\mathrm{extr}}$ varied with precipitation ($p = 0.023$) and with the non-significant savanna P_A dependency ($p = 0.58$) in marked contrast to the increasing forest $[\mathrm{P}]_{\mathrm{extr}}$ as P_A declined (for which $p < 0.001$). In all soils, the bulk of the $[\mathrm{P}]_{\mathrm{extr}}$ pool was made up of the less accessible NaOH extractable organic and inorganic fractions ($\mathrm{P_{NaOH(o)}}$ and $\mathrm{P_{NaOH(i)}}$ respectively). Small amounts of mineral P were also present in some of the lower P_A soils as indicated through the presence of an HCl extractable component.

Further site information (including other soil characteristics of the study plots) may be found in the Supplement (Table S1) from which we note both a tendency for the savanna plots to be sandier than their nearby forest counterparts though with no consistent difference between $\mathbb{F}$ and $\mathbb{S}$ in terms of their plant available water holding capacity (θ_{P}) which was itself highly variable (ranging from 0.18 to 0.74 m). Also of note is that – with the exception of the driest TUC-01 and TUC-03 plots which were Cambisols – all soils were of the highly weathered Acrisol, Arenosol or Ferralsol WRB great soil group.

3.2 Canopy characteristics

All three canopy structural properties showed differences both in absolute values and precipitation dependencies for forest vs. savanna plots (Fig~~s. 2 and~~ 4). Specifically, there was a clear decline in forest canopy area index (C_W) with declining precipitation ($p < 0.001$), but with the best fit line for savanna plots (which were on average of a lower C_W than their forest counterparts) only significant at $p = 0.183$ (Fig. 4a).

Also observed was a tendency for the increase in 0.95 quantile canopy height with rainfall to approach it's maximum at high P_A (overall response significant at $p < 0.001$) but with no systematic dependency of H^* on P_A for $\mathbb{S}$ ($p = 0.106$): the trees in savanna plots being on average 10.5 m shorter than their forest counterparts (Fig. 4b).

Aboveground biomass (B_U) estimates showed similar patterns as for C_W and H^* (Fig. 4c), though in this case (interestingly) with the slight increase in savanna B_U as P_A declines statistically significant ($p < 0.001$).

Overall then, we find a marked decline in stature and canopy area with precipitation for forest sites, but not for savannas. Thus, savanna and forest are much more similar in their above ground structural characteristics at lower P_A.

3.3 Leaf traits

3.3.1 Variance partitioning (mass based traits)

Through fitting the multilevel model of Eq. (4), a partitioning of the variance to genetic- and plot-level components was achieved with results presented for leaf mass per unit area (M_a), mass-based nutrient concentrations and estimated leaf construction costs (Eq. 2) shown in Fig. 5. Here, because each species could be assigned as primarily affiliated with either "forest" or "savanna" it was further possible to partition the genetic-component into that systematically associated with where a species typically grows (its "affiliation") as opposed to genetic variation within the "forest" and "savanna" grouping themselves. This analysis shows not only that relative contributions of the genetic- vs.

plot-components vary from trait to trait, but that the relative magnitude of the residual component (representing within-species variability and experimental error) is also trait dependent.

For the genetic component, that systematically associated with a species' affiliation was typically a small proportion of the overall variability, the one exception being for potassium ($\mathrm{K_m}$) where the relative contributions were approximately equal. With the exception of phosphorus ($\mathrm{P_m}$), the variance explained by the combined genetic components was of equal or greater magnitude than the plot-dependent ("environmental") component and with the latter being only a minor contributor to the overall variations in $\mathrm{C_m}$ and the associated leaf construction costs (K).

Whether or not one should attempt to assign error estimates and associated inferred level of significance to random effect estimates as used in deriving Fig. 5 is a point of contention (Wood, 2006), but in any case, the "affiliation" of forest vs. savanna species is just as readily perceivable as a fixed effect allowing reasonable error estimates and associated significance levels to be obtained. When this is done, species affiliation (forest vs. savanna) is found to exert a significant influence on all trait values investigated in Fig. 5 except $\mathrm{P_m}$. (Table S3). That is to say, even after accounting for differences in soil properties, intrinsic differences between forest and savanna in all traits except $\mathrm{P_m}$ existed. From Table S3 it can be seen in some cases these differences – although significant – are relatively small (e.g. M_a, $\mathrm{N_m}$, $\mathrm{C_m}$, $\mathrm{Mg_m}$, and K all having savanna species mean values all within 20 % of the forest species' mean) but with $\mathrm{Ca_m}$ and $\mathrm{K_m}$ showing much larger differences (savanna affiliated species showing reductions of 34 and 39 % respectively as compared to forest species: Table S3).

3.3.2 Mass-based trait variation in relation to vegetation type and precipitation

Across the precipitation gradient, leaves of trees within savanna formations ($\mathbb{S}$) had consistently higher leaf mass per unit area than those where the dominant species mix consisted of forest species ($\mathbb{F}$) (Fig. 6a). From the generalised additive model fit (Eq. 5), this overall $\langle M_\mathrm{a} \rangle$ difference ($\alpha = 32 \pm 9\,\mathrm{g\,m^{-2}}$) was significant ($p = 0.001$). Overall, the

P_A dependencies observed were highly significant ($p < 0.001$ for both $\mathbb{V}$) but with the differing fitted trends not so ($p = 0.183$). That is to say, little credence should be placed on the greater difference between the two vegetation formation types at highest P_A.

For stand-level leaf nitrogen there was also a significant difference in overall concentrations between the two $\mathbb{V}$ ($\mathbb{F} - \mathbb{S} = 6.0 \pm 1.5\,\mathrm{mg\,g^{-1}}$; $p = 0.001$; Fig. 6b) with the fitted precipitation dependencies showing an increase with declining P_A significant at $p < 0.001$ and $p = 0.065$ for $\mathbb{F}$ and $\mathbb{S}$ respectively. As for $\langle M_a \rangle$ there was, however, no significant difference in the fitted P_A dependencies for $\langle \mathrm{N_m} \rangle$ once differences in absolute values were taken into account ($p = 0.588$). Thus, after accounting for differences in intercept both $\mathbb{V}$ can be considered as increasing with declining P_A in a similar manner.

For $\langle \mathrm{P_m} \rangle$ there was no effect of $\mathbb{V}$ on overall leaf concentrations (Fig. 6c: $p = 0.283$). Nor was there any significant difference in the fitted P_A response patterns ($p = 0.098$).

A similar lack of significant difference was also observed for leaf carbon concentrations (Fig. 6d) where although $\langle \mathrm{C_m} \rangle$ were $11\,\mathrm{mg\,g^{-1}}$ higher for $\mathbb{S}$ plots this effect was significant only at $p = 0.091$. The fitted P_A dependencies were, nevertheless, significant ($p < 0.001$) in both cases, but not significantly different in pattern to each other ($p = 0.687$).

Despite the $\langle \mathrm{Ca_m} \rangle$ differences between $\mathbb{F}$ and $\mathbb{S}$ plots at lower P_A, the overall contrast ($\mathbb{F} - \mathbb{S}$) of $1.4\,\mathrm{mg\,g^{-1}}$ was not significant ($p = 0.161$), presumably a consequence of significant overlap between the two $\mathbb{V}$ at around $P_A = 1.5$ m and the high variance of the community weighted means at higher overall $\langle \mathrm{Ca_m} \rangle$, especially for forest plots at low P_A (Fig. 7a). The fitted P_A dependencies were highly significant in both cases ($p < 0.001$), but with overall patterns not significantly different ($p = 0.687$).

For $\langle \mathrm{K_m} \rangle$, $\mathbb{F}$ and $\mathbb{S}$ values were significantly different overall ($p = 0.015$) with savanna plots being estimated as, on average as $1.8 \pm 0.7\,\mathrm{mg\,g^{-1}}$ less than forest (Fig. 7b). Overall fitted P_A dependency patterns – which were significant at $p < 0.001$ and $p = 0.025$ for $\mathbb{F}$ and $\mathbb{S}$ respectively – were also significantly different from each other ($p = 0.010$). Thus for $\langle \mathrm{K_m} \rangle$ we can conclude that for $\mathbb{F}$ the rate of increase with declining precipitation was more or less constant across the transect. This is as opposed to $\mathbb{S}$ where the increase in $\langle \mathrm{K_m} \rangle$ with declining P_A was more moderate, also occurring only towards the drier end of the transect.

Overall, the $0.67\,\mathrm{mg\,g^{-1}}$ lower $\langle \mathrm{Mg_m} \rangle$ observed for the savanna plots (Fig. 7c) did not make them significantly different to their forest counterparts ($p = 0.155$) and with no difference between the two $\mathbb{V}$ in the nature of their P_A dependencies ($p = 0.192$) which were themselves both significant ($p = 0.001$ and $p = 0.047$ for $\mathbb{F}$ and $\mathbb{S}$ respectively). As for $\langle \mathrm{Ca_m} \rangle$ and $\langle \mathrm{K_m} \rangle$, within plot variation at the lowest P_A forest plot (TUC-01) was exceptionally high.

Leaf construction costs showed a slight overall dependence on $\mathbb{V}$ with $\langle K \rangle$ for $\mathbb{S}$ being on average $0.077 \pm 0.037\,\mathrm{mg\,glucose\,g^{-1}}$ DW higher than $\mathbb{F}$ ($p = 0.053$). Although the individually fitted curves are different in form for $\mathbb{F}$ vs. $\mathbb{S}$ (Fig. 7d) this difference in shape was not significant ($p > 0.999$).

Although a lack of knowledge for many of the species studied prevents rigorous inferences of trends in leaf habit, from those species for which this information was available (Table S2), it can be confidently stated that at the driest Tucavaca sites all species were deciduous (both forest and savanna) with semi-deciduous and brevi-deciduous and then evergreen species becoming more common as precipitation increased. At all sites other than Tucavaca, evergreen species were more common in the forests and with purely deciduous species more common in the savanna.

3.3.3 Vegetation–soil nutrient associations

Estimates on canopy nutrient contents (Eq. 2) as a function of soil exchangeable nutrient contents (Eq. 1) showed no clear relationship for calcium ($\mathrm{Ca_C}$: Fig. 8a), magnesium ($\mathrm{Mg_C}$: Fig. 8b) and phosphorus ($\mathrm{P_C}$: Fig. 8d), but with some association being more clear for potassium ($\mathrm{K_C}$: Fig. 8c). Using a robust regression procedure (relatively immune to outliers) significance levels as estimated through a dispersion test being $p = 0.062$, 0.266, 0.026 and 0.402 for $\mathrm{Ca_C}$, $\mathrm{Mg_C}$, $\mathrm{K_C}$, and $\mathrm{P_C}$ respectively).

As the graphs of Fig. 8 express both plant and soil nutrients on the same per unit ground area basis, they provide a ready means to evaluate the relative amounts of any nutrient in the foliage vs. the soil. Here we then see that, as approaching the asymptote, $\mathrm{Ca_C} \simeq 0.1[\mathrm{Ca}]_{\mathrm{sa}}$; $\mathrm{Mg_C} \simeq 0.1[\mathrm{Mg}]_{\mathrm{sa}}$ and $\mathrm{P_C} \simeq 0.08[\mathrm{P}]_{\mathrm{sa}}$. But that for $\mathrm{K_C} : [\mathrm{K}]_{\mathrm{sa}}$ there is no real flattening out and with canopy potassium contents quite similar to those of calcium and magnesium despite much lower soil concentrations That is to say, relative to the amount of soil nutrient present, there is much less K in the canopy foliage than is the case for Ca and Mg. This is in addition to a much clearer relationship between the nutrient stocks in the canopy vs. soil pools for K than for the other cations examined. For phosphorus the generally overall lower canopy foliar contents of savanna plots are not associated with a lower $[\mathrm{P}]_{\mathrm{sa}}$.

3.4 Photosynthesis and related traits

3.4.1 Variance partitioning (area based traits)

In contrast to the mass-based traits, in no case was the proportion of the total dataset variance in light and CO_2 saturated assimilation rates (A_{max}), area-based nitrogen and phosphorus concentrations ($\mathrm{N_a}$ and $\mathrm{P_a}$ respectively), photosynthetic N and P use efficiencies (A_{N} and A_{P} respectively) and foliar δ^{13}C attributable to species affiliation per se. But still – with the exception of $\mathrm{P_a}$ – and to a lesser extent δ^{13}C – a notable portion of the explained variance was attributable to species identity. Plot identity as estimated through the environmental components was also an appreciable source of variation in all cases, especially for δ^{13}C and – in relative terms – also for $\mathrm{P_a}$.

3.4.2 Area-based trait variation in relation to vegetation type and precipitation

Stand level species-abundance weighted maximum CO_2 assimilation rates (Fig. 10a) did not vary overall between the two $\mathbb{V}$ ($p = 0.851$) and nor, despite their fitted slopes being of a different sign, did their precipitation dependencies differ significantly ($p = 0.302$). Amongst this general "noise" of note, however, are two noticeably high $\langle A_{\mathrm{max}} \rangle$

plots; the relatively low precipitation forest OTT-01 and the mid-precipitation savanna LFB-03.

Contrasting to $\langle \mathrm{N_m} \rangle$, there was no overall difference between $\mathbb{F}$ and $\mathbb{S}$ in $\langle \mathrm{N_a} \rangle$ across the dataset (Fig. 10b), though with very different patterns in terms of their P_{A} dependencies ($p = 0.006$). Specifically, there was virtually no systematic variation of $\langle \mathrm{N_a} \rangle$ with precipitation for the savanna plots, but with a significant increase in forest plot $\langle \mathrm{N_a} \rangle$ as P_{A} decreased ($p < 0.001$).

For $\langle \mathrm{P_a} \rangle$ there was a small effect of $\mathbb{V}$ on mean values (Fig. 10c) with savanna plots typically being $0.022\,\mathrm{g\,m^{-2}}$ higher than their forest counterparts. As for $\langle A_{\mathrm{max}} \rangle$ and $\langle \mathrm{N_a} \rangle$, opposing patterns of variations with P_{A} were observed, here with a decline in $\langle \mathrm{P_a} \rangle$ coinciding with an increase in precipitation for $\mathbb{F}$. But with a less significant and opposite pattern observed for $\mathbb{S}$ These patterns were significantly different at $p = 0.058$.

Finally, we note the clear contrasting patterns in $\langle \delta^{13}\mathrm{C} \rangle$ observed for $\mathbb{F}$ vs. $\mathbb{S}$ with a more or less constant decline with increasing precipitation observed for the forest plots. But with this pattern only being replicated for savanna plots at lower P_{A} (Fig. 10d). Here the fitted curves were both significant at $p < 0.001$ and statistically different to each other ($p = 0.011$).

3.4.3 Identifying key drivers of variation in $\langle A_{\mathrm{max}} \rangle$ and $\langle \delta^{13}\mathrm{C} \rangle$

With Fig. 10 suggesting broad-scale interacting patterns of variations in $\langle A_{\mathrm{max}} \rangle$ with $\mathbb{V}$ and P_{A} in form quite similar as for $\langle \mathrm{N_a} \rangle$ and $\langle \mathrm{P_a} \rangle$, Kendall's non-parametric regression co-efficients (τ) were calculated for these and other stand level properties of interest (Table 1). This shows that, contrary to expectation, the only significant univariate correlation with was $\langle A_{\mathrm{max}} \rangle$ was a negative one with soil potassium. Of note $[\mathrm{K}]_{\mathrm{sa}}$ also exhibited strong positive correlations with a range of stand-level structural properties such as crown area index, canopy height (both mean and 0.95 quantile) as well as $\langle \delta^{13}\mathrm{C} \rangle$.

Building on this negative $\langle A_{\mathrm{max}} \rangle : [\mathrm{K}]_{\mathrm{sa}}$ association through the development of a OLS multivariate regression model using a forward regression procedure, a best fit linear-log relationship of $\langle A_{max} \rangle$ with $[K]_{sa}$, $[P]_{sa}$, $\langle N_a \rangle$, and $\langle H_U \rangle$ was found, details of which are given in Table 2a. Here, along with unstandardised coefficients, standardized values are also given, together with the appropriate collinearity statistics, the latter giving VIF < 10 (tolerance > 0.1) which suggests that cross-correlations between predictor variables was not an issue in the model fit. From the standardised co-efficients we can conclude that the dominant effect is, indeed, the negative $[K]_{sa}$ association and with the other three positive factors viz. $[P]_{sa}$, $\langle N_a \rangle$ and $\langle H_U \rangle$ all contributing to a lesser degree. The reasons for the complex multivariate association can be seen in Fig. 11 where $\langle A_{max} \rangle$ is individually plotted as a function of each of $[K]_{sa}$, $[P]_{sa}$, $\langle N_a \rangle$, and $\langle H_U \rangle$. Here, for example, although the forest plot OTT-01 is a clear outlier when considered just in terms of $[K]_{sa}$, this apparently anomalously high $\langle A_{max} \rangle$ can, however, be explained in terms of a very high $\langle N_a \rangle$. The lower precipitation forest plot TUC-01 also has a high $\langle N_a \rangle$, but its case $[K]_{sa}$ is very high and $\langle H_U \rangle$ relatively low: these factors then combine (at least according to the model) to give a relatively low $\langle A_{max} \rangle$. For the savanna plot LFB-03 the main contributing factor to its high $\langle A_{max} \rangle$ is suggested by the model to arise through a very low $[K]_{sa}$ combined with a reasonably high $[P]_{sa}$.

Given the relatively strong association between soil exchangeable K and the other base cations (Table 1) it was of interest to see if these could substitute for potassium as a predictor of $\langle A_{max} \rangle$; this also being tested for other potentially important soil properties such as pH and soil and clay content. This analysis confirmed potassium as the defining soil predictor, with the best alternative predictor as detected through a substitution of the $[K]_{sa}$ term in the model of Table 2a being $[Mg]_{sa}$ term with an r^2 of only of 0.15 (c.f. 0.71 for $[K]_{sa}$). This "best alternative model" had an Akaike's Information Criterion (AIC) of 117.6 as compared to 98.4 for the equation of Table 2a.

Soil potassium status was also negatively related to species-abundance-weighted photosynthetic nitrogen use efficiency; $\langle A_N \rangle = \langle A_{max}/N_a \rangle$: and indeed, following a similar procedure as for $\langle A_{max} \rangle$, significant associations were again found for $[K]_{sa}$, $[P]_{sa}$ and $\langle H_U \rangle$ with soil exchangeable potassium again the dominant (negatively associated) predictor variable (Table 2b). As for $\langle A_{max} \rangle$, alternative soil predictors gave a markedly

inferior fit, the "best alternative model" again being with $[Mg]_{sa}$ but with an r^2 of only of 0.15 (c.f. 0.68 for $[K]_{sa}$). This model had an Akaike's Information Criterion (AIC) of 87.1 as compared to 68.7 for the equation of Table 2b. In both the above cases, substituting either the soil $[K]_{sa}$ variable with its canopy equivalent $\langle K_a \rangle$ and/or the soil $[P]_{sa}$ variable with its canopy equivalent $\langle P_a \rangle$ also gave rise to a markedly inferior fit (data not shown).

This was similarly the case for nitrogen in the case of a fit of species-abundance-weighted photosynthetic phosphorus-use efficiency; $\langle A_P \rangle = \langle A_{max}/P_a \rangle$ where soil C : N was a significant better predictor than $\langle N_a \rangle$ and with $[K]_{sa}$ and $\langle H_U \rangle$ again included in the best fit model (Table 2c). Here again, other soil properties could not substitute for $[K]_{sa}$ with the best alternative predictor being $[Ca]_{sa}$ giving an AIC of 226.7 as compared to 222.8 for the equation of Table 2c.

Soil exchangeable potassium also showed a relatively high Kendall's τ when considered as a univariate predictor of $\langle \delta^{13}C \rangle$ (Table 1). And, indeed, a model consisting of $[K]_{sa}$ and $\langle H_U \rangle$ provided a statistically reasonable model fit, with an increases in $[K]_{sa}$ or a decrease in $\langle H_U \rangle$ predicted to cause higher (less negative) $\langle \delta^{13}C \rangle$. It is also of note, however, that in this case soil calcium (ground-area basis) turns out to be a better predictor of $\langle \delta^{13}C \rangle$ when taken in conjunction with $\langle H_U \rangle$ ($r^2 = 0.383$) giving an AIC of 40.7 as compared to 44.1 for the equation of Table 2c.

Especially as on its own P_A gave a reasonably strong correlation with $[K]_{sa}$ (Table 1), mean annual precipitation was also tested as a predictor variable for $\langle A_{max} \rangle$, $\langle A_N \rangle$, $\langle A_P \rangle$ and $\langle \delta^{13}C \rangle$. But in no case, either on its own or in conjunction with the other predictor variables in Table 2 did it give rise to an r^2 even closely approximating $[K]_{sa}$ (data not shown).

3.5 Predicting canopy structural properties

In addition to an important role as a modulator of leaf-level photosynthetic properties, Table 1 also suggests a strong associations between $[K]_{sa}$ and C_W and both canopy height measures. With C_W relating directly to both leaf area index and fractional canopy cover (Veenendaal et al., 2015) and these providing commonly used measures of woody plant plenteousness in tropical ecosystems (Lloyd et al., 2008; Hirota et al., 2011; Staver et al., 2011; Murphy and Bowman, 2012; Torello-Raventos et al., 2013; Veenendaal et al., 2015) we therefore first applied a simple OLS log-log model relating C_W to $[K]_{sa}$. And indeed, even when simply considered on its own, this area-based soil potassium measure accounted for 0.31 of the total dataset C_W variation (Model 1: Table 3a). Although this was substantially more than when precipitation was considered on its own ($r^2 = 0.00$), when P_A was considered along with $\log[K]_{sa}$ as a predictor of $\log(C_W)$, then a substantial improvement in the model fit was achieved (Model 2: Table 4b; $r^2 = 0.57$; $\Delta AIC = -8.6$). Further, although the simple addition of plant available soil water storage capacity (θ_P: see Table S1) did not improve the model fit (Model 3: Table 3c) addition of a $P_A \times \theta_P$ interaction term did provide substantial model improvement (Model 4: Table 3d; $r^2 = 0.68$; $\Delta AIC = -5.3$). However, in this model, the P_A term is insignificant at only $p = 0.553$ and very high VIF (low tolerances) for θ_P and the $P_A \times \theta_P$ interaction as well. Removal of the P_A term from Model 4 but with all other variables retained (including the interaction) resulted in a model that was as good, if not even better (Model 5: Table 3e; $r^2 = 0.71$; $\Delta AIC = -1.9$).

Overall, predictions of C_W according to Model 5 were of acceptable fidelity (Fig. 12a) with the wide range of savanna C_W well predicted in particular by this simple mixture of soil chemical and hydrological properties. Some differentiation of the forest plots would also seem to have been achieved by the model. Nevertheless, there was a tendency for the model to under-predict forest C_W and vv. for savanna plots.

~~In order to help~~ illustrate how Model 5 works, the input data is presented in the ordinal space of the interacting P_A and θ_P terms in Fig. 12b. Here the colour of the symbols relate to C_W and the symbol size relates to $[K]_{sa}$. From Fig. 12b it can be seen that in any one region of the plot that the smaller symbols (lower $[K]_{sa}$) tend to be of a redder hue (lower C_W) and consideration of similarly sized symbols shows a tendency for increased greenness (higher C_W) as one moves along the main diagonal. Reddish

symbols (of low C_W) are typically smaller (of lesser $[K]_{sa}$) at higher P_A, although the pattern of variation with θ_P is less systematic.

As illustration, model predictions of canopy area index ($\hat{C}_W$) variations as a function of $[K]_{sa}$ are shown in Fig. 12c for $P_A = 1.0\,\mathrm{m\,a^{-1}}$ and $P_A = 1.5\,\mathrm{m\,a^{-1}}$ ($\theta_P = 0.5\,\mathrm{m}$). This shows the model to be especially responsive to $[K]_{sa}$ below about $0.2\,\mathrm{mol\,m^{-2}}$ and with a greater sensitivity of $\hat{C}_W$ to $[K]_{sa}$ at higher P_A. Thus, in relative terms, $\hat{C}_W$ is modelled to become most sensitive to P_A at low $[K]_{sa}$.

Figure 12d–f shows how the $P_A \times \theta_P$ interaction affects $\hat{C}_W$ at three different $[K]_{sa}$. Here (where white areas are for $\hat{C}_W < 0$ and for which we therefore assume in practise $C_W = 0$) we see first for Fig. 12d that at a very low $[K]_{sa}$ of $0.1\,\mathrm{mol\,m^{-2}}$ the model suggests that any sort of woody leaf area is simply not possible for $P_A < 1.5\,\mathrm{m\,a^{-1}}$; and even then only when θ_P is relatively high. As P_A increases the θ_P for which $\hat{C}_W \geqslant 0$ increases, with a $\hat{C}_W$ of around $2\,\mathrm{m^2\,m^{-2}}$ at the highest P_A; θ_P combination examined considered possible.

At double potassium availability with $[K]_{sa} = 0.2\,\mathrm{mol\,m^{-2}}$ the response observed is very different (Fig. 12e). Here by comparison with Fig. 12d we can again see the generally higher $\hat{C}_W$ anticipated for the higher P_A; θ_P combinations. But at around $P_A \simeq 1.3\,\mathrm{m\,a^{-1}}$ the area delineated by the $\hat{C}_W = 0$ shifts from a concave to a convex form. That is to say, the model then predicts that for $P_A \lessapprox 1.3\,\mathrm{m\,a^{-1}}$, rather than increase, C_W should decline with increasing θ_P.

At an even higher $[K]_{sa}$ of $0.4\,\mathrm{mol\,m^{-2}}$ the general concave/convex pattern is maintained (Fig. 12f) and with higher $\hat{C}_W$ at all P_A; θ_P combinations. The domain for which $\hat{C}_W \geqslant 0$ is also shifted compared to Fig. 12e with additional combinations of lower P_A/higher θ_P also deemed possible. At the lowest simulated P_A of $0.8\,\mathrm{m\,a^{-1}}$, $\hat{C}_W \geqslant 0$ is now modelled as possible for all θ_P less than about 0.5 m.

Application of Model 5 to other structural variables also gave rise to a reasonable fit. For example as shown in Table 3f a reasonable fit of $r^2 = 0.41$ was found when $\langle H_U \rangle$ was substituted as the dependent variable. Above ground biomass (B_U) was also reasonably well predicted by the model (Table 5g: $r^2 = 0.47$), in both cases with a role for potassium still evident at $p = 0.001$.

When taken in conjunction with P_A and θ_P, $[\mathrm{K}]_\mathrm{sa}$ further proved to be a much better predictor for each of the three structural variables examined than any other measured soil property. For example, the next best alternative to $[\mathrm{K}]_\mathrm{sa}$ as a co-predictor for C_W in Model 5 was $[\mathrm{Mg}]_\mathrm{sa}$ which gave a $r^2 = 0.65$ and an AIC of 31.9 as compared to $r^2 = 0.74$ and AIC = 26.5 for $[\mathrm{K}]_\mathrm{sa}$ (Table 2e). For both $\langle H_\mathrm{U} \rangle$ and B_U it also emerged that $[\mathrm{Mg}]_\mathrm{sa}$ was the next best substitute for $[\mathrm{K}]_\mathrm{sa}$, but in both cases with the differences between the two cations in their statistical efficacy much less marked with $\Delta\mathrm{AIC} = -0.4$ for $\langle H_\mathrm{U} \rangle$ and -1.9 for B_U.

3.6 Soil water simulations

Given the results of Sect. 3.5 where the statistical modelling of C_W, $\langle H_\mathrm{U} \rangle$ and B_U in terms of climate and soil factors suggested a significant interaction between mean annual precipitation and soil water storage (Fig. 12) we conducted numerical simulations of soil water balances investigating the specific proposition that a low θ_P arising through the existence of some sort of impermeable layer close to the soil surface could actually have a positive effect on ecosystem annual water balances at low P_A: this occurring as a consequence of reductions in vertical water flow to depths below the rooting zone (Appendix A). And indeed, as is detailed is Sect. A3, it turns out that, due to reductions in drainage not necessarily being offset by high runoff rates, restricted root zones need not always be considered as having a detrimental effect on plant water relations. Indeed, in many cases potentially the opposite and with this more likely to be the case where P_A is low.

4 Discussion

Utilising the relatively novel situation found in South America where two distinct tropical vegetation formation types ($\mathbb{V}$) occur in close proximity across a wide precipitation range, we have demonstrated here systematic differences between forest ($\mathbb{F}$) and savanna ($\mathbb{S}$) in terms of soil, vegetation structure and some of the sampled physiologically relevant foliar characteristics. Further, we have shown that the large contrasts in structure between forest and savanna (Figs. 2 and 4) can be explained with a simple statistical model based on "effective plant available soil water" θ_P and upper layer exchangeable potassium concentrations $[\mathrm{K}]_\mathrm{sa}$ (Table 3).

In terms of our unusual situation of forest-savanna contrasts existing over such a wide precipitation range, the underlying reasons seem well understood in terms of underlying geomorphology and past landscape evolution (Cole, 1960, 1986). In short (and as a gross simplification) outside the Amazon forest region proper, forests tend to be found on slopes and escarpments with reasonably young and hence fertile (but often shallow) soils, with cerrado savanna on plateaus and other planation surfaces characterised by deep and usually heavily weathered soils. These differences in soil parent material, landscape position and/or soil age (degree of weathering) then lead to differences in soil properties (Fig. 3, Table S1) which – as has already been noted by others (Cochrane, 1989; Silva et al., 2006; Cochrane and Cochrane, 2010) – are intimately associated with the different vegetation types found across the landscape mosaic. At larger scales than the study here an important role for soil cations as a modulator of tropical vegetation structure and function has already been implied, for example from the canonical correspondence analysis (CCA) of vegetation distributions across the Amazon Basin where – in addition to P_A – effective soil cation exchange capacity (ECEC) and subsoil texture were found to be important determinants of vegetation type and with vegetation formations characterised by a higher C_W tending to be found at higher ECEC (Lloyd et al., 2009). Similarly, taking interpolated estimates of total exchangeable bases ($\Sigma_\mathrm{B} = [\mathrm{Ca}]_\mathrm{ex} + [\mathrm{Mg}]_\mathrm{ex} + [\mathrm{K}]_\mathrm{ex} + [\mathrm{Na}]_\mathrm{ex}$) as a measure of "soil fertility", Lehmann et al. (2011) found a significant positive effect of inclusion of Σ_B into a precipitation based model of global savanna distribution. Using a crude water balance metric (W), Veenendaal et al. (2015) found that both intra- and inter-continental differences in transition zone W were related to differences in $[Ca]_{ex} + [Mg]_{ex} + [K]_{ex}$ (drier transition zones typically having higher cation status) and with that study (of which the soil and vegetation data here forms a subset) also finding significant cation/soil moisture interactions.

4.1 Mass-related trait variations in relation to species, soils and climate

In terms of their constituent taxon, data interpretation is facilitated by there being almost no species overlap between forest and savanna plots anywhere along the precipitation gradient (Torello-Raventos et al., 2013) – hence our ability to refer to "forest" and "savanna" species. Within each vegetation type there is, however significant overlap between plots and, although forest plot species composition changes systematically in accordance with changes in both precipitation regime and soil characteristics along our study gradient (Torello-Raventos et al., 2013), when examined at the community level changes in plot mean trait values were, with the exception of the cations and $\delta^{13}C$, surprisingly small (Figs. 6, 7 and 10). This is especially the case when compared to the dramatic changes in forest stand-level canopy cover, tree height and biomass characteristics (Figs. 2 and 4). This is even all the more surprising in so much as there was also a clear change in leaf deciduousness along the transect, with almost all the forest species deciduous at the lowest P_A TUC-01 and mostly evergreen at the highest P_A TAP-01 and TAP-04 sites (Table S2). Moreover, as is evident from the relatively modest "environmental component" in the variance partitioning of Fig. 3 and the error bars of Figs. 6, 7 and 10, within-plot variability – a reasonable portion of which could be attributed to species identity (Fig. 3) – accounted for much more of the variation in trait characteristics than soil or climate. This then suggests that, at least within the one vegetation type, that species differences in leaf-level traits such as M_a, N_m and P_m are more or less irrelevant in terms of any habitat filtering that might be occurring.

Some changes in savanna species composition along the transect in response to the obvious edaphic and climatic gradients also occurred, though with this being to a lesser extent than for the forest species (Torello-Raventos et al., 2013), and in general, the changes in community level trait values were even more muted for $\mathbb{S}$ than was the case for $\mathbb{F}$. The lack of any effect of precipitation on community-averaged M_a~~,~~ of savanna species was also observed by Schrodt et al. (2014) ~~for~~ West Africa. They, also noting this observation to be contrary to the generally accepted dogma that M_a~~,~~ should increase with declining rainfall (Poorter et al., 2009), attributed lack of precipitation response to an increased rainfall seasonality (shorter growing season) as precipitation declines in their study – as is also the case here (Fig. 1).

An overall higher M_a (Fig. 6a) and lower N_m (Fig. 6b) of savanna trees was also noted by Schrodt et al. (2014) and has ~~similarly~~ been observed in tropical Australia by Bloomfield et al. (2014) and in the phylogenetically controlled Brazilian cerrado-gallery forest ~~comparisons of~~ Hoffmann et al. (2005). This suggests a consistent difference and, as is discussed in the next section, ~~the~~ tendency for leaf nitrogen concentrations to increase with decreasing rainfall also seems to be a consistent pattern and is probably related to reductions in canopy leaf areas as P_A declines. Also involved might be lesser N lixiviation and denitrification (e.g. through urease) at lower rainfall.

Differences between $\mathbb{F}$ and $\mathbb{S}$ in mass based phosphorus concentrations are less consistent across studies with Schrodt et al. (2014) finding no difference in West Africa (as was the case here – Fig. 6d), but with Bloomfield et al. (2014) finding lower values in their Australian savanna species. Nevertheless, at least within ZOT, this apparent discrepancy between vegetation types disappears when P is considered on a leaf area basis (Sect. 4.2).

It was the cations, however, for which the most dramatic changes with P_A occurred and for which the differences between $\mathbb{F}$ and $\mathbb{S}$ were the greatest: especially at low P_A. Again these trends and differences are as for West Africa, with in that case the higher K_m at low rainfall not being associated with increases in soil cation availability. As discussed by Schrodt et al. (2014) given its prime role as an osmotically active cation (Leigh and Wyn Jones, 1984) it seems likely that leaves of trees exposed to a lower P_A regime have a high potassium content in association with the more negative osmotic potentials required ~~in order~~ to survive more extended rain-free periods (also likely to be times of higher than average evaporative demand) during the dry season. We also note a recent literature survey where it was found that the leaves of "tropical-dry" woody species tend to have more negative osmotic potentials than their "tropical-wet" counterparts (Bartlett et al., 2012).

The West African study of Schrodt et al. (2014) similarly found, as here, lower K_m for savanna trees which – although also related to lower potassium in the savanna soils within ZOT, was further attributable to a genetic component. This is also the case here as re-running Eq. (2) but with the affiliation term treated as fixed rather than random gave an intrinsic savanna-forest difference of $3.0 \pm 0.7\,\mathrm{mg\,g^{-1}}$ (Table S3f). That is to say, it is not just the different soil chemistry of the forest vs. savanna plots that leads to their lower $\langle K_m \rangle$: but with intrinsically lower K_m for savanna species also contributing. Specifically, our model predicts K_m to be – on average – only 0.6 that of their forest counterparts under identical edaphic conditions. Also inferred to be intrinsically lower for savanna species were both Ca_m (Table S3e) and (more marginally) Mg_m (Table S3g) and as discussed by Schrodt et al. (2014) underlying this forest-savanna difference may be typically contrasting plant strategies in terms of leaf construction costs, with the tendency for low M_a in leaves of high mineral content. This is presumably attributable to a low tissue density associated with thinner, less lignified cell walls with the higher cation content presumably also balanced by higher levels of organic acids which are, themselves, of a relatively low C content. Generally with a lower C_m as well, forest leaves thus have lower overall construction costs (K) especially at low P_A (Fig. 7d; Table S3g).

As noted in Sect. 3.3.3 there was a tendency towards increased deciduousness as P_A declined and indeed, with a simple ANOVA on the data in Table S2 (data not shown) we find a significantly lower K for deciduous species as compared to evergreen species and the semi- and brevi-deciduous types as defined in Sect. 2.4 ($p < 0.01$), but only for

forest species. The lower $\langle K \rangle$ for forest plots are not therefore associated with a greater dominance of deciduous species per se. Indeed, if anything the opposite occurs with more evergreen-type species in the transitional forests (Sect. 3.3.3).

4.2 Area-based trait variations

Despite individual estimates of A_{max} at the leaf level varying more than two fold across the dataset, little of this variation appeared systematic in terms of differences in $\langle A_{max} \rangle$ between $\mathbb{F}$ and $\mathbb{S}$ plots, or in relation to variations in P_A (Fig. 10a). This lack of any rainfall dependence was also observed for savanna plot $\langle N_a \rangle$ and $\langle P_a \rangle$. There was, however a slight and significant tendency for forest plot $\langle N_a \rangle$ and $\langle P_a \rangle$ to increase with declining rainfall (in a general pattern similar to the non-significant $\langle A_a \rangle$ trend) consistent with the idea that leaves functioning at lower P_A should have a higher photosynthetic capacity than at high P_A – also operating a lower ratio of intercellular to ambient [CO_2], C_i/C_a (Buckley et al., 2002; Farquhar et al., 2002). The latter effect would be expected to be detectable through such leaves having a higher (less negative) $\delta^{13}C$ as was indeed observed to be the case for forest plots across the transect (Fig. 10d). It was, however, only at the lowest P_A savanna site that $\langle \delta^{13}C \rangle$ was increased for savanna trees. This lack of a community-level savanna $\delta^{13}C$ response has also been observed along a precipitation gradient in Australia where it has been assumed that the pattern is due to "species switching" (Schulze et al., 1998; Miller et al., 2001). That is to say, as P_A declines, then species increasingly adapted to more severe and/or extended soil water deficits replace those whose physiological characteristics are better suited to more mesic conditions; presumably primarily through the former having intrinsically higher root: shoot ratios (Schenk and Jackson, 2002; Mokany et al., 2006; Zerihun et al., 2006).

Taking savanna and forest together, simple linear multivariate modelling (Table 2) showed changes in $\langle N_a \rangle$ to be positively correlated with higher $\langle A_{max} \rangle$ as would be expected on the basis of leaf level studies (Domingues et al., 2010, 2014; Bloomfield et al., 2014) but with the soil associated $[P]_{sa}$ rather than the community weighted foliar

$\langle P_a \rangle$ being the better predictor in terms of stand level phosphorus status. Moreover, in addition to a statistically significant positive effect of mean canopy height $\langle H_U \rangle$ on $\langle A_{max} \rangle$ also detected ($p < 0.01$), there was a very strong negative effect of soil exchangeable potassium $[K]_{sa}$.

Taking the phosphorus effect first: one likely explanation for soil concentrations being better predictors than those of the foliage itself is that – at the individual leaf level – N and P may not be simple additive constraints on photosynthetic capacity. But rather – and depending on their relative concentrations – either one of these two elements can be limiting and with both forms of limitation often existing within the one stand (Domingues et al., 2010, 2014). With the higher the $[P]_{sa}$ the less the chance of a given tree having its photosynthetic rate limited by P_a, this would then mean that a soil phosphorus effect as shown here should be evident and with this not necessarily being simply reflected through the addition of a $\langle P_a \rangle$ term.

But what of the canopy height and soil potassium effects? Dealing with $\langle H_U \rangle$ first: although there is a strong tendency for taller trees with a greater probability of access to full sunlight to have higher area based nutrient concentrations and associated higher CO_2 assimilation capacities (Kenzo et al., 2006; Lloyd et al., 2010), this effect applies only within individual stands and there is no reason why that phenomenon should readily translate to differences in mean canopy height between different stands. Moreover, with $\langle N_a \rangle$ also included in the multivariate model (Table 2a) this means that it is also the mean photosynthetic N use efficiency which is modelled to decline with decreasing $\langle H_U \rangle$. But with the $\langle H_U \rangle$ of forest plots showing a clear negative dependence on P_A especially at the drier end of the transect (and savanna plots being less variable: Figs. 4b and 11d). Perhaps this effect relates to concurrent changes on other forest stand-forest properties which also correlate with $\langle H_U \rangle$: For example an increase in deciduousness associated with the shorter growing season as noted in Sect. 4.1. Here for example, to facilitate rapid leaf and shoot expansion during the limited periods of plant water availability at sites such as TUC-01, we might reasonably expect relatively large amounts of nitrogen to be allocated away from photosynthesis and towards amino-acid production

(Funk et al., 2013) and with increased allocation to N-based plant defence strategies also expected for the inevitably short lived leaves (Stamp, 2003) on trees growing in – as is strongly suggested by their soil and leaf δ^{15}N (Nardoto et al., 2013) – a relatively replete nitrogen environment.

Although at first sight the negative correlation between soil potassium and both leaf-area based photosynthetic capacities and the photosynthetic nutrient efficiencies of both N and P may seem surprising, this association is broadly consistent with previous work in the forest-savanna transition zone in both Africa and Australia where savanna species – typically found on lower potassium status soils than their forest counterparts as was the case here – have been observed to have greater A_{max} and/or A_N than their forest counterparts (Domingues et al., 2010, 2014; Bloomfield et al., 2014). Indeed, undertaking simple non-parametric correlations between photosynthetic capacity and a range of climatic and edaphic conditions for a (combined) dataset of nearly 200 forest and savanna tree measurements in Far North Queensland (Australia) Bloomfield et al. (2014) also found soil exchangeable potassium to be the best predictor of photosynthetic properties and with a negative relationship as found here.

In interpreting this relationship between community-level mean trait values and soil properties it is important to remember that edaphic effects may be mediated via intrinsic differences in the physiological characteristics of the various species making up the different plant communities (Fyllas et al., 2012), this being in addition to any direct effects of the soil property on the physiological traits of the species making up that community per se. In this respect, there is some indication that both these effects are likely to be important with Fig. 9 suggesting about equivalent amounts of the explained variance in the dataset attributable to both species and environment for A_{max} and A_N. Akin with this may then be, that associated with the typically lower cation status low $[K]_{sa}$ soils are typically slower growing species which, on average have less of their N allocated to defence or amino acids as growth reserves as compared to the species. Also related to differences in leaf nitrogen chemistry may be the tendency for tropical trees on higher cation status soils to use as their primary source NO_3^- which is subsequently assimilated in the foliage as opposed to root assimilated NH_4^+ (Stewart et al., 1988; Schmidt and Stewart, 1998; Aidar et al., 2003). This could affect photosynthesis and photosynthetic nitrogen efficiency in two ways. First with the leaves of trees on higher nutrient status soil having the main site of nitrogen processing in the leaves as opposed to roots on more dystric soils, more N-containing compounds not directly associated with CO_2 assimilation would inevitably be present in the foliage, this leading to a lower A_N. Second, with some of the NO_3^- reduction reactions of such trees occurring in the chloroplast (Halliwell, 1981) then it is also possible there could be direct competition with the photosynthetic carbon reduction cycle for the reducing equivalents ATP and NADPH.

But how to specifically invoke a role for soil potassium in the above scheme? Especially as differing forms of nitrogen uptake observed on eutric vs. dystric soils are generally considered to largely reflect differences in the relative availabilities of NO_3^- and NH_4^+ (Britto and Kronzucker, 2013) which in turn relate to pH sensitivities of ammonia-oxidizing bacteria and archaea (Yao et al., 2011). It is, however, now clear that other edaphic factors may influence soil nitrification rates at low pH (de Gannes et al., 2014) including a likely role for potassium (Norman and Barrett, 2014). Moreover, when one considers that a likely cause of nitrogen assimilation being mostly in the roots at low pH is a prevention of ammonium toxicity in the stem and leaf tissues (Givan, 1979) and with alleviation of NH_4^+ toxicity by K^+ supply well documented (Mengel et al., 1976; Britto and Kronzucker, 2013) then a specific role of soil potassium in influencing leaf photosynthetic characteristics through a range of interactions with plant nitrogen utilisation characteristics seems likely; especially given the close linkages between nitrogen and potassium in the modulation of numerous plant signalling pathways as discovered in recent years (Tsay et al., 2011). It has also been suggested that there may be plant specific advantages to storing C as organic acids (rather than sugars/starch) when it is to be subsequently used for the assimilation and/or use for N (Xu et al., 2012); this also linking to potassium's likely role as a balancing cation for organic anions (see Sect. 4.1).

Along with $\langle H_U \rangle$, $[K]_{sa}$ was ~~also~~ found to be associated with variations in $\langle \delta^{13}C \rangle$, with forest stands growing on soils of a higher exchangeable potassium status having a tendency towards higher $\langle \delta^{13}C \rangle$ (Table 2d). Although this potassium effect could potentially be considered an "artefact" of the general tendency of $[K]_{sa}$ to increase with declining P_A and with the latter exerting the direct effect on $\langle \delta^{13}C \rangle$ through reductions in $\langle C_i/C_a \rangle$ (Lloyd and Farquhar, 1994; Schulze et al., 1998; Miller et al., 2001; Bird et al., 2004) substitution of the $[K]_{sa}$ term with P_A – either in the presence or absence of the $\langle H_U \rangle$ – resulted in a markedly inferior model fit ($r^2 < 0.10$). And indeed, when patterns of variation in $\langle \delta^{13}C \rangle$ and $\langle K_m \rangle$ as a function of P_A are compared (Figs. 7b and 10c) they are remarkably similar~~— though~~ with some differences in the offset between forest and savanna. This then suggests a direct effect of potassium on photosynthetic physiology at the leaf level with the implied lower $\langle C_i/C_a \rangle$ at higher $[K]_{sa}$ perhaps associated with the stimulation of canopy leaf areas under conditions of high $[K]_{sa}$ as discussed in Sect. 4.3.

Despite being an important predictor of photosynthetic properties, $\langle H_U \rangle$ was unrelated to variations in $\langle \delta^{13}C \rangle$ when considered on its own (Table 1). Nevertheless, when taken in conjunction with variations in $[K]_{sa}$ a reasonably high association became apparent (Table 3c) with the inferred tendency being for $\langle \delta^{13}C \rangle$ to decrease with increasing $\langle H_U \rangle$. This implied increase in C_i/C_a as trees become taller is at odds with the often cited notion that taller trees tend to have less negative $\langle \delta^{13}C \rangle$ as a reflection of strong stomatal limitations to their gas exchange (Lloyd et al., 2010; McDowell et al., 2011). It is, however, important to remember that here we are looking at the relationship between average tree height and average foliar $\delta^{13}C$ across different stands, rather than comparing individual trees within the one stand. This difference, taken in conjunction with the observation that there is actually little dependence of $\langle H_U \rangle$ on P_A except at either very low P_A or – at the other extreme – beyond the magnitude of P_A being of sufficient magnitude to allow canopy closure to occur (Veenendaal et al., 2015) – see also Fig. 4b; suggests then that perhaps it is changes in light regime at the higher C_W

associated with greater $\langle H_\mathrm{U} \rangle$ driving this response. And, indeed, when considered in conjunction with $[\mathrm{K}]_\mathrm{sa}$, C_W is also a reasonably good predictor of $\langle \delta^{13}\mathrm{C} \rangle$ (multivariate $r^2 = 0.37$).

4.3 Soil–vegetation–climate relationships

In both managed and natural ecosystems, physiologically relevant reductions in soil nutrient availability can be considered as most likely to manifest either through changes in tissue nutrient concentrations and/or reductions in the extent of standing biomass (for example reductions in leaf area) and so through Eq. (3) we have attempted to see which of our studied nutrients was likely to be more limiting by examining the relationships between total canopy and soil amounts when both are expressed on a ground area basis (Fig. 8). When looked at this way, suggestions of any sort of relationship were, however, found only for calcium (Fig. 8a) and potassium (Fig. 8c) with – in marked contrast to the wetter forests of the Amazon Basin (Quesada and Lloyd, 2015) – no relationship being found between canopy and soil phosphorus amounts. It is accepted of course that Eq. (3) is an approximation: ignoring for example nutrients in boles, branches and roots as well as in grasses and understorey shrubs. Nevertheless, with their fast foliage turnover times and an general equivalence between fine root and leaf concentrations in tropical ecosystems (Vitousek and Sanford, 1986) such plots should still give a general indication of the relationship between ecosystem nutrient stocks/uptake rates and so the lack of any sort of relationship for magnesium and phosphorus remains particularly telling. It is also clear that whilst there are typically 5 fold higher concentrations of calcium in the soil as compared to potassium (see also Fig. 3a), differences in the total amount of foliar nutrient per unit ground area are much less marked (Fig. 8a and c). This – along with the non-saturating relationship of Fig. 8c then suggests – at least when considered in terms of vegetation requirements in relation to soil availability – that of the nutrients examined it is potassium that is the more likely candidate in terms of a nutrient constraint on ecosystem function.

Further evidence pointing in this direction comes from the observation that, as well as being associated with a range of different foliar properties such as photosynthetic nitrogen and phosphorus use efficiencies and varying systematically between forest and savanna stands, as a univariate predictor, $[\mathrm{K}]_\mathrm{sa}$ was the only edaphic or climatic variable significantly correlated with C_W (Table 1) and with none of $[\mathrm{Mg}]_\mathrm{sa}$, $[\mathrm{Ca}]_\mathrm{sa}$, pH, sand or clay content nearly as good a predictor of C_W, when considered either on their own or when considered in conjunction with P_A and θ_P (Sect. 3.5). Thus we may postulate not only that low soil potassium availability serves to decrease leaf areas though with this effect somewhat offset by higher photosynthetic capacities per unit leaf area, but also – with this response also mimicking what is expected under conditions of increasingly more severe water deficits (Buckley et al., 2002; Farquhar et al., 2002) – that potassium may somehow be involved in the signalling of the latter. Although such a strong effect, attributable to a single cation may be surprising, especially in terms of generally assumed belief that nitrogen and/or phosphorus are the two factors likely to be limiting plant productivity – and through the associated modulation of C supply other attributes such as leaf area and stand level biomass (Ostle et al., 2009; Scheiter and Higgins, 2009; Mercado et al., 2011; Alvarez-Clare et al., 2013; Pavlick et al., 2013) – in the agricultural literature the importance of potassium for crop yields is particularly well appreciated (Römheld and Kirkby, 2010; Wang et al., 2013; Zörb et al., 2014). This is especially the case under conditions of soil water deficit where a range of factors have been implicated: these including enhanced root longevity, reduction of stress-associated reactive oxygen species production, maintenance of tissue water relations through increases in leaf and/or root osmotic potential, as well as through effects on photosynthetic carbon acquisition via effects on stomatal and/or chloroplast metabolism (Mengel and Arneke, 1982; Egilla et al., 2001, 2005; Umar, 2006; Lebaudy et al., 2008; El-Mesbahi et al., 2012; Wang et al., 2013; Shabala and Pottosin, 2014). An important role of potassium as a prime signaller of plant responses to abiotic stresses has also recently been postulated by several groups (Osakabe et al., 2013; Ahmad and Maathuis, 2014; Anschütz et al., 2014; Hafsi et al., 2014; Shabala and Pottosin, 2014), which – along with a previously unrecognised likely role for potassium as an osmoticum in woody stem tissues capable of high water storage (Braun et al., 1968; Hart, 1984; Borchert and Pockman, 2005; Pineda-Garcia et al., 2013; Hietz et al., 2014; Spicer, 2014) all point to this element as a key chemical in soil water deficit signalling and response.

An active involvement of potassium in modulating plant responses to soil water deficit is also consistent with the additional involvement of mean annual precipitation and total plant available water as key factors modulating canopy structural properties (Table 3): In particular as a determinant of C_{W} for which θ_{P} seems just as important as P_{A} in accounting for the variations observed (Fig. 12d–f). Although perhaps surprising, numerical simulations have shown that this should indeed be the case. For example, the theoretical study of Feng et al. (2012) showed that – along with seasonality, the key factor controlling ecosystem evaporation rates – themselves expected to link broadly to differences in plant productivity (Beer et al., 2009) – was $\gamma = \theta_P / \dot{P}$ where $\dot{P}$ is the mean precipitation depth per event. The dimensionless nature of γ itself immediately points to an interaction between precipitation and soil water storage as detected here and is also as expected on the basis of maximum rooting depths increasing with mean annual rainfall in water-limited ecosystems (Collins and Bras, 2007; Schenk, 2008). Moreover, as one might intuitively expect, the study of Feng et al. (2012) also served to show that lower values of γ provide increasingly greater constraints on annual ecosystem evaporation rates as precipitation seasonality increases. Thus, in less seasonal environments than those investigated here it may well be that θ_{P} is less important a factor in the modulation of precipitation effects than as found for the current study.

Nevertheless, none of the above considerations can account for our fitted model prediction that for P_{A} 1.5 m a decline in θ_{P} may actually be associated with an increase in C_{W}. Nevertheless, as is verified numerically in Appendix A, this phenomenon is, however, readily understandable when it is considered that – with the exception of only a few sites – lower values of θ_{P} for the current study arose through the presence of some physical barrier restricting the depth below which roots could penetrate (Table S1). We suggest that because such layers are also effectively impermeable to water flow, then associated with a lower θ_{P} was also less drainage and more water generally being available for plant water use above that layer. Of course, were any such layer not to be present then roots could still access water below that depth. But presumably with this also involving additional structural carbon investment as compared to the restricted rootzone case: the maximum rooting depth on that case presumably reflecting the point at which the marginal carbon cost of adding deeper roots is balanced by the marginal carbon benefit of the increased transpiration then made possible (Guswa, 2008).

As characterised through the forest-savanna species dichotomy, a strong influence of soil physical and chemical properties on tropical vegetation structure as detected here are also indicative of a significant edaphic influence on woody plant community composition consistent with numerous regional studies where landscape-scale variations in vegetation structure/floristics have been related to effects of landscape position, underlying geology and/or soil texture: as for example: in Brigalow woodland in Central Queensland (Australia) (Dowling et al., 1986), Mopane Woodland in Botswana (Mlambo, 2007), for Nylsvley Nature Reserve (Coetzee et al., 1976), Kruger National Park (Fraser et al., 1987; Ben-Shahar, 1991; Baldeck et al., 2014; Scholtz et al., 2014), northern Transvaal (O'Connor, 1992) and Klaserie Nature Reserve (Witkowski and O'Connor, 1996) in South Africa; for the southern Kalahari Desert (Botswana, Namibia and South Africa) (Werger, 1978); in Etosha National Park in Namibia (Le Roux et al., 1988); for the Turkana District in Kenya (Coughenour and Ellis, 1993); across northern Yucatan Peninsula in Mexico (White and Hood, 2004); at Assis Ecological Station in southeast Brazil (de Assis et al., 2011); in W Regional Park in Southwest Niger (Diouf et al., 2012); in the Zambesi Valley (Guy, 1977), at Malilangwe Wildlife Reserve (Clegg and O'Connor, 2012) and Gonarezhou National Park (Gandiwa et al., 2014) in Zimbabwe, and for Emas National Park in central Brazil (Dantas et al., 2014). At larger scales, soil specific texture and depth effects on vegetation structure have also been noted for Zimbabwe (Dye and Walker, 1980) and, in conjunction with rainfall variations for Australia (Williams et al., 1996) Botswana (Skarpe, 1986; Ringrose et al., 2003) and

Sudan (Smith, 1951). Although it has been suggested that one general theme emerging from these studies is the importance of soil texture, with heavy textured soil generally having a lower woody vegetation density than coarser textured soils, apparently due to lower infiltration rates associated with the swelling of 2 : 1 minerals (Clegg and O'Connor, 2012), high clay contents are also possible for even the most highly weathered soils dominated by 1 : 1 clays for which water infiltration and retention properties are, if anything, more favourable than more coarsely textured soils (Sanchez, 1976; Hodnett and Tomasella, 2002; Quesada et al., 2011; Quesada and Lloyd, 2015). Moreover, variations in both soil organic matter and silt fraction also contribute importantly to differences in plant available soil volumetric water content (Rawls et al., 2003; Collins and Bras, 2007; Shukla, 2013). This means that, along with variations in rooting depth (as potentially affected by physical limitations), simple measures of upper-soil sand and clay content are likely to be only broadly reflective of the θ_P parameter as identified here. Although our estimates of θ_P were based simply on observations of maximum rooting depth and translating the categorized soil texture for each depth increment to a water holding capacity using a simple look up table (Hodnett and Tomasella, 2002), this clearly provides an improved estimate of soil moisture storage and buffering as compared to simple measures of upper surface clay and/or sand content as seems to have been the generally employed metric to date (Williams et al., 1996; Sankaran et al., 2005, 2008; Lehmann et al., 2014). It is, however, important to note that the fitted $P_\mathrm{A} : \theta_\mathrm{P}$ interaction term should not be independent of precipitation seasonality (Good and Caylor, 2011; Feng et al., 2012) and with any (presumably small) changes in seasonality with P_A incorporated into our fitted regression coefficients.

Although a few of the above studies demonstrating strong effects of soil physical properties and landscape position of vegetation structure did also measure soil nutrients, prior to this study little attempt had been made to ascertain if variations in tropical vegetation structure could be explained on the basis of differences in soil chemistry: either in isolation – or in addition to the soil physical effects interacting with water supply as described above. One exception is the interesting recent study of Mills et al. (2013)

who found that for measures of woody cover on 364 plots at 20 sites in Namibia that C_W tended to peak at intermediate nutrient contents. They interpreted their data as indicating that at the highest soil nutrient availabilities the "metabolic power" of grasses exceeded that of woody plants. Noting significant differences on several foliar traits between species growing in a "seasonally dry forest" vs. a *cerradão* (closed savanna woodland) stand in south-eastern Brazil, Viani et al. (2014) finger-pointed a low pH as the main factor driving differences in stand structure between the two vegetation formation types. But, as was found here (Fig. 7b), foliar potassium concentrations were also markedly higher in the forest species as compared to their savanna counterparts and with similar large contrasts in soil exchangeable cations (Fig. 3) between the two vegetation types (Viani et al., 2011). In terms of model fits, we found pH to be a far inferior predictor when substituted with $[\mathrm{K}]_\mathrm{sa}$ with $r^2 < 0.1$ for all multivariate predictor combinations as presented in Table 3. Indeed, as was the case for the photosynthetic properties examined, when considered in association with the appropriate covariates, no other soil parameter come even close to potassium in terms of its efficacy as a predictor of C_W with the best alternative (viz. $[\mathrm{Mg}]_\mathrm{sa}$) yielding a ΔAIC of −5.4 (Sect. 3.5).

4.4 Implications

Obviously there is much work to be done in terms of verifying what might be termed the "combined water and potassium" (CWAK) concept in terms of its applicability to other tropical systems. But, nevertheless, the idea that variations in canopy structure both within and between different forest and savanna vegetation formation types can be explained through a simple concurrent consideration of water and nutrients does not sit comfortably with most current theories of tropical vegetation structure where notions of disturbance and the existence of alternative stable states (ASS) as mediated by fire (or herbivory) as the prime drivers of structural and floristic variations in tropical ecosystems have assumed dogma status over recent years (Warman and Moles, 2009; Hirota et al., 2011; Lehmann et al., 2011, 2014; Staver et al., 2011; Favier et al., 2012; Hoffmann et al., 2012; Murphy and Bowman, 2012). Nevertheless, observational evidence for ASS is at best circumstantial (Veenendaal et al., 2015).

The CWAK hypothesis, of course, does not require there to be no effect of fire on tropical vegetation structure. But rather, that fire be more a passive response to the presence of flammable C_4 grasses (Lloyd et al., 2008) as opposed to fire being a major factor accounting for differences in savanna structure and the nature of forest-savanna transitions per se (Bond, 2008). And indeed, when examined in this context, recent results do actually point to the “passive response hypothesis being correct” (Diouf et al., 2012; Dantas et al., 2014), although interacting effects of fire on long-term soil nutrient availabilities and physical properties cannot be discounted (Cook, 1994; Cawson et al., 2012; Oliveras et al., 2013; Kugbe et al., 2014). Moreover although some researchers have argued that the spatial scale of variability in soil chemical variations is insufficient to account for observed spatial patterns in vegetation structure (Lehmann et al., 2011; Favier et al., 2012) this would seem to, more fundamentally, simply reflect a basic misunderstanding of the purpose of large scale soil maps such as are generally employed at the national or continental scale (Levels 4 and 5 in Table 6.1 of Dent and Young, 1981). Such maps were never constructed with the intention of providing an indication of the exact soil resource at any location, but rather to simply provide a broad overview of the soil resource at national or regional levels, this often being as a first step to more detailed mapping for future land use planning (Young, 1980; Dent and Young, 1981). And indeed, due to practical limits in the number of field observations possible when mapping at medium to high resolution, the hectare scale soil–vegetation associations as mentioned above in Sect. 4.3 often end up being one important factor in the generation of the smaller-scale soil map itself (Trapnell et al., 1950; Young, 1980; Breimer et al., 1986; Nyamapfene, 1988). As noted by Guy (1977) working in the Zambesi Valley: “The very close relationships between vegetation types and soils is well illustrated. . . . Because of this close relationship it is not hard to see why that structure of each vegetation type changes over short distances where pockets of soils unlike those surrounding them occur”.

Of course, we are by no means suggesting that all observed variations in tropical vegetation structure should be explainable on the simple basis of the CWAK hypothesis. For example, there are numerous cases where poor drainage may be the reason for savanna vegetation types under conditions otherwise suitable for forest (Cole, 1960, 1986; Haase and Beck, 1989; Cronje et al., 2008; Mantlana et al., 2008; Cochrane and Cochrane, 2010) and it also seems reasonable to speculate that in some cases that woody savanna tree extent could be constrained by supra-low calcium concentrations in the sub-soil (Cochrane, 1989). Also, with sodium capable of replacing potassium in many of its physiological functions when available at moderate concentrations (Wakeel et al., 2011; Kronzucker et al., 2013) of considerable interest in terms of refinement of the CWAK hypothesis is the existence of very high biomass stands of *Colophospermum mopane* (J.Kirk ex Benth.) J.Kirk ex J.Léonard and *Acacia harophylla* F. Muell. in southern Africa and north-eastern Australia respectively: in both cases sometimes at low precipitation ($< 0.8\,\mathrm{m\,a^{-1}}$) but then also on soils with a high exchangeable sodium content and often some also form of physical constraint at depth (Russell et al., 1967; Guy, 1977, 1981; Dye and Walker, 1980; Dowling et al., 1986). Whatever the case, as has also recently been shown for Amazon forests at a basin-wide scale (Quesada et al., 2012), it is now clear that a simple sampling of soils for a few selected parameters such as upper surface sand and clay content can in no way allow for a reasonable assessment of likely edaphic effects of tropical vegetation structure and function. to have been achieved.

5 Conclusions

Irrespective of rainfall regime savannas are found on soils of a consistently lower cation status than their forest counterparts: these soils also being characterised by lower phosphorus concentrations and higher C/N ratios. Leaves of trees growing within savanna stands are also typically of lower N and K concentrations (dry-mass basis) than for forest stands, but with little systematic difference in other elements (including phosphorus) or photosynthetic capacity. Contrasts between forest and savanna in the magnitude of their canopy cover for any given precipitation regime are appreciably greater than any differences in leaf area based physiological traits.

Especially for savannas, canopy cover is not closely associated with mean annual rainfall. But when considered in conjunction with soil water storage capacity and mean annual precipitation, soil exchangeable K (expressed on an area basis) emerges as an excellent predictor of canopy cover. Soil exchangeable Mg or Ca, pH or texture metrics are much less well associated. Soil exchangeable potassium is also well associated with a range of structural and photosynthesis associated traits with, in almost all cases, other cations, pH or soil texture metrics again of an inferior predictive ability.

For canopy cover and other stand-level structural traits such as mean canopy height and standing live biomass, this potassium effect is modulated by variations in soil water availability as evidenced by a co-occurring soil water storage/precipitation interaction term in OLS multivariate predictive model fits. This modelled interaction is complex, and although the intuitive increase in canopy cover with increasing soil water storage capacity is simulated to occur at relatively high rates of mean annual precipitation ($P_\mathrm{A} \gtrsim 1/5\,\mathrm{m\,a^{-1}}$), the opposite is observed for $P_\mathrm{A} \not\gtrsim 1/5\,\mathrm{m\,a^{-1}}$. With most of the variation in soil water storage capacity in the current dataset being attributable to differences in rooting zone depth as opposed to plant available water storage per unit soil volume, it was confirmed through numerical simulation that the presence of an impermeable layer close to the soil surface can potentially have a beneficial effect on annual water balances in a strongly seasonal environment. This unexpected effect arises as a consequence of reduced drainage rates out of the shallow rooting zone more than offsetting any higher runoff rates associated with extreme rainfall events.

Appendix A: Numerical demonstration of potential beneficial effects of restricted root zones

Given the results of Sect. 3.6 where our best fit statistical model predicted that, other things being equal, a reduced water storage capacity to be associated with higher canopy leaf areas than for potentially deeper rooting systems under low rainfall conditions ($P_\mathrm{A} \lessapprox 1.5\,\mathrm{m\,a^{-1}}$) but with the opposite true at under higher rainfall regimes; we investigate here the nature of this soil water storage/precipitation interaction using a simple water balance model as described on pp. 136–138 of Moene and van Dam (2014) with and without a physical barrier in the upper soil layers.

A1 Model description

The model is constructed by first considering all in- and out-flowing water amounts viz.

$$\Delta W = (P - E - R - D)\Delta t, \tag{A1}$$

where W is the amount of water stored in the soil column (m), P denotes the precipitation rate ($\mathrm{m\,d^{-1}}$), E is the evaporation rate ($\mathrm{m\,d^{-1}}$), R is surface runoff ($\mathrm{m\,d^{-1}}$), D is drainage or deep percolation rate ($\mathrm{m\,d^{-1}}$) and Δt is the considered time interval (d).

Here the soil is considered as a uniform reservoir of depth Z_t which can be filled with precipitation and which gradually releases water to the vegetation and the subsoil. All precipitation is assumed to infiltrate unless the reservoir is saturated in which case surplus precipitation flows away as surface runoff.

Reduction of potential evaporation E_P is assumed to occur when the soil moisture content drops below a critical value θ_C according to

$$E(\theta) = \beta_\mathrm{W}(\theta)E_\mathrm{P} \text{ with } \beta_\mathrm{W} = \begin{cases} 1 & \text{for } \theta_\mathrm{C} \le \theta < \theta_\mathrm{S} \\ \frac{\theta-\theta_\mathrm{W}}{\theta_\mathrm{C}-\theta_\mathrm{W}} & \text{for } \theta_\mathrm{W} \le \theta < \theta_\mathrm{C} \\ 0 & \text{for } \theta < \theta_\mathrm{W} \end{cases}, \tag{A2}$$

where E denotes the actual evapotranspiration, θ is the soil reservoir moisture content ($\mathrm{m^3\,m^{-3}}$), β_W is a reduction coefficient for transpiration (dimensionless) and θ_S, θ_C and θ_W are the saturated, critical and wilting point moisture contents ($\mathrm{m^3\,m^{-3}}$) respectively.

In the absence of any restriction to vertical water flow, percolation is described with free drainage below the soil reservoir using a hydraulic conductivity function where

$$D = k_h(\theta), \tag{A3}$$

where k_h ($\mathrm{m\,h^{-1}}$) is the soil hydraulic conductivity, the moisture dependence of which is described here according to the Brooks and Corey (1964) model as applied to the conductivity equation of Mualem (1976) by Tomasella and Hodnett (1997) viz.

$$k_h = k_{sat}\left(\frac{\theta - \theta_W}{\theta_S - \theta_W}\right)^{\eta}, \tag{A4a}$$

where k_{sat} is the saturated soil hydraulic conductivity ($\mathrm{m\,h^{-1}}$) and η is a function of parameter b in the water release curve retention mode of Brooks and Corey (1964), denoted herein as b_{BC} according to

$$\eta = \eta_1 b_{BC} + \eta_2. \tag{A4b}$$

To estimate k_{sat} we utilise the Ahuja et al. (1984) generalization of the Kozeny–Caraman equation as applied by Tomasella and Hodnett (1997) viz.

$$k_{sat} = B\phi_e^n, \tag{A5}$$

where ϕ_e is the effective porosity of the soil, defined as the total porosity (ϕ) minus the water content at a matric potential (ψ) of −33 kPa, and B and n are fitted parameters.

To relate ψ to θ we used the tropical soil van Genuchten (VG) pedotransfer function as applied to tropical soil by (Hodnett and Tomasella, 2002). The van Genuchten function is

$$\theta = \theta_R + \frac{\theta_S - \theta_R}{[1 + (\alpha/\psi)^a]^b}, \tag{A6}$$

where θ_R is the "residual" water content and α, a and b are empirical constants (and for which b is generally taken to be equal to $1 - 1/a$). To avoid confusion with the Brooks and Corey (BC) equation (whose parameters are used in Eq. A4b) we from here denote a and b of Eq. (A6) as a_{VG} and b_{VG} also noting the numerical equivalences between the parameters of these two different equations (Morel-Seytoux et al., 1996).

To define the required parameters for the running of the model, we first must specify a specific soil type; the one chosen here being the soil below the stunted forest at TUC-01; a silty loam at the driest end of the transect. On the basis of that texture classification the five parameter values of the pedotransfer functions of Hodnett and Tomasella (2002) were obtained, these being $\alpha = 0.191\,\mathrm{kPa^{-1}}$, $a_{VG} = 1.644$, $b_{VG} = 0.391$, $\theta_R = 0.223\,\mathrm{m^3\,m^{-3}}$ and $\theta_S = 0.601\,\mathrm{m^3\,m^{-3}}$. Soil water content at field capacity θ_{FC} was then estimated using Eq. (A6) with $\psi = -33\,\mathrm{kPa}$ yielding a value of $\theta_R = 0.336\,\mathrm{m^3\,m^{-3}}$. This then allowed ϕ_e (Eq. A5) to be estimated according to (Shukla, 2013):

$$\phi_e = 1 - \frac{\rho}{2.65} - \theta_{FC}, \tag{A7}$$

with ρ being the measured average soil bulk density ($1.47\,\mathrm{g\,cm^{-3}}$) and the 2.65 representing a (default) soil particle density. To obtain values of B and n for inclusion into Eq. (A5), we took the values obtained by Tomasella and Hodnett (1997) as derived from a regression of $\log(k_{sat})$ on $\log(\phi_e)$ across a range of tropical soil types viz $B = 56\,540$ and $n = 4.5359$ yielding $k_{sat} = 26.40\,\mathrm{mm\,h^{-1}}$. The soil moisture dependence of the soil hydraulic conductivity was then estimated through Eq. (A4), with $\eta_1 = 3.701$ and $\eta_2 = 1.843$ as suggested by Tomasella and Hodnett (1997), this with $b_{BC} = 0.644$ then yielding $\eta = 4.89$.

To obtain an estimate of β_W in Eq. (A2) we took $\theta_W = \theta_R$ and $\theta_W = 0.3\theta_{FC*}$ (Dunin and Aston, 1984) where θ_{FC*} is a slightly modified field capacity to that used in Eq. (A7), being taken at $\psi = -10\,\mathrm{kPa}$ (Moene and van Dam, 2014), this then yielding $\theta_{FC*} = 0.445\,\mathrm{m^3\,m^{-3}}$.

A2 Driving variables and model progression

To drive the model, we first used meteorological data collected as part of an study into Amazon forest productivity at the dry margin of the Amazon Basin in Bolivia (Araujo-Murakami et al., 2014; Doughty et al., 2014), taking data from the first year of measurements and estimating on a half-hourly basis values of E_P for input into Eq. (2) according to the FAO Penman method (Allen et al., 1998) viz.:

$$E_\mathrm{P} = \frac{0.408(R_\mathrm{n} - G) + \gamma \frac{900}{T_\mathrm{K}} u_2 (e_\mathrm{s} - e_\mathrm{a})}{\Delta + \gamma(1 + 0.34u_2)}, \tag{A8}$$

where E_P is the reference (potential) evapotranspiration (mm d^{-1}), R_n is the net radiation at the crop surface (MJ m^{-2} d^{-1}), G is the soil heat flux density (MJ m^{-2} day^{-1}), T_K mean daily air temperature at 2 m height (K), u is the wind speed at 2 m height (m s^{-}1), e_s is the saturation vapour pressure (kPa), e is actual vapour pressure (kPa), Δ is the slope of the vapour pressure/temperature curve (kPa °C^{-1}) and γ is the psychometric constant (kPa °C^{-1}).

Although with measurements of incoming solar radiation Q, neither R_n nor G had been directly determined at the KEN-01 site. In estimating the $(R_\mathrm{n} - G)$ term in Eq. (A8), we therefore made the simple assumption that $G = 0.1R_\mathrm{n}$ (Moene and van Dam, 2014) also assuming $R_\mathrm{n} = 0.8Q$ (Miranda et al., 1997). On a half-hourly basis (the resolution of the provided meteorological data) the estimation of E_P then allowed an estimate of the change of soil moisture with time in the absence a relatively impenetrable layer to be made viz.

$$\frac{\mathrm{d}\theta}{\mathrm{d}t} = \frac{1}{Z_\mathrm{r}} \left[P - \beta E_\mathrm{P} - k_\mathrm{sat} \left(\frac{\theta - \theta_\mathrm{W}}{\theta_\mathrm{S} - \theta_\mathrm{W}} \right)^{\eta} \right]. \tag{A9}$$

To simulate the effects of an impenetrable layer, the k_sat term in Eq. (A9) above was set to 1.0 mm s^{-1}; a value in the range of those reported for an almost totally impermeable layer in the subsoil of an Amazon Plinthosol (de Moraes et al., 2006).

We then undertook two sets of analysis with water supply and demand always as described as above, but with varying k_sat. For both scenarios simulations were undertaken for a range of soil depths by repeated model runs with the effective rooting depth Z_r increasing from 0.08 to 2.40 m in 10 mm increments.

As well as being evaluated at the KEN-01, we also investigated the effect of different precipitation regimes through substitution of the KEN-01 precipitation values (P_A = 1.51 m a^{-1}) with the hourly record of a site close to TUC-01 and made in an apparently very dry year (Steininger et al., 2013) (P_A = 0.54 m a^{-1}) and the wettest year of an hourly six year record from a site in the Amazon forest region proper (TAP-04) as provided by Kim et al. (2012) (P_A = 2.15 m a^{-1}). Providing a fourth (so as to provide a series of precipitation regimes in approximately 0.5 m increments) we also generated an artificial regime of P_A = 1.1 m a^{-1} by simply multiplying each KEN-01 precipitation event by 0.7.

Figure A1 shows the seasonality of these four precipitation patterns are shown along with the simulated potential evaporation rate (as obtained using input radiation, wind speed, temperature and humidity data from KEN-01 and held as invariant across all four sites).

A3 Simulation results

Figure A2 shows the simulated dependencies of all water fluxes into and out of the soil according to the model as dependent on the rooting depth (Z_r) where, for the "restricted" case it is assumed that an impermeable layer constrains the depth to which the supported vegetation can extract water. In the case of "unrestricted" rooting, free drainage is allowed to occur below Z_r which then reflects – in some sort of crude way – the ecological strategy of the vegetation above in terms of its below-ground carbon investment directed towards water acquisition.

Starting with the lowest precipitation regime (Fig. A2a: TUC-01) it can clearly be seen that in neither case is extending $Z_\mathrm{r} \gtrsim 0.8$ m likely to be any profit for the vegetation (with both drainage and runoff being zero beyond this value). The water flux through evapotranspiration does, however, increase with Z_{r} up until around 0.6 m, but with a far more rapid increase in E with Z_{r} occurring for $Z_{\mathrm{r}} \gtrsim 0.2$ m in the restricted case. This can be seen to be because of much less drainage than the unrestricted case at low Z_{r}; something which is only offset to a minor degree by the marginally increased runoff.

At the ca. 100 % higher precipitation regime of Fig. A2b, very different patterns emerge with an increase in E with Z_{r} up till at least 2.4 m in both cases. Though with this dependency in both cases distinctly non-linear and, as for the lowest rainfall regime, with the restricted case showing a much more rapid rise in vegetation water use as rooting depth increases up until about 0.25 m and, at any given Z_{r} always with high E predicted for the restricted vs. unrestricted case. The latter effect can be attributed to the reduction in drainage associated with the impeded layer being less than offset by the higher runoff.

A broadly similar pattern is observed at a higher rainfall of about 1.5 m a^{-1} (KEN-01: Fig. A2c) though here drainage fluxes for the restricted case show a different pattern: first increasing then decreasing with increased Z_{r}. This can be regarded as a consequence of R declining faster than E as the restricted layer depth decreases; the implication being that of the extra water infiltrating the soil as rooting depth increases at lower Z_{r}, only some of it can be used by the vegetation above; the rest necessarily going as drainage. Beyond $Z_{\mathrm{r}} \cong 0.6$ m – this also being the minimum soil depth for which R is modelled to be zero – the expected decline in D with increased Z_{r} occurs, this being complemented entirely by increased E.

Under the highest examined precipitation regime of TAP-04 ($P = 2.15$ m a^{-1}) a broadly similar pattern to KEN-01 is observed, but with the more rapid increase in E with Z_{r} in the restricted case now extending to about 0.6 m. Beyond this depth there is simulated to be little effect of the higher precipitation regime on D for either the restricted or unrestricted case as compared to KEN-01, with all the extra rainfall being utilised by the vegetation (Fig. A2d).

Overall, Fig. A2 suggests that, according to these simulations at least – as hypothesized – a restricted root zone may be beneficial in at least some situations – at least

when compared to the unrestricted case at the same Z_{r}. Yet, it is also important to bear in mind that also when compared at the same E, there are very different temporal patterns for the two cases examined here. This is shown in Table A1, where for each of the four precipitation regimes examined in Fig. A2, we have calculated both the numbers of days at which $\theta < \theta_{\mathrm{C}}$ (indicating some degree of simulated effect of soil water deficit on E as modulated by the β_{W} term in Eq. A2) and those for which the air filled porosity (ϕ) was modelled as being less than 0.1 m^3 m^{-3}; this being one general indicator of potentially waterlogged conditions (Wesseling et al., 1957). Here for each P_{A} regime the unrestricted-restricted comparison is at the same simulated E as that found for the restricted case with $Z_{\mathrm{r}} = 0.3$ m. For all four P_{A} the equivalent Z_{r} for the unrestricted case is just over 0.7 m.

This shows that for all four P_{A} regimes there are no simulated indications of any water logging in the well-drained case but with up to three months of unfavourable conditions of soil aeration predicted with a restricted layer present. On the other hand, time spent under conditions of some sort of soil water deficit is reduced by the presence of the restricting layer with differences of nearly 50 days under the highest TAP-04 rainfall regime examined.

This effect is probed further in Fig. A3 where the simulated annual patterns (daily values) of P, R, D, E and θ are shown for KEN-01 with the yearly total evapotranspiration in both cases equal to the $Z_{\mathrm{r}} = 0.3$ m restricted case. Here can be seen the higher runoff of the restricted case, with the unrestricted soil showing a corresponding lagged drainage response immediately after high precipitation periods (Fig. A3a and b). This general "buffering" in the absence of any root zone restriction is also seen in both the E and θ responses during periods of soil water depletion or refill (Fig. A3c and d) with, most noticeably, θ always at a much lower value for the unrestricted case – even during the wet season when E is clearly not limited by soil water availability.

A4 Caveats

It must be emphasised that in many ways the model applied here is a crude one. For example – in terms of defects – see also page 138 of Moene and van Dam (2014):

1. It assumes that runoff occurs only when a soil becomes saturated; in reality runoff will also occur when the precipitation flux is higher than the maximum infiltration flux into the soil In savannas that bias may potentially be a large one because of hydrophobicity caused by fire (DeBano, 2000), this also being the case for more strongly seasonal environments with extreme dry-wetting events, especially in soils with a relatively abundant clay content (Shukla, 2013; Moene and van Dam, 2014).
2. The critical moisture content θ_C is a merely an assumed one, defined on the basis of one Australian study (Dunin and Aston, 1984). Most likely it would also vary according to variations in Z_r and in response to the presence/absence of any restrictive layer (Guswa, 2010).
3. Likewise in both cases we have assumed that β_W (a dimensionless coefficient relating E to E_P – see Eq. A2) is dependent only upon the soil water content. In practise it will vary with other factors such as leaf area index, which also vary seasonally, this probably giving rise to a more linear E vs. θ relationship than that prescribed here (Quesada et al., 2008). As an example, with the restricted $Z_\mathrm{r} = 0.3$ m soil most likely supporting a deciduous forest under KEN-01 conditions (Torello-Raventos et al., 2013) the simulated out of season vegetation water uptake around day 150 would be most unlikely to actually occur due to an absence of leaves. It might also be expected than when Z_r is restricted that the supported vegetation would have a more aggressive water use strategy that would otherwise be the case so as to deplete the root zone more quickly – this then creating space to absorb the next rain(s) (Guswa, 2010).
4. Any evaporation direct from the soil surface has been ignored.

5. Vertical variations in root distributions have not been accounted for.
6. Capillary rise has not been considered.
7. The simulated pattern in E_P comes from a single site (KEN-01). Thus, for example, anti-correlations between precipitation amount and potential evaporation rates (due to reduced radiation inputs and low vapour pressure deficits on wetter, cloudy days) have been broken for the TUC-01 and TAP-04 simulations.

Nevertheless, whilst the above means that little emphasis should be placed on the precise nature of the various individual predictions, the general principles as established by the simulations still remain valid.

The Supplement related to this article is available online at doi:10.5194/bgd-12-7879-2015-supplement.

Acknowledgements. We gratefully acknowledge the many generous individuals who took part in the making of this work either in the field or in the UK. Shiela Lloyd assisted with manuscript preparation and anger management. This work was funded as part of the UK Natural Environment Research Council TROBIT Consortium project (Award NE/D005590/1). We gratefully acknowledge to CNPq to the productivity grant and "Ciência sem Fronteiras" grant granted by CNPq to BH Marimon Junior and BS Marimon. Meteorological data for KEN-01 as used in the Appendix was provided by C. Doughty and Y. Malhi (University of Oxford) with data for TAP-04 having been made available by M. Goulden (University of California, Irvine). Original data as presented here available through the TRY' plant trait database (www.try-db.org/).

References

Ahmad, I. and Maathuis, F. J. M.: Cellular and tissue distribution of potassium: physiological relevance, mechanisms and regulation, J. Plant Physiol., 171, 708–714, doi:10.1016/j.jplph.2013.10.016, 2014.

Ahuja, L., Naney, J., Green, R., and Nielsen, D.: Macroporosity to characterize spatial variability of hydraulic conductivity and effects of land management, Soil Sci. Soc. Am. J., 48, 699–702, 1984.

Aidar, M., Schmidt, S., Moss, G., Stewart, G., and Joly, C.: Nitrogen use strategies of neotropical rainforest trees in threatened Atlantic Forest, Plant Cell Environ., 26, 389–399, 2003.

Allen, R. G., Pereira, L. S., Raes, D., and Smith, M.: Crop Evapotranspiration – Guidelines for Computing Crop Water Requirements – FAO Irrigation and Drainage Paper 56, FAO, Rome, 300, 6541, 1998.

Alvarez-Clare, S., Mack, M., and Brooks, M.: A direct test of nitrogen and phosphorus limitation to net primary productivity in a lowland tropical wet forest, Ecology, 94, 1540–1551, 2013.

Anderson, J. M. and Ingram, J. S. I.: Tropical Soil Biology and Fertility: a Handbook of Methods, CAB International, Wallingford, UK, 1–221, 1993.

Anschütz, U., Becker, D., and Shabala, S.: Going beyond nutrition: regulation of potassium homoeostasis as a common denominator of plant adaptive responses to environment, J. Plant Physiol., 171, 670–687, doi:10.1016/j.jplph.2014.01.009, 2014.

Araujo-Murakami, A., Doughty, C. E., Metcalfe, D. B., Silva-Espejo, J. E., Arroyo, L., Heredia, J. P., Flores, M., Sibler, R., Mendizabal, L. M., and Pardo-Toledo, E.: The productivity, allocation and cycling of carbon in forests at the dry margin of the Amazon forest in Bolivia, Plant Ecol. Divers., 7, 55–69, 2014.

Askew, G., Moffatt, D., Montgomery, R., and Searl, P.: Interrelationships of soils and vegetation in the savanna-forest boundary zone of North-Eastern Mato Grosso, Geogr. J., 136, 370–376, 1970.

Avenard, J.-M. and Tricart, J.: Le contact forêt-savane: rôle des régimes hydriques des sols dans l'Ouest de la Côte-d'Ivoire, Ann. Geogr., 81, 421–450, 1972.

Baldeck, C. A., Colgan, M. S., Féret, J. B., Levick, S. R., Martin, R. E., and Asner, G. P.: Landscape-scale variation in plant community composition of an African savanna from airborne species mapping, Ecol. Appl., 24, 84–93, doi:10.1890/13-0307.1, 2014.

Bartlett, M. K., Scoffoni, C., and Sack, L.: The determinants of leaf turgor loss point and prediction of drought tolerance of species and biomes: a global meta-analysis, Ecol. Lett., 15, 393–405, doi:10.1111/j.1461-0248.2012.01751.x,doi:, 2012.

Beer, C., Ciais, P., Reichstein, M., Baldocchi, D., Law, B., Papale, D., Soussana, J. F., Ammann, C., Buchmann, N., and Frank, D.: Temporal and among-site variability of inherent water use efficiency at the ecosystem level, Global Biogeochem. Cy., 23, 1–13. 2009.

Ben-Shahar, R.: Abundance of trees and grasses in a woodland savanna in relation to environmental factors, J. Veg. Sci., 2, 345–350, doi:10.2307/3235926, 1991.

Bevington, P. R. and Robinson, D. K.: Data Reduction and Error Analysis for the Physical Sciences, McGraw-Hill, New York, 1969.

Bird, M. I., Veenendaal, E. M., and Lloyd, J. J.: Soil carbon inventories and δ^{13}C along a moisture gradient in Botswana, Glob. Change Biol., 10, 342–349, doi: 10.1046/j.1365-2486.2003.00695.x, 2004.

Bloomfield, K. J.: The Nature of Photosynthetic Phosphorus Limitations for Tropical Tree Species, Ph.D. thesis, School of Geography, University of Leeds, 160 pp., 2012.

Bloomfield, K. J., Domingues, T. F., Saiz, G., Bird, M. I., Crayn, D. M., Ford, A., Metcalfe, D. J., Farquhar, G. D., and Lloyd, J.: Contrasting photosynthetic characteristics of forest versus savanna species (Far North Queensland, Australia), Biogeosciences, 11, 7331–7347, doi: 10.5194/bg-11-7331-2014, 2014.

Bond, W. J.: What limits trees in C_4 grasslands and savannas?, Annu. Rev. Ecol. Evol. S., 39, 641–659, 2008.

Bond, W. J.: Do nutrient-poor soils inhibit development of forests? A nutrient stock analysis, Plant Soil, 334, 47–60, doi:10.1007/s11104-010-0440-0, 2010.

Borchert, R. and Pockman, W. T.: Water storage capacitance and xylem tension in isolated branches of temperate and tropical trees, Tree Physiol., 25, 457–466, doi:10.1093/treephys/25.4.457, 2005.

Braun, H. J., Versteegh, C., and Böhme, H.: Holz-Bautypen tropischer Bäume und ihre Einordnung in die Organisation des Hydrosystems, Holzforschung, 22, 16–21, 1968.

Breimer, R. F., Van Kekem, A., and Van Reuler, H.: Guidelines for soil survey and land evaluation in ecological research, Unesco, 1986.

Briggs, R. D.: Site Classification Field Guide, Maine Agriculture and Forest Experiment Station, 1994.

Britto, D. T. and Kronzucker, H. J.: Ecological significance and complexity of N-source preference in plants, Ann. Bot.-London, 112, 957–963, doi:10.1093/aob/mct157, 2013.

Brooks, R. and Corey, A.: Hydraulic properties of porous media, Hydrology Papers, Colorado State University 1964.

Buckley, T. N., Miller, J. D., and Farquhar, G. D.: The mathematics of linked optimisation for water and nitrogen use in a canopy, Silva Fenn., 36, 639–669, 2002.

Cawson, J., Sheridan, G., Smith, H., and Lane, P.: Surface runoff and erosion after prescribed burning and the effect of different fire regimes in forests and shrublands: a review, Int. J. Wildland Fire, 21, 857–872, 2012.

Cernusak, L. A., Hutley, L. B., Beringer, J., Holtum, J. A., and Turner, B. L.: Photosynthetic physiology of eucalypts along a sub-continental rainfall gradient in northern Australia, Agr. Forest Meteorol., 151, 1462–1470, 2011.

Clegg, B. and O'Connor, T.: The vegetation of Malilangwe Wildlife Reserve, south-eastern Zimbabwe, Afr. J. Range For. Sci., 29, 109–131, 2012.

Cleveland, C. C., Townsend, A. R., Taylor, P., Alvarez-Clare, S., Bustamante, M. M. C., Chuyong, G., Dobrowski, S. Z., Grierson, P., Harms, K. E., Houlton, B. Z., Marklein, A., Parton, W., Porder, S., Reed, S. C., Sierra, C. A., Silver, W. L., Tanner, E. V. J., and Wieder, W. R.: Relationships among net primary productivity, nutrients and climate in tropical rain forest: a pantropical analysis, Ecol. Lett., 14, 939–947, doi:10.1111/j.1461-0248.2011.01658.x, 2011.

Cochrane, T. T.: Chemical properties of native savanna and forest soils in central Brazil, Soil Sci. Soc. Am. J., 53, 139–141, 1989.

Cochrane, T. T. and Cochrane, T. A.: Amazon Forest and Savanna lands: A Guide to the Climates, Vegetation, Landscapes and Soils of Central Tropical South America, CreateSpace, 2010.

Coetzee, B., Meulen, F., Zwanziger, S., Gonsalves, P., and Weisser, P.: A phytosociological classification of the Nylsvley Nature Reserve, Bothalia, 12, 137–160, 1976.

Cole, M. M.: Cerrado, Caatinga and Pantanal: the distribution and origin of the savanna vegetation of Brazil, Geogr. J., 126, 168–179, 1960.

Cole, M. M.: The Savannas, Biogeography and Geobotany, Academic Press, 1986.

Collins, D. B. G. and Bras, R. L.: Plant rooting strategies in water-limited ecosystems, Water Resour. Res., 43, W06407, doi:10.1029/2006WR005541, 2007.

Comins, H. and McMurtrie, R.: Long-term response of nutrient-limited forests to CO_2 enrichment; equilibrium behavior of plant-soil models, Bulletin of the Ecological Society of America, 3, 666–681, 1993.

Cook, G.: The fate of nutrients during fires in a tropical savanna, Aust. J. Ecol., 19, 359–365, 1994.

Coughenour, M. B. and Ellis, J. E.: Landscape and climatic control of woody vegetation in a dry tropical ecosystem: Turkana District, Kenya, J. Biogeogr., 383–398, 20, 1993.

Cronje, H. P., Panagos, M. D., and Reilly, B. K.: The plant communities of the Andover Game Reserve, South Africa: original research, Koedoe: African Protected Area Conservation and Science, 50, 184–201, 2008.

Daly, D. C. and Mitchell, J. D.: Lowland vegetation of tropical South America – an overview, in: Imperfect Balance Landscape Transformations in the Pre-Columbian Americas, edited by: Lentz, D., Columbia University Press, New York, 391–454, 2000.

Dantas, V. D. L., Batalha, M. A., França, H., and Pausas, J. G.: Resource availability shapes fire-filtered savannas, J. Veg. Sci., 26, 395–403, doi:10.1111/jvs.12247, 2015.

de Assis, A., Coelho, R., da Silva Pinheiro, E., and Durigan, G.: Water availability determines physiognomic gradient in an area of low-fertility soils under Cerrado vegetation, Plant Ecol., 212, 1135–1147, doi:10.1007/s11258-010-9893-8, 2011.

de Gannes, V., Eudoxie, G., and Hickey, W. J.: Impacts of edaphic factors on communities of ammonia-oxidizing archaea, ammonia-oxidizing bacteria and nitrification in tropical soils, Plos One, 9, V.9, doi:10.1371/journal.pone.0089568, 2014.

de Moraes, J. M., Schuler, A. E., Dunne, T., Figueiredo, R. D. O., and Victoria, R. L.: Water storage and runoff processes in plinthic soils under forest and pasture in eastern Amazonia, Hydrol. Process., 20, 2509–2526, doi:10.1002/hyp.6213, 2006.

DeBano, L. F.: The role of fire and soil heating on water repellency in wildland environments: a review, J. Hydrol., 231, 195–206, 2000.

Dent, D. and Young, A.: Soil Survey and Land Evaluation, George Allen & Unwin., 1981.

Diouf, A., Barbier, N., Lykke, A. M., Couteron, P., Deblauwe, V., Mahamane, A., Saadou, M., and Bogaert, J.: Relationships between fire history, edaphic factors and woody vegetation structure and composition in a semi-arid savanna landscape (Niger, West Africa), Appl. Veg. Sci., 15, 488–500, doi: 10.1111/j.1654-109X.2012.01187.x, 2012.

Domingues, T. F., Berry, J. A., Martinelli, L. A., Ometto, J. P. H. B., and Ehleringer, J. R.: Parameterization of canopy structure and leaf-level gas exchange for an Amazonian tropical rain forest (Tapajós National Forest, Pará, Brazil), Earth Interact., 9, 1–23, doi:10.1175/EI149.1, 2005.

Domingues, T. F., Meir, P., Feldpausch, T. R., Saiz, G., Veenendaal, E. M., Schrodt, F., Bird, M., Djagbletey, G., Hien, F., Compaore, H., Diallo, A., Grace, J., and Lloyd, J.: Co-limitation of photosynthetic capacity by nitrogen and phosphorus in West Africa woodlands, Plant Cell Environ., 33, 959–980, doi: 10.1111/j.1365-3040.2010.02119.x, 2010.

Domingues, T. F., Ishida, F. Y., Feldpausch, T. R., Grace, J., Meir, P., Saiz, G., Sene, O., Schrodt, F., Sonké, B., Taedoumg, H., Veenendaal, E. M., Lewis, S. L., and Lloyd, J.: Biome-specific effects of nitrogen and phosphorus on the photosynthetic characteristics of trees at a forest-savanna boundary in Cameroon, Oecologia, doi: 10.1007/s00442-015-3250-5, 2015.

Doughty, C. E., Malhi, Y., Araujo-Murakami, A., Metcalfe, D. B., Silva-Espejo, J. E., Arroyo, L., Heredia, J. P., Pardo-Toledo, E., Mendizabal, L. M., and Rojas-Landivar, V. D.: Allocation trade-offs dominate the response of tropical forest growth to seasonal and interannual drought, Ecology, 95, 2192–2201, 2014.

Dowling, A. J., Webb, A. A., and Scanlan, J. C.: Surface soil chemical and physical patterns in a Brigalow–Dawson gum forest, Central Queensland, Aust. J. Ecol., 11, 155–162, doi: 10.1111/j.1442-9993.1986.tb01386.x, 1986.

Dunin, F. and Aston, A.: The development and proving of models of large scale evapotranspiration: an Australian study, Agr. Water Manage., 8, 305–323, 1984.

Durigan, G. and Ratter, J. A.: Successional changes in cerrado and cerrado/forest ecotonal vegetation in Western São Paulo State, Brazil, 1962–2000, Edin. J. Bot., 63, 119–130, doi: 10.1017/S0960428606000357, 2006.

Dye, P. and Walker, B.: Vegetation–environment relations on sodic soils of Zimbabwe Rhodesia, J. Ecol., 68, 589–606, 1980.

Egilla, J. N., Davies, F. T. J., and Drew, M. C.: Effect of potassium on drought resistance of *Hibiscus rosa-sinensis* cv. *Leprechaun*: plant growth, leaf macro- and micronutrient content and root longevity, Plant Soil, 229, 213–224, doi:10.1023/A:1004883032383, 2001.

Egilla, J. N., Davies, F. T. J., and Boutton, T. W.: Drought stress influences leaf water content, photosynthesis, and water-use efficiency of *Hibiscus rosa-sinensis* at three potassium concentrations, Photosynthetica, 43, 135–140, doi:10.1007/s11099-005-5140-2, 2005.

Eiten, G.: Delimitation of the cerrado concept, Plant Ecol., 36, 169–178, doi:10.1007/bf02342599, 1978.

El-Mesbahi, M. N., Azcon, R., Ruiz-Lozano, J. M., and Aroca, R.: Plant potassium content modifies the effects of arbuscular mycorrhizal symbiosis on root hydraulic properties in maize plants, Mycorrhiza, 22, 555–564, doi:10.1007/s00572-012-0433-3, 2012.

Farquhar, G. D., Ehleringer, J. R., and Hubick, K. T.: Carbon isotope discrimination and photosynthesis, Annu. Rev. Plant Phys., 40, 503–537, 1989.

Farquhar, G. D., Buckley, T. N., and Miller, J. M.: Optimal stomatal control in relation to leaf area and nitrogen content, Silva Fenn., 36, 625–637, 2002.

Favier, C., Aleman, J., Bremond, L., Dubois, M. A., Freycon, V., and Yangakola, J.-M.: Abrupt shifts in African savanna tree cover along a climatic gradient, Global Ecol. Biogeogr., 21, 787–797, doi:10.1111/j.1466-8238.2011.00725.x, 2012.

Feldpausch, T. R., Banin, L., Phillips, O. L., Baker, T. R., Lewis, S. L., Quesada, C. A., Affum-Baffoe, K., Arets, E. J. M. M., Berry, N. J., Bird, M., Brondizio, E. S., de Camargo, P., Chave, J., Djagbletey, G., Domingues, T. F., Drescher, M., Fearnside, P. M., França, M. B., Fyllas, N. M., Lopez-Gonzalez, G., Hladik, A., Higuchi, N., Hunter, M. O., Iida, Y., Salim, K. A., Kassim, A. R., Keller, M., Kemp, J., King, D. A., Lovett, J. C., Marimon, B. S., Marimon-Junior, B. H., Lenza, E., Marshall, A. R., Metcalfe, D. J., Mitchard, E. T. A., Moran, E. F., Nelson, B. W., Nilus, R., Nogueira, E. M., Palace, M., Patiño, S., Peh, K. S.-H., Raventos, M. T., Reitsma, J. M., Saiz, G., Schrodt, F., Sonké, B., Taedoumg, H. E., Tan, S., White, L., Wöll, H., and Lloyd, J.: Height-diameter allometry of tropical forest trees, Biogeosciences, 8, 1081–1106, doi:10.5194/bg-8-1081-2011, 2011.

Feng, X., Vico, G., and Porporato, A.: On the effects of seasonality on soil water balance and plant growth, Water Resour. Res., 48, W05543, doi:10.1029/2011WR011263, 2012.

Fraser, S., Van Rooyen, T., and Verster, E.: Soil–plant relationships in the central Kruger National Park, Koedoe, 30, 19–34, 1987.

Fromm, J.: Wood formation of trees in relation to potassium and calcium nutrition, Tree Physiol., 30, 1140–1147, doi:10.1093/treephys/tpq024, 2010.

Funk, J. L., Glenwinkel, L. A., and Sack, L.: Differential allocation to photosynthetic and non-photosynthetic nitrogen fractions among native and invasive species, PloS one, 8, e64502, 10.1371/journal.pone.0064502, 2013

Furley, P. A. and Ratter, J. A.: Soil resources and plant communities of the central Brazilian cerrado and their development, J. Biogeogr., 15, 97–108, 1988.

Fyllas, N. M., Patiño, S., Baker, T. R., Bielefeld Nardoto, G., Martinelli, L. A., Quesada, C. A., Paiva, R., Schwarz, M., Horna, V., Mercado, L. M., Santos, A., Arroyo, L., Jiménez, E. M., Luizão, F. J., Neill, D. A., Silva, N., Prieto, A., Rudas, A., Silviera, M., Vieira, I. C. G., Lopez-Gonzalez, G., Malhi, Y., Phillips, O. L., and Lloyd, J.: Basin-wide variations in foliar properties of Amazonian forest: phylogeny, soils and climate, Biogeosciences, 6, 2677–2708, doi:10.5194/bg-6-2677-2009, 2009.

Fyllas, N. M., Quesada, C. A., and Lloyd, J.: Deriving plant functional types for Amazonian forests for use in vegetation dynamics models, Perspect. Plant Ecol., 14, 97–110, doi: 10.1016/j.ppees.2011.11.001, 2012.

Fyllas, N. M., Gloor, E., Mercado, L. M., Sitch, S., Quesada, C. A., Domingues, T. F., Galbraith, D. R., Torre-Lezama, A., Vilanova, E., Ramírez-Angulo, H., Higuchi, N., Neill, D. A., Silveira, M., Ferreira, L., Aymard C., G. A., Malhi, Y., Phillips, O. L., and Lloyd, J.: Analysing Amazonian forest productivity using a new individual and trait-based model (TFS v.1), Geosci. Model Dev., 7, 1251–1269, doi: 10.5194/gmd-7-1251-2014, 2014.

Gandiwa, E., Zisadza-Gandiwa, P., Goza, D., Mashapa, C., and Muboko, N.: Diversity and structure of woody vegetation across areas with different soils in Gonarezhou National Park, Zimbabwe, South. Forests, 76, 111–116, doi:10.2989/20702620.2014.921007, 2014.

Gee, G. W. and Bauder, J. W.: Particle-size analysis, in: Methods in Soil Analysis, Part 1, Physical and Mineralogical Methods, edited by: Klute, A., American Society of Agronomy and Soil Science Society of America, Madison, Wisconsin, USA, 383–409, 1986.

Givan, C. V.: Metabolic detoxification of ammonia in tissues of higher plants, Phytochemistry, 18, 375–382, 1979.

Good, S. P. and Caylor, K. K.: Climatological determinants of woody cover in Africa, P. Natl. Acad. Sci. USA, 108, 4902–4907, doi:10.1073/pnas.1013100108, 2011.

Goodland, R. and Pollard, R.: The Brazilian cerrado vegetation: a fertility gradient, J. Ecol., 61, 219–224, 1973.

Grace, J. B. and Bollen, K. A.: Interpreting the results from multiple regression and structural equation models, Bull. Ecol. Soc. Am., 86, 283–295, doi: 10.1890/0012-9623(2005)86[283:itrfmr]2.co;2, 2005.

Grigal, D. F.: A soil-based aspen productivity index for Minnesota, Forest Ecol. Manag., 257, 1465–1473, doi:10.1016/j.foreco.2008.12.022, 2009.

Guo, S., Zhou, Y., Shen, Q., and Zhang, F.: Effect of ammonium and nitrate nutrition on some physiological processes in higher plants – growth, photosynthesis, photorespiration, and water relations, Plant Biol., 9, 21–29, doi:10.1055/s-2006-924541, 2007.

Guswa, A. J.: The influence of climate on root depth: a carbon cost-benefit analysis, Water Resour. Res., 44, W02427, doi:10.1029/2007WR006384, 2008.

Guswa, A. J.: Effect of plant uptake strategy on the water – optimal root depth, Water Resour. Res., 46, 1–5, 2010.

Guy, P. R.: Notes on the vegetation types of the Zambezi Valley, Rhodesia, between the Kariba and Mpata gorges, Kirkia, 10, 543–557, 1977.

Guy, P. R.: Changes in the biomass and productivity of woodlands in the Sengwa Wildlife Research Area, Zimbabwe, J. Appl. Ecol., 18, 507–519, doi:10.2307/2402412, 1981.

Haase, R. and Beck, G.: Structure and composition of savanna vegetation in northern Bolivia: a preliminary report, Brittonia, 41, 80–100, doi:10.2307/2807594, 1989.

Hafsi, C., Debez, A., and Abdelly, C.: Potassium deficiency in plants: effects and signaling cascades, Acta Physiol. Plant, 36, 1055–1070, doi:10.1007/s11738-014-1491-2, 2014.

Halliwell, B.: Chloroplast Metabolism. The Structure and Function of Chloroplasts in Green Leaf Cells, Clarendon Press, Oxford, 1981.

Hanan, N. P., Tredennick, A. T., Prihodko, L., Bucini, G., and Dohn, J.: Analysis of stable states in global savannas: is the CART pulling the horse?, Global Ecol. Biogeogr., 23, 259–263, 2013.

Hänsch, R. and Mendel, R. R.: Physiological functions of mineral micronutrients (Cu, Zn, Mn, Fe, Ni, Mo, B, Cl), Curr. Opin. Plant Biol., 12, 259–266, 2009.

Hart, C.: Relative humidity, EMC, and collapse shrinkage in wood, Forest Prod. J., 32, 45–54, 1984.

Hedley, M. J., Stewart, J. W. B., and Chauhan, B. S.: Changes in inorganic and organic soil phosphorus fractions induced by cultivation practices and by laboratory incubations, Soil Sci. Soc. Am. J., 46, 970–976, 1982.

Hietz, P., Horsky, M., Prohaska, T., Lang, I., and Grabner, M.: High-resolution densitometry and elemental analysis of tropical wood, Trees, 1–11, 2014.

Hijmans, R. J., Cameron, S. E., Parra, J. L., Jones, P. G., and Jarvis, A.: Very high resolution interpolated climate surfaces for global land areas, Int. J. Climatol., 25, 1965–1978, doi:10.1002/joc.1276, 2005.

Hirota, M., Holmgren, M., Van Nes, E. H., and Scheffer, M.: Global resilience of tropical forest and savanna to critical transitions, Science, 334, 232–235, doi:10.1126/science.1210657, 2011.

Hodnett, M. G. and Tomasella, J.: Marked differences between van Genuchten soil water-retention parameters for temperate and tropical soils a new water-retention pedo-transfer functions developed for tropical soils, Geoderma, 108, 155–180, doi:10.1016/S0016-7061(02)00105-2, 2002.

Hoffmann, W. A., Franco, A. C., Moreira, M. Z., and Haridasan, M.: Specific leaf area explains differences in leaf traits between congeneric savanna and forest trees, Funct. Ecol., 19, 932–940, 2005.

Hoffmann, W. A., Geiger, E. L., Gotsch, S. G., Rossatto, D. R., Silva, L. C., Lau, O. L., Haridasan, M., and Franco, A. C.: Ecological thresholds at the savanna-forest boundary: how plant traits, resources and fire govern the distribution of tropical biomes, Ecol. Lett., 15, 759–768, 2012.

Hollander, M. and Wolfe, D. A.: Nonparametric Statistical Methods, J. Wiley & Sons, New York, 1999.

Kenzo, T., Ichie, T., Watanabe, Y., Yoneda, R., Nonomiya, I., and Koike, T.: Changes in photosynthesis and leaf characteristics with tree height in five diperocarp species in a tropical rain forest, Tree Physiol., 26, 865–873, doi:10.1093/treephys/26.7.865, 2006.

Killeen, T. J., Jardim, A., Mamani, F., and Rojas, N.: Diversity, composition and structure of a tropical semideciduous forest in the Chiquitania region of Santa Cruz, Bolivia, J. Trop. Ecol., 14, 803–827, 1998.

Killeen, T. J., Chavez, E., Peña-Claros, M., Toledo, M., Arroyo, L., Caballero, J., Correa, L., Guillén, R., Quevedo, R., and Saldias, M.: The Chiquitano dry forest, the transition between humid and dry forest in eastern lowland Bolivia, in: Neotropical Savannas and Seasonally Dry Forests: Plant Diversity, Biogeography, and Conservation, edited by: Pennington, R. T., Lewis, G. P., and Ratter, J. A., CRC Press, Boca Rato, 213–233, 2006.

Kim, Y., Knox, R. G., Longo, M., Medvigy, D., Hutyra, L. R., Pyle, E. H., Wofsy, S. C., Bras, R. L., and Moorcroft, P. R.: Seasonal carbon dynamics and water fluxes in an Amazon rainforest, Glob. Change Biol., 18, 1322–1334, doi:10.1111/j.1365-2486.2011.02629.x, 2012.

Kronzucker, H., Coskun, D., Schulze, L., Wong, J., and Britto, D.: Sodium as nutrient and toxicant, Plant Soil, 369, 1–23, doi:10.1007/s11104-013-1801-2, 2013.

Kugbe, J., Fosu, M., and Vlek, P. G.: Impact of season, fuel load and vegetation cover on fire mediated nutrient losses across savanna agro-ecosystems: the case of northern Ghana, Nutr. Cycl. Agroecosys., doi:10.1007/s10705-014-9635-8, 2014.

Le Roux, C., Grunow, J., Morris, J., Bredenkamp, G., and Scheepers, J.: Classification of the vegetation of the Etosha National Park, S. Afr. J. Bot., 54, 1–10, 1988.

Lebaudy, A., Vavasseur, A., Hosy, E., Dreyer, D., Leonhardt, N., Thibaud, J. B., Véry, A.-A., Simonneau, T., and Hervé, S.: Plant adaptation to fluctuating environment and biomass production are strongly dependent on guard cell potassium channels, P. Natl. Acad. Sci. USA, 105, 5271–5276, doi:10.1073/pnas.0709732105, 2008.

Lehmann, C. E. R., Archibald, S. A., Hoffmann, W. A., and Bond, W. J.: Deciphering the distribution of the savanna biome, New Phytol., 191, 197–209, doi:10.1111/j.1469-8137.2011.03689.x, 2011.

Lehmann, C. E. R., Anderson, T. M., Sankaran, M., Higgins, S. I., Archibald, S., Hoffmann, W. A., Hanan, N. P., Williams, R. J., Fensham, R. J., Felfili, J.,Hutley, L. B., Ratnam, J., San Jose, J., Montes, R., Franklin, D., Russell-Smith, J., Ryan, C. M., Durigan, G., Hiernaux, P., Haidar, R., Bowman, D. M. J. S., and Bond, W. J.: Savanna vegetation–fire–climate relationships differ among continents, Science, 343, 548–552, 2014.

Leigh, R. A. and Wyn Jones, R. G.: A hypothesis relating critical potassium concentrations for growth to the distribution and function of this ion in the plant cell, New Phytol., 97, 1–13, doi:10.1111/j.1469-8137.1984.tb04103.x, 1984.

Lloyd, J. and Farquhar, G. D.: ^{13}C discrimination during CO_2 assimilation by the terrestrial biosphere, Oecologia, 99, 201–215, doi:10.1007/bf00627732, 1994.

Lloyd, J., Bird, M. I., Vellen, L., Miranda, A. C., Veenendaal, E. M., Djagbletey, G., Miranda, H. S., Cook, G., and Farquhar, G. D.: Contributions of woody and herbaceous vegetation to tropical savanna ecosystem productivity: a quasi-global estimate, Tree Physiol., 28, 451–468, doi:10.1093/treephys/28.3.451, 2008.

Lloyd, J., Goulden, M., Ometto, J. P., Fyllas, N. M., Quesada, C. A., and Patino, S.: Ecophysiology of forest and savanna vegetation, in: Amazonia and Climate Change, edited by: Keller, M., Gash, J., and Silva Dias, P., American Geophysical Union, Washington D.C., 463–484, 2009.

Lloyd, J., Patiño, S., Paiva, R. Q., Nardoto, G. B., Quesada, C. A., Santos, A. J. B., Baker, T. R., Brand, W. A., Hilke, I., Gielmann, H., Raessler, M., Luizão, F. J., Martinelli, L. A., and Mercado, L. M.: Optimisation of photosynthetic carbon gain and within-canopy gradients of associated foliar traits for Amazon forest trees, Biogeosciences, 7, 1833–1859, doi:10.5194/bg-7-1833-2010, 2010.

Lopes, A. and Cox, F.: Cerrado vegetation in Brazil: an edaphic gradient, Agron. J., 69, 828–831, 1977.

Lopez-Gonzalez, G., Lewis, S. L., Burkitt, M., and Phillips, O. L.: ForestPlots. net: a web application and research tool to manage and analyse tropical forest plot data, J. Veg. Sci., 22, 610–613, 2011.

Maathuis, F. J. M.: Physiological functions of mineral macronutrients, Curr. Opin. Plant Biol., 12, 250–258, doi:10.1016/j.pbi.2009.04.003, 2009.

Male, P. S.: Site index studies of established exotic species for the Granite Belt, Research Paper no. 11., Department of Forestry, Queensland, Australia, 1981.

Mantlana, K. B., Arneth, A., Veenendaal, E. M., Wohland, P., Wolski, P., Kolle, O., Wagner, M., and Lloyd, J.: Photosynthetic properties of C$_4$ plants growing in an African savanna/wetland mosaic, J. Exp. Bot., 59, 3941–3952, doi:10.1093/jxb/ern237, 2008.

Mapaure, I.: The distribution of *Colophospermum mopane* (Leguminosae: Caesalpinioideae) in Africa, Kirkia, 15, 1–5, 1994.

Marimon, B. S., Lima, E. de S. , Duarte, T., Chieregatto, L., and Ratter, J. A.: Observations on the vegetation of northeastern Mato Grosso, Brazil. IV. An analysis of the Cerrado-Amazonian Forest ecotone, Edin. J. Bot., 63, 323–341, 2006.

McDowell, N., Bond, B., Dickman, L., Ryan, M., and Whitehead, D.: Relationships between tree height and carbon isotope discrimination, in: Size- and Age-Related Changes in Tree Structure and Function, edited by: Meinzer, F. C., Lachenbruch, B., and Dawson, T. E., Tree Physiology, Springer Netherlands, 255–286, 2011.

McKean, J. W., Terpstra, J. T., and Kloke, J. D.: Computational rank-based statistics, Wiley Interdisciplinary Reviews: Computational Statistics, 1, 132–140, doi:10.1002/wics.29, 2009.

Mengel, K. and Arneke, W.-W.: Effect of potassium on the water potential, the pressure potential, the osmotic potential and cell elongation in leaves of *Phaseolus vulgaris*, Physiol. Plantarum, 54, 402–408, 1982.

Mengel, K., Viro, M., and Hehl, G.: Effect of potassium on uptake and incorporation of ammonium-nitrogen of rice plants, Plant Soil, 44, 547–558, 1976.

Mercado, L. M., Patiño, S., Domingues, T. F., Fyllas, N. M., Weedon, G. P., Sitch, S., Quesada, C. A., Phillips, O. L., Aragão, L. E. O. C., Malhi, Y., Dolman, A. J., Restrepo-Coupe, N., Saleska, S. R., Baker, T. R., Almeida, S., Higuchi, N., and Lloyd, J.: Variations in Amazon forest productivity correlated with foliar nutrients and modelled rates of photosynthetic carbon supply, Philos. T. R. Soc. B, 366, 3316–3329, doi:10.1098/rstb.2011.0045, 2011.

Mews, H., Marimon, B. S., and Ratter, J. A.: Observations on the vegetation of Mato Grosso, Brazil. V. Changes in the woody species diversity of a forest in the Cerrado–Amazonian forest transition zone and notes on the forests of the region, Edin. J. Bot., 69, 239–253, 2012.

Miller, J. M., Williams, R. J., and Farquhar, G. D.: Carbon isotope discrimination by a sequence of Eucalyptus species along a subcontinental rainfall gradient in Australia, Funct. Ecol., 15, 222–232, doi:10.1046/j.1365-2435.2001.00508.x, 2001.

Mills, A. J., Rogers, K. H., Stalmans, M., and Witkowski, E. T. F.: A framework for exploring the determinants of savanna and grassland distribution, Bioscience, 56, 579–589, 2006.

Mills, A. J., Milewski, A. V., Fey, M. V., Gröngröft, A., Petersen, A., and Sirami, C.: Constraint on woody cover in relation to nutrient content of soils in western southern Africa, Oikos, 122, 136–148, doi:10.1111/j.1600-0706.2012.20417.x, 2013.

Miranda, A. C., Miranda, H. S., Lloyd, J., Grace, J., Francey, R. J., McIntyre, J. A., Meir, P., Riggan, P., Lockwood, R., and Brass, J.: Fluxes of carbon, water and energy over Brazilian cerrado: an analysis using eddy covariance and stable isotopes, Plant, Cell Environ., 20, 315-328, doi: 10.1046/j.1365-3040.1997.d01-80.x, 1997.

Mitchard, E. T., Feldpausch, T. R., Brienen, R. J., Lopez-Gonzalez, G., Monteagudo, A., Baker, T. R., Lewis, S. L., Lloyd, J., Quesada, C. A., and Gloor, M.: Markedly divergent estimates of Amazon forest carbon density from ground plots and satellites, Global Ecol. Biogeogr., 23, 945-956, doi:10.1111/geb.12168, 2014.

Mlambo, D.: Influence of soil fertility on the physiognomy of the African savanna tree *Colophospermum mopane*, Afr. J. Ecol., 45, 109–111, doi:10.1111/j.1365-2028.2006.00676.x, 2007.

Moene, A. F. and van Dam, J. C.: Transport in the Atmosphere–Vegetation–Soil Continuum, Cambridge University Press, New York, 436 pp., 2014.

Mokany, K., Raison, R. J., and Prokushkin, A. S.: Critical analysis of root: shoot ratios in terrestrial biomes, Glob. Change Biol., 12, 84–96, doi:10.1111/j.1365-2486.2005.001043.x, 2006.

Morel-Seytoux, H. J., Meyer, P. D., Nachabe, M., Tourna, J., van Genuchten, M. T., and Lenhard, R. J.: Parameter equivalence for the Brooks-Corey and Van Genuchten soil characteristics: preserving the effective capillary drive, Water Resour. Res., 32, 1251–1258, doi: 10.1029/96WR00069, 1996.

Mualem, Y.: A new model for predicting the hydraulic conductivity of unsaturated porous media, Water Resour. Res., 12, 513–522, 1976.

Murdoch, G., Ojo Atere, J., Colborne, G., Olomu, E., and Odugbesan, E.: Soils of the Western State savanna in Nigeria, Vol. 1, The Environment, Land Resource Study (UK), no. 23., 1976.

Murphy, B. P. and Bowman, D. M.: What controls the distribution of tropical forest and savanna?, Ecol. Lett., 15, 748–758, 2012.

Nardoto, G. B., Quesada, C. A., Patiño, S., Saiz, G., Baker, T. R., Schwarz, M., Schrodt, F., Feldpausch, T. R., Domingues, T. F., Marimon, B. S., Marimon Junior, B.-H., Vieira, I. C. G., Silveira, M., Bird, M. I., Phillips, O. L., Lloyd, J., and Martinelli, L. A.: Basin-wide variations in Amazon forest nitrogen-cycling characteristics as inferred from Plant Soil ^{15}N : ^{14}N measurements, Plant Ecol. Divers., 7, 173–187, doi:10.1080/17550874.2013.807524, 2013.

Nelson, D. W. and Sommers, L. E.: Total carbon and total nitrogen, in: Methods of Soil Analysis: Part 3 – Chemical Methods, edited by: Sparks, D. L., SSSA Book Series No 5, American Society of Agronomy/Soil Science Society of America, Madison, WI, 961–1010, 1996.

Norman, J. S. and Barrett, J. E.: Substrate and nutrient limitation of ammonia-oxidizing bacteria and archaea in temperate forest soil, Soil Biol. Biochem., 69, 141–146, doi: 10.1016/j.soilbio.2013.11.003, 2014.

Nyamapfene, K.: A note on some Zimbabwean soil–vegetation relationships of important indicator value in soil survey, Kirkia, 13, 239–242, 1988.

O'Connor, T.: Woody vegetation–environment relations in a semi-arid savanna in the northern Transvaal, S. Afr. J. Bot., 58, 268–274, 1992.

Oliveira-Filho, A. T. and Ratter, J. A.: Vegetation physiognomies and woody flora of the cerrado biome, in: The Cerrados of Brazil. Ecology and Natural History of a Neotropical Savanna, Columbia University Press, 91–120, 2002.

Oliveras, I., Meirelles, S. T., Hirakuri, V. L., Freitas, C. R., Miranda, H. S., and Pivello, V. R.: Effects of fire regimes on herbaceous biomass and nutrient dynamics in the Brazilian savanna, Int. J. Wildland Fire, 22, 368–380, doi:10.1071/WF10136, 2013.

Olsen, S. R. and Sommers, E. L.: Phosphorus soluble in sodium bicarbonate, in: Methods of Soil Analysis, Part 2, Chemical and Microbiological Properties, edited by: Page, A. L., Miller, RH. H., and Keeney, D. R., American Society of Agronomy, Soil Science Society of America, Madison, WIS, 404–430, 1982.

Osakabe, Y., Arinaga, N., Umezawa, T., Katsura, S., Nagamachi, K., Tanaka, H., Ohiraki, H., Yamada, K., Seo, S.-U., Abo, M., Yoshimura, E., Shinozaki, K., and Yamaguchi-Shinozaki, K.: Osmotic stress responses and plant growth controlled by potassium transporters in arabidopsis, The Plant Cell Online, 25, 609–624, doi:10.1105/tpc.112.105700, 2013.

Ostle, N. J., Smith, P., Fisher, R., Ian Woodward, F., Fisher, J. B., Smith, J. U., Galbraith, D., Levy, P., Meir, P., McNamara, N. P., and Bardgett, R. D.: Integrating plant–soil interactions into global carbon cycle models, J. Ecol., 97, 851–863, doi:10.1111/j.1365-2745.2009.01547.x, 2009.

Pavlick, R., Drewry, D. T., Bohn, K., Reu, B., and Kleidon, A.: The Jena Diversity-Dynamic Global Vegetation Model (JeDi-DGVM): a diverse approach to representing terrestrial biogeography and biogeochemistry based on plant functional trade-offs, Biogeosciences, 10, 4137–4177, doi:10.5194/bg-10-4137-2013, 2013.

Pella, E.: Elemental organic analysis, Part 2, State of the art, Am. Lab., 22, 28–32, 1990.

Pennington, R. T., Lewis, G. P., and Ratter, J. A.: An overview of the plant diversity, biogeography and conservation of neotropical savannas and seasonally dry forests, in: Neotropical Savannas and Seasonally Dry Forests: Plant Biodiversity, Biogeography and Conservation, 1–29, 2006.

Pineda-Garcia, F., Paz, H., and Meinzer, F. C.: Drought resistance in early and late secondary successional species from a tropical dry forest: the interplay between xylem resistance to embolism, sapwood water storage and leaf shedding, Plant Cell Environ., 36, 405–418, 2013.

Pleysier, J. L. and Juo, A. S. R.: A single-extraction method using silver-thiourea for measuring exchangeable cations and effective CEC in soils with variable charges, Soil Sci., 129, 205–211, 1980.

Poorter, H. and de Jong, R.: A comparison of specific leaf area, chemical composition and leaf construction costs of field plants from 15 habitats differing in productivity, New Phytol., 143, 163–176, doi:10.1046/j.1469-8137.1999.00428.x, 1999.

Poorter, H., Niinemets, U., Poorter, L., Wright, I. J., and Villar, R.: Causes and consequences of variation in leaf mass per area (LMA): a meta-analysis, New Phytol., 182, 565–588, doi: 10.1111/j.1469-8137.2009.02830.x, 2009.

Prado, D. E. and Gibbs, P. E.: Patterns of species distributions in the dry seasonal forests of South America, Ann. Mo. Bot. Gard., 80, 902–927, 1993.

Priess, J., Then, C., and Fölster, H.: Litter and fine-root production in three types of tropical premontane rain forest in SE Venezuela, Plant Ecol., 143, 171–187, 1999.

Quesada, C. A. and Lloyd, J.: Soil–vegetation interactions in Amazonia, in: The Large-scale Biosphere–Atmosphere Programme in Amazonia, edited by: Nagy, L., Forsberg, B., and Artaxo, P., Ecological Studies, Springer-Verlag, in press, 2014.

Quesada, C. A., Hodnett, M. G., Breyer, L. M., Santos, A. J. B., Andrade, S., Miranda, H. S., Miranda, A. C., and Lloyd, J.: Seasonal variations in soil water in two woodland savannas of central Brazil with different fire histories, Tree Physiol., 28, 405–415, doi:10.1093/treephys/28.3.405, 2008.

Quesada, C. A., Lloyd, J., Schwarz, M., Patiño, S., Baker, T. R., Czimczik, C., Fyllas, N. M., Martinelli, L., Nardoto, G. B., Schmerler, J., Santos, A. J. B., Hodnett, M. G., Herrera, R., Luizão, F. J., Arneth, A., Lloyd, G., Dezzeo, N., Hilke, I., Kuhlmann, I., Raessler, M., Brand, W. A., Geilmann, H., Moraes Filho, J. O., Carvalho, F. P., Araujo Filho, R. N., Chaves, J. E., Cruz Junior, O. F., Pimentel, T. P., and Paiva, R.: Variations in chemical and physical properties of Amazon forest soils in relation to their genesis, Biogeosciences, 7, 1515–1541, doi:10.5194/bg-7-1515-2010, 2010.

Quesada, C. A., Lloyd, J., Anderson, L. O., Fyllas, N. M., Schwarz, M., and Czimczik, C. I.: Soils of Amazonia with particular reference to the RAINFOR sites, Biogeosciences, 8, 1415–1440, doi:10.5194/bg-8-1415-2011, 2011.

Quesada, C. A., Phillips, O. L., Schwarz, M., Czimczik, C. I., Baker, T. R., Patiño, S., Fyllas, N. M., Hodnett, M. G., Herrera, R., Almeida, S., Alvarez Dávila, E., Arneth, A., Arroyo, L., Chao, K. J., Dezzeo, N., Erwin, T., di Fiore, A., Higuchi, N., Honorio Coronado, E., Jimenez, E. M., Killeen, T., Lezama, A. T., Lloyd, G., López-González, G., Luizão, F. J., Malhi, Y., Monteagudo, A., Neill, D. A., Núñez Vargas, P., Paiva, R., Peacock, J., Peñuela, M. C., Peña Cruz, A., Pitman, N., Priante Filho, N., Prieto, A., Ramírez, H., Rudas, A., Salomão, R., Santos, A. J. B., Schmerler, J., Silva, N., Silveira, M., Vásquez, R., Vieira, I., Terborgh, J., and Lloyd, J.: Basin-wide variations in Amazon forest structure and function are mediated by both soils and climate, Biogeosciences, 9, 2203–2246, doi:10.5194/bg-9-2203-2012, 2012.

R: A language and environment for statistical computing, available at: http://www.R-project.org/, 2014.

Ratter, J. A.: Transition between cerrado and forest vegetation in Brazil, in: Nature and Dynamics of Forest–Savanna Boundaries, edited by: Furley, P. A., Proctor, J., and Ratter, J. A., Chapman and Hall, London, 417–430, 1992.

Rawls, W. J., Pachepsky, Y. A., Ritchie, J. C., Sobecki, T. M., and Bloodworth, H.: Effect of soil organic carbon on soil water retention, Geoderma, 116, 61–76, doi:10.1016/S0016-7061(03)00094-6, 2003.

Ringrose, S., Matheson, W., Wolski, P., and Huntsman-Mapila, P.: Vegetation cover trends along the Botswana Kalahari transect, J. Arid Environ., 54, 297–317, doi:10.1006/jare.2002.1092, 2003.

Ritchie, M. W. and Hamann, J. D.: Individual-tree height-, diameter-and crown-width increment equations for young Douglas-fir plantations, New Forest., 35, 173–186, 2008.

Römheld, V. and Kirkby, E. A.: Research on potassium in agriculture: needs and prospects, Plant Soil, 335, 155–180, 2010.

Rossatto, D.: Spatial patterns of species richness and phylogenetic diversity of woody plants in the neotropical savannas of Brazil, Braz. J. Bot, 37, 1–10, doi:10.1007/s40415-014-0070-5, 2014.

Rossatto, D., Hoffmann, W., de Carvalho Ramos Silva, L., Haridasan, M., Sternberg, L. L., and Franco, A.: Seasonal variation in leaf traits between congeneric savanna and forest trees in Central Brazil: implications for forest expansion into savanna, Trees, 27, 1139–1150, doi:10.1007/s00468-013-0864-2, 2013.

Russell, J., Moore, A., and Coaldrake, J.: Relationships between subtropical, semiarid forest of *Acacia harpophylla* (Brigalow), microrelief, and chemical properties of associated gilgai soil, Aust. J. Bot., 15, 481–498, doi:10.1071/BT9670481, 1967.

Saiz, G., Bird, M. I., Domingues, T., Schrodt, F., Schwarz, M., Feldpausch, T. R., Veenendaal, E., Djagbletey, G., Hien, F., Compaore, H., Diallo, A., and Lloyd, J.: Variation in soil carbon stocks and their determinants across a precipitation gradient in West Africa, Glob. Change Biol., 18, 1670–1683, doi:10.1111/j.1365-2486.2012.02657.x, 2012.

Sanchez, P. A.: Properties and Management of Soils in the Tropics, Wiley, New York, 1976.

Sankaran, M., Hanan, N. P., Scholes, R. J., Ratnam, J., Augine, D. J., Cade, B. S., Gignoux, J., Higgins, S. I., Le Roux, X., Ludwig, F., Ardo, J., Banyikwa, F., Bronn, A., Bucini, G., Caylor, K. K., Coughenour, M. B., Diouf, A., Ekaya, W., Feral, C. J., Feb, E. C., Frost, P. G. H., Hiernaux, P., Hrabar, H., Metzger, K. L., Prins, H. H. T., Ringrose, S., Sea, W., Tews, J., Worden, J., and Zambatis, N.: Determinants of woody cover in African savannas, Nature, 438, 846–849, 2005.

Sankaran, M., Ratnam, J., and Hanan, N.: Woody cover in African savannas: the role of resources, fire and herbivory, Global Ecol. Biogeogr., 17, 236–245, 2008.

Santiago, L. S., Wright, S. J., Harms, K. E., Yavitt, J. B., Korine, C., Garcia, M. N., and Turner, B. L.: Tropical tree seedling growth responses to nitrogen, phosphorus and potassium addition, J. Ecol., 100, 309–316, doi:10.1111/j.1365-2745.2011.01904.x, 2012.

Sayer, E. J., Wright, S. J., Tanner, E. V., Yavitt, J. B., Harms, K. E., Powers, J. S., Kaspari, M., Garcia, M. N., and Turner, B. L.: Variable responses of lowland tropical forest nutrient status to fertilization and litter manipulation, Ecosystems, 15, 387–400, 2012.

Scheiter, S. and Higgins, S. I.: Impacts of climate change on the vegetation of Africa: an adaptive dynamic vegetation modelling approach, Glob. Change Biol., 15, 2224–2246, doi:10.1111/j.1365-2486.2008.01838.x, 2009.

Schenk, H. J.: The shallowest possible water extraction profile: a null model for global root distributions, Vadose Zone J., 7, 1119–1124, doi:10.2136/vzj2007.0119, 2008.

Schenk, H. J. and Jackson, R. B.: Rooting depths, lateral root spreads and below-ground/above-ground allometries of plants in water-limited ecosystems, J. Ecol., 90, 480–494, 2002.

Schmidt, S. and Stewart, G. R.: Transport, storage and mobilization of nitrogen by trees and shrubs in the wet/dry tropics of northern Australia, Tree Physiol., 18, 403–410, doi:10.1093/treephys/18.6.403, 1998.

Schmimper, A. F. W.: Plant-geography upon a Physiological Basis, Clarendon Press, Oxford, 839 pp., 1903.

Scholtz, R., Kiker, G. A., Smit, I. P. J., and Venter, F. J.: Identifying drivers that influence the spatial distribution of woody vegetation in Kruger National Park, South Africa, Ecosphere, 5, art71, doi:10.1890/ES14-00034.1, 2014.

Schrodt, F., Domingues, T. F., Feldpausch, T., Saiz, G., Quesada, C. A., Schwarz, M., Ishida, F. Y., Compaore, H., Diallo, A., Djagbletey, G., Hien, F., Hiernaux, P., Mougin, E., Sonké, B., Zapfack, L., Bird, M. I., Lewis, S. L., Meir, P., Phillips, O. L., Grace, J., Veenendaal, E., and Lloyd, J.: Foliar trait contrasts between African forest and savanna trees: genetic versus environmental effects, Funct. Plant Biol., 42, 63–83, doi:10.1071/FP14040, 2014.

Schulze, E.-D., Williams, R. J., Farquhar, G. D., Schulze, W., Langridge, J., Miller, J. M., and Walker, B. H.: Carbon and nitrogen isotope discrimination and nitrogen nutrition of trees along a rainfall gradient in northern Australia, Funct. Plant Biol., 25, 413–425, doi:10.1071/PP97113, 1998.

Shabala, S. and Pottosin, I.: Regulation of potassium transport in plants under hostile conditions: implications for abiotic and biotic stress tolerance, Physiol. Plantarum, 151, 257–279, doi:10.1111/ppl.12165, 2014.

Shukla, M. K.: Soil Physics: an Introduction, CRC Press, 2013.

Silva, J., Fariñas, M., Felfili, J., and Klink, C.: Spatial heterogeneity, land use and conservation in the cerrado region of Brazil, J. Biogeogr., 33, 536–548, 2006.

Silva, L. C., Hoffmann, W. A., Rossatto, D. R., Haridasan, M., Franco, A. C., and Horwath, W. R.: Can savannas become forests? A coupled analysis of nutrient stocks and fire thresholds in central Brazil, Plant Soil, 373, 1–14, 2013.

Skarpe, C.: Plant community structure in relation to grazing and environmental changes along a north–south transect in the western Kalahari, Vegetatio, 68, 3–18, doi:10.1007/BF00031575, 1986.

Smith, J.: Distribution of tree species in the Sudan in relation to rainfall and soil texture, Agricultural Publications Committee, Khartoum, 1951.

Spicer, R.: Symplasmic networks in secondary vascular tissues: parenchyma distribution and activity supporting long-distance transport, J. Exp. Bot., 65, 1829–1848, doi:10.1093/jxb/ert459, 2014.

Stamp, N.: Out of the quagmire of plant defense hypotheses, Q. Rev. Biol., 78, 23–55, 2003.

Staver, A. C., Archibald, S., and Levin, S. A.: The global extent and determinants of savanna and forest as alternative biome states, Science, 334, 230–232, doi:10.1126/science.1210465, 2011.

Steininger, M. K., Tabor, K., Small, J., Pinto, C., Soliz, J., and Chavez, E.: A satellite model of forest flammability, Environ. Manage., 52, 136–150, 2013.

Stewart, G. R., Hegarty, E. E., and Specht, R. L.: Inorganic nitrogen assimilation in plants of Austrlian rainforest communities, Physiol. Plantarum, 74, 26–33, doi:10.1111/j.1399-3054.1988.tb04936.x, 1988.

Thomas, M. F.: Tropical Geomorphology: a Study of Weathering and Landform Development in Warm Climates, Focal Problems in Geography Series, The McMillan Press, London, 331 pp., 1974.

Thompson, J., Viana, J., Proctor, J., and Ratter, J. A.: Contrasting forest-savanna boundaries on Maraca Island, Roraima, Brazil, in: Nature and Dynamics of Forest-Savanna Boundaries, edited by: Furley, P., Proctor, J., and Ratter, J. A., Chapman and Hall, London, 367–391, 1992.

Tomasella, J. and Hodnett, M. G.: Estimating unsaturated hydraulic conductivity of Brazilian soils using soil–water retention data, Soil Sci., 162, 703–712, 1997.

Torello-Raventos, M., Feldpausch, T. R., Veenendaal, E., Schrodt, F., Saiz, G., Domingues, T. F., Djagbletey, G., Ford, A., Kemp, J., Marimon, B. S., Marimon, B. H., Lenza, E., Ratter, J. A., Maracahipes, L., Sasaki, D., Sonke, B., Zapfack, L., Taedoumg, H., Villarroel, D., Schwarz, M., Quesada, C. A., Ishida, F. Y., Nardoto, G. B., Affum-Baffoe, K., Arroyo, L., Bowman, D. M. J. S., Compaore, H., Davies, K., Diallo, A., Fyllas, N. M., Gilpin, M., Hien, F., Johnson, M., Killeen, T. J., Metcalfe, D., Miranda, H. S., Steininger, M., Thomson, J., Sykora, K., Mougin, E., Hiernaux, P., Bird, M. I., Grace, J., Lewis, S. L., Phillips, O. L., and Lloyd, J.: On the delineation of tropical vegetation types with an emphasis on forest/savanna transitions, Plant Ecol. Divers., 6, 101–137, doi:10.1080/17550874.2012.762812, 2013.

Tripler, C. E., Kaushal, S. S., Likens, G. E., and Todd Walter, M.: Patterns in potassium dynamics in forest ecosystems, Ecol. Lett., 9, 451–466, 2006.

Tsay, Y.-F., Ho, C.-H., Chen, H.-Y., and Lin, S.-H.: Integration of nitrogen and potassium signaling, Annu. Rev. Plant Biol., 62, 207–226, 2011.

Turner, J., Thompson, C., Turvey, N., Hopmans, P., and Ryan, P.: A soil technical classification system for *Pinus radiata* (D. Don) plantations. I. Development, Aust. J. Soil Res., 28, 797–811, doi: 10.1071/SR9900797, 1990.

Umar, S.: Alleviating adverse effects of water stress on yield of sorghum, mustard and groundnut by potassium application, Pak. J. Bot., 38, 1373–1380, 2006.

Van Reeuwijk, L. P.: Procedures for Soil Analysis, 6th edn., International Soil Reference Information Centre, ISRIC, Wageningen, the Netherlands, 120 pp., 2002.

Veenendaal, E. M., Torello-Raventos, M., Feldpausch, T. R., Domingues, T. F., Gerard, F., Schrodt, F., Saiz, G., Quesada, C. A., Djagbletey, G., Ford, A., Kemp, J., Marimon, B. S., Marimon-Junior, B. H., Lenza, E., Ratter, J. A., Maracahipes, L., Sasaki, D., Sonké, B., Zapfack, L., Villarroel, D., Schwarz, M., Yoko Ishida, F., Gilpin, M., Nardoto, G. B., Affum-Baffoe, K., Arroyo, L., Bloomfield, K., Ceca, G., Compaore, H., Davies, K., Diallo, A., Fyllas, N. M., Gignoux, J., Hien, F., Johnson, M., Mougin, E., Hiernaux, P., Killeen, T., Metcalfe, D., Miranda, H. S., Steininger, M., Sykora, K., Bird, M. I., Grace, J., Lewis, S., Phillips, O. L., and Lloyd, J.: Structural, physiognomic and aboveground biomass variation in savanna-forest transition zones on three continents. How different are co-occurring savanna and forest formations?, Biogeosciences, 12, 2927–2951, doi:10.5194/bg-12-2927-2015, 2015.

Viani, R. A. G., Rodrigues, R. R., Dawson, T. E., and Oliveira, R. S.: Savanna soil fertility limits growth but not survival of tropical forest tree seedlings, Plant Soil, 349, 341–353, doi:10.1007/s11104-011-0879-7, 2011.

Viani, R. A. G., Rodrigues, R. R., Dawson, T. E., Lambers, H., and Oliveira, R. S.: Soil pH accounts for differences in species distribution and leaf nutrient concentrations of Brazilian woodland savannah and seasonally dry forest species, Perspect. Plant Ecol., 16, 64–74, doi:10.1016/j.ppees.2014.02.001, 2014.

Villarroel, D., Catari, J. C., Calderon, D., Mendez, R., and Feldpausch, T.: Estructura, composición y diversidad arbórea de dos áreas de Cerrado sensu stricto de la Chiquitanía (Santa Cruz, Bolivia), Ecología en Bolivia, 45, 116–130, 2010.

Vitousek, P. M. and Sanford, R. L.: Nutrient cycling in moist tropical forest, Annu. Rev. Ecol. Syst., 17, 137–167, doi:10.1146/annurev.es.17.110186.001033, 1986.

Wakeel, A., Farooq, M., Qadir, M., and Schubert, S.: Potassium substitution by sodium in plants, Crit. Rev. Plant Sci., 30, 401–413, doi:10.1080/07352689.2011.587728, 2011.

Wang, M., Zheng, Q., Shen, Q., and Guo, S.: The critical role of potassium in plant stress response, Int. J. Mol. Sci., 14, 7370–7390, 2013.

Warman, L. and Moles, A. T.: Alternative stable states in Australia's Wet Tropics: a theoretical framework for the field data and a field-case for the theory, Landscape Ecol., 24, 1–13, 2009.

Weiskittel, A. R., Hann, D. W., Kershaw Jr, J. A., and Vanclay, J. K.: Forest Growth and Yield Modeling, John Wiley & Sons, 2011.

Werger, M. J. A.: Vegetation Structure in the Southern Kalahari, J. Ecol., 66, 933–941, doi:10.2307/2259305, 1978.

Wesseling, J., van Wijk, W. R., Fireman, M., van't Woudt, B. D., and Hagan, R. M.: Land drainage in relation to soils and crops, in: Drainage of Agricultural Lands, edited by: Luthin, J. N., Agronomy Monograph, American Society of Agronomy, 461–578, 1957.

White, D. A. and Hood, C. S.: Vegetation patterns and environmental gradients in tropical dry forests of the northern Yucatan Peninsula, J. Veg. Sci., 15, 151–160, doi: 10.1111/j.1654-1103.2004.tb02250.x, 2004.

Williams, R., Duff, G., Bowman, D., and Cook, G.: Variation in the composition and structure of tropical savannas as a function of rainfall and soil texture along a large-scale climatic gradient in the Northern Territory, Australia, J. Biogeogr., 23, 747–756, 1996.

Witkowski, E. T. F. and O'Connor, T. G.: Topo-edaphic, floristic and physiognomic gradients of woody plants in a semi-arid African savanna woodland, Vegetatio, 124, 9–23, doi:10.1007/BF00045140, 1996.

Wood, S. N.: Generalized Additive Models: an Introduction with R, Chapman & Hall/CRC, Bota Racon, 2006.

Wood, S. N.: Fast stable restricted maximum likelihood and marginal likelihood estimation of semiparametric generalized linear models, J. Roy. Stat. Soc. B, 73, 3–36, 2011.

Wright, S. J., Yavitt, J. B., Wurzburger, N., Turner, B. L., Tanner, E. V. J., Sayer, E. J., Santiago, L. S., Kaspari, M., Hedin, L. O., Harms, K. E., Garcia, M. N., and Corre, M. D.: Potassium, phosphorus, or nitrogen limit root allocation, tree growth, or litter production in a lowland tropical forest, Ecology, 92, 1616–1625, doi:10.1890/10-1558.1, 2011.

Xu, G., Fan, X., and Miller, A. J.: Plant nitrogen assimilation and use efficiency, Annu. Rev. Plant Biol., 63, 153–182, 2012.

Yao, H., Gao, Y., Nicol, G. W., Campbell, C. D., Prosser, J. I., Zhang, L., Han, W., and Singh, B. K.: Links between ammonia oxidizer community structure, abundance, and nitrification potential in acidic soils, Appl. Environ. Microb., 77, 4618–4625, doi:10.1128/aem.0136-11, 2011.

Young, A.: Tropical Soils and Soil Survey, CUP Archive, 1980.

Zerihun, A., Montagu, K., Hoffmann, M., and Bray, S.: Patterns of below- and aboveground biomass in *Eucalyptus populnea* woodland communities of Northeast Australia along a rainfall gradient, Ecosystems, 9, 501–515, doi: 10.1007/s10021-005-0155-x, 2006.

Zörb, C., Senbayram, M., and Peiter, E.: Potassium in agriculture – status and perspectives, J. Plant Physiol., 171, 656–669, 2014.

Zuur, A., Ieno, E. N., Walker, N., Saveliev, A. A., and Smith, G. M.: Mixed Effects Models and Extensions in Ecology with R, Springer, 2009.

Table 1. Kendall's bivariate correlation coefficients for stand level photosynthetic capacity $\langle A_{\mathrm{max}}\rangle$, photosynthetic nitrogen use use efficiency $\langle A_{\mathrm{N}}\rangle$, photosynthetic phosphorus use efficiency $\langle A_{\mathrm{P}}\rangle$ and their association with a range of canopy, soil and climatic factors viz.; community-weighted-means of area-based leaf nitrogen $\langle \mathrm{N_a}\rangle$ and phosphorus $\langle \mathrm{P_a}\rangle$ concentrations; leaf carbon stable isotopic composition $\langle \delta^{13}\mathrm{C}\rangle$; total woody canopy area index C_{W}; upper 0.95 quantile upper-canopy height $\langle H_{\mathrm{U}}\rangle$; community-weighted-mean upper-canopy height H^{*}; area based measures of soil nutrient availability for calcium, potassium and magnesium viz. $[\mathrm{Ca}]_{\mathrm{sa}}$, $[\mathrm{K}]_{\mathrm{sa}}$ and $[\mathrm{Mg}]_{\mathrm{sa}}$; soil carbon/nitrogen ratio (CN), and mean annual precipitation (P_{A}). Values significant at $p < 0.05$ are shown in bold.

$\langle A_{\mathrm{max}}\rangle$															
0.65	$\langle A_{\mathrm{N}}\rangle$														
0.43	**0.54**	$\langle A_{\mathrm{P}}\rangle$													
0.17	−0.18	−0.12	$\langle N_{\mathrm{a}}\rangle$												
−0.12	−0.26	**−0.7**	0.22	$\langle \mathrm{P_a}\rangle$											
−0.09	**−0.27**	**−0.29**	0.25	**0.31**	$\langle \delta^{13}\mathrm{C}\rangle$										
−0.07	−0.02	0.11	0.08	−0.2	0.01	C_{W}									
0.01	0.08	0.20	0.16	−0.25	0.02	**0.74**	$\langle H_{\mathrm{U}}\rangle$								
−0.01	0.06	0.22	0.16	−0.26	0.02	**0.73**	**0.86**	H^{*}							
−0.13	−0.3	−0.15	0.20	0.05	**0.53**	0.13	0.13	0.18	$[\mathrm{Ca}]_{\mathrm{sa}}$						
−0.37	**−0.42**	−0.15	0.20	0.01	**0.32**	**0.42**	**0.37**	**0.42**	**0.53**	$[\mathrm{K}]_{\mathrm{sa}}$					
−0.15	**−0.29**	−0.09	0.19	−0.03	**0.38**	0.12	0.10	0.16	**0.85**	**0.54**	$[\mathrm{Mg}]_{\mathrm{sa}}$				
−0.05	−0.12	0.03	0.12	−0.1	**0.31**	0.14	0.08	0.17	**0.50**	**0.52**	**0.53**	$[\mathrm{P}]_{\mathrm{sa}}$			
0.15	0.22	−0.07	−0.07	**0.28**	−0.2	−0.05	−0.16	−0.15	**−0.53**	**−0.41**	**−0.56**	**−0.38**	$\mathrm{CN_s}$		
0.2	**0.35**	0.05	−0.13	0.16	−0.25	0.06	0.03	−0.01	**−0.46**	**−0.37**	**−0.59**	**−0.43**	**−0.85**	P_{A}	

Table 2. Multivariate regression statistics relating estimates of community-weighted canopy-level average maximum CO_2 assimilation rates, nitrogen use efficiency, phosphorus use efficiency and foliar $^{13}C/^{12}C$ to canopy and soil variables. Abbreviations: $[K]_{sa}$ – soil potassium ($mmol\,m^{-2}$); $[P]_{sa}$ ($\mu mol\,m^{-2}$); $\langle N_a \rangle$ – species-abundance-weighted area-based leaf nitrogen ($g\,m^{-2}$), $\langle H_U \rangle$ – average canopy height (trees > 0.1 m diameter at beast height, in m); CN_s – soil CN ratio ($g\,g^{-1}$), VIF – variance inflation factor. In all cases predictor variates have been centred with the unstandardised intercept giving then the predicted value when all predictor variables are at their mean values. In the standardized case, all variables have been centred and scaled by their SD.

	Coefficients								
	Unstandardised coefficients		Standardized			0.95 confidence interval for *b*		Collinearity statistics	
	b	s.e.	*β*	*t*	*p*	Lower	Upper	Tolerance	VIF
a. Light/CO_2 saturated assimilation rate ($\mu mol\,CO_2\,m^{-2}\,s^{-1}$): $r^2 = 0.71$, $p = 0.0004$									
Intercept	28.73	0.74	–	38.74	0.000	27.07	30.53	–	–
$\log_e[K]_{sa}$	−6.98	1.19	−1.212	−5.86	0.000	−11.04	−4.75	0.387	2.59
$\log_e[P]_{sa}$	3.80	0.83	0.630	3.67	0.003	0.75	6.00	0.575	1.73
$\log_e\langle N_a \rangle$	3.62	1.98	0.660	4.58	0.001	0.87	5.21	0.875	1.14
$\log_e\langle H_U \rangle$	2.44	0.98	0.425	2.50	0.027	1.39	5.45	0.604	1.65
b. Photosynthetic nitrogen use efficiency: ($\mu mol\,CO_2\,g^{-1}\,N\,s^{-1}$) $r^2 = 0.68$, $p = 0.0003$									
Intercept	12.81	0.33	–	38.72	0.000	11.86	13.28	–	–
$\log_e[K]_{sa}$	−3.16	0.52	−1.393	−6.12	0.000	−4.88	−2.41	0.411	2.43
$\log_e[P]_{sa}$	1.59	0.44	0.630	3.67	0.003	0.574	2.72	0.585	1.71
$\log_e\langle H_U \rangle$	1.04	0.44	0.463	2.40	0.031	0.326	2.10	0.607	1.65
c. Photosynthetic phosphorus use efficiency ($\mu mol\,CO_2\,mg^{-1}\,P\,s^{-1}$): $r^2 = 0.30$, $p = 0.0469$									
Intercept	312.4	23.90	–	13.07	0.000	258.3	354.1	–	–
$\log_e\,[K]_{sa}$	−91.59	33.61	−0.857	−2.73	0.016	−173.0	−31.8	0.507	1.97
$\log_e\,(CN_s)$	−58.78	27.53	−0.542	−2.13	0.051	−126.1	−3.48	0.754	1.33
$\log_e\langle H_U \rangle$	71.34	31.50	0.586	2.27	0.040	11.6	129.3	0.610	1.64
d. Foliar $^{13}C/^{12}C$ (‰): $r^2 = 0.26$, $p = 0.040$									
Intercept	−29.37	0.170	–	−180	0.000	−29.61	−28.93	–	–
$\log_e\,[K]_{sa}$	0.592	0.219	0.787	3.63	0.016	0.301	1.143	0.609	1.64
$\log_e\langle H_U \rangle$	−0.526	0.225	−0.604	−2.88	0.034	−0.974	−0.133	0.609	1.64

Table 3. Multivariate regression statistics relating canopy area index (C_W), mean upper stratum canopy height $\langle H_U \rangle$, and above ground biomass (B_U) to soil and climatic variables. From (a) to (d) occur increasingly complex models for the prediction of C_W; (e) represents an application of model (d) to $\langle H_U \rangle$ and (f) is model (d) but applied to B_U. Other abbreviations: $[K]_{sa}$ – soil potassium ($mmol\,m^{-2}$), P_A mean annual precipitation (m); VIF – variance inflation factor. In all cases predictor variates have been centred with the unstandardised intercept giving then the predicted value when all predictor variables are at their mean values. In the standardized case, all variables have been centred and scaled by their SD.

	Coefficients								
	Unstandardised coefficients		Standardized			0.95 confidence interval for *b*		Collinearity statistics	
	b	s.e.	*β*	*t*	*p*	Lower	Upper	Tolerance	VIF
a. $\log_e$ [Crown area index] (Model 1): $r^2 = 0.31$, $p = 0.010$, AIC = 42.43									
Intercept	1.42	0.457	–	3.12	0.007	0.456	2.40	–	–
$\log_e[K]_{sa}$	0.748	0.258	0.573	2.91	0.010	0.204	1.30	–	–
b. $\log_e$ [Crown area index] (Model 2): $r^2 = 0.57$, $p = 0.000$, AIC = 34.70									
Intercept	−0.55	0.701	–	1.70	0.794	−2.04	0.945	–	–
$\log_e[K]_{sa}$	1.14	0.236	0.874	5.15	0.000	0.640	1.645	0.740	1.35
P_A	1.78	0.542	0.633	3.47	0.001	0.623	2.93	0.740	1.35
c. $\log_e$ [Crown area index] (Model 3): $r^2 = 0.58$, $p = 0.001$, AIC = 35.19									
Intercept	−0.926	0.774	–	−1.17	0.111	−2.58	0.733	–	–
$\log_e[K]_{sa}$	1.121	0.235	1.022	4.77	0.000	0.618	1.624	0.735	1.36
P_A	1.775	0.539	0.686	3.30	0.005	0.620	2.930	0.740	1.35
θ_P	0.827	0.743	0.140	1.13	0.285	−0.767	2.421	0.991	1.00
d. $\log_e$ [Crown area index] (Model 4): $r^2 = 0.72$, $p = 0.000$ AIC = 28.27									
Intercept	1.821	1.140	–	0.67	0.498	−0.643	4.289	–	–
$\log_e[K]_{sa}$	0.949	0.199	0.726	4.76	0.000	0.518	1.380	0.670	1.49
P_A	−0.372	0.863	0.931	4.99	0.886	−2.234	1.492	0.189	5.27
θ_P	−9.274	−2.610	0.281	2.16	0.050	−16.95	−1/598	0.028	35.10
$\theta_P \times P_A$	7.090	2.458	0.445	2.89	0.012	1.780	12.400	0.026	37.85
e. $\log_e$ [Crown area index] (Model 5): $r^2 = 0.74$, $p = 0.000$ AIC = 26.52									
Intercept	1.362	0.395	–	2.05	0.030	0.515	2.21	–	–
$\log_e[K]_{sa}$	0.992	0.167	0.643	5.94	0.000	0.634	1.35	0.896	1.11
θ_P	−7.975	1.819	−1.404	−4.39	0.001	−11.88	−4.07	0.102	9.77
$\theta_P \times P_A$	6.177	0.326	1.673	5.12	0.000	3.59	8.77	0.103	9.68
f. $\log_e$ [Mean canopy height]: $r^2 = 0.41$, $p = 0.016$									
Intercept	2.926	0.329	–	8.90	0.000	2.221	3.631	–	–
$\log_e[K]_{sa}$	0.503	0.139	0.766	3.62	0.003	0.205	0.802	0.897	1.12
θ_P	−2.113	1.514	1.286	−1.39	0.184	−5.361	1.134	0.102	9.77
$\theta_P \times P_A$	1.702	1.004	−1.102	1.70	0.112	−0.451	3.857	0.103	9.69
g. $\log_e$ [Woody biomass]: $r^2 = 0.47$, $p = 0.007$									
Intercept	5.614	0.725	–	7.75	0.000	4.06	7.168	–	–
$\log_e[K]_{sa}$	1.238	0.307	0.637	4.03	0.001	0.581	1.896	0.897	1.11
θ_P	−3.228	3.339	−0.528	−0.96	0.350	−10.38	3.933	0.102	9.77
$\theta_P \times P_A$	3.004	2.214	0.695	1.35	0.197	−1.745	7.753	0.103	9.68

Table A1. Effect of presence of restricted soil layer on simulated total duration of low aeration ($\phi > 0.1\,\mathrm{m^3\,m^{-3}}$) or low soil moisture status ($\theta < \theta_\mathrm{C}$) for the four precipitation scenarios shown in Fig. A1. In all cases the evapotranspiration rate refers to that estimated for a soil with a restricted layer at 0.3 m depth and with the number of days calculated and compared (with in brackets) that predicted to be the case in simulations giving the same annual evapotranspiration rate but with no restricted layer present: KEN-01* = all rainfall events at KEN-01 multiplied by 0.7. (see text)

Weather Station Site	Precipitation ($\mathrm{m\,a^{-1}}$)	Evapotranspiration ($\mathrm{m\,a^{-1}}$)	Days ($\phi > 0.1\,\mathrm{m^3\,m^{-3}}$)	Days ($\theta < \theta_\mathrm{C}$)
TUC-01	0.54	0.52	0(0)	342(350)
KEN-01*	1.01	0.71	28(0)	284(303)
KEN-01	1.51	0.87	94(0)	248(285)
TAP-04	2.15	1.51	62(0)	168(215)

Table A2. List of symbols and abbreviations (with typical units as appropriate).

$\hat{C}_\mathrm{W}$	model predicted crown area index ($\mathrm{m^2\,m^{-2}}$)
$\langle H_\mathrm{U} \rangle$	mean canopy height ($d > 0.1$ m)
ρ_b	soil bulk density ($\mathrm{kg\,dm^{-3}}$)
$\langle \Theta \rangle$	average value of canopy trait within plot (weighted according to species abundance)
$[\mathrm{Ca}]_\mathrm{ex}$	soil exchangeable calcium on a mass basis ($\mathrm{mmol\,eq^+\,kg^{-1}}$)
$[\mathrm{Ca}]_\mathrm{s,\,a}$	soil exchangeable calcium on a ground area basis ($\mathrm{mol\,m^{-2}}$)
$[\mathrm{K}]_\mathrm{ex}$	soil exchangeable potassium on a mass basis ($\mathrm{mmol\,eq^+\,kg^{-1}}$)
$[\mathrm{K}]_\mathrm{s,\,a}$	soil exchangeable potassium on a ground area basis ($\mathrm{mol\,m^{-2}}$)
$[\mathrm{Mg}]_\mathrm{ex}$	soil exchangeable magnesium on a mass basis ($\mathrm{mmol\,eq^+\,kg^{-1}}$)
$[\mathrm{Mg}]_\mathrm{s,\,a}$	soil exchangeable magnesium on a ground area basis ($\mathrm{mol\,m^{-2}}$)
$[\mathrm{Na}]_\mathrm{ex}$	soil exchangeable sodium on a mass basis ($\mathrm{mmol\,eq^+\,kg^{-1}}$)
$[\mathrm{P}]_\mathrm{extr}$	soil extractable phosphorus ($\mathrm{mg\,kg^{-1}}$)
$[\mathrm{P}]_\mathrm{s,\,a}$	soil extractable phosphorus on a ground area basis ($\mathrm{mol\,m^{-2}}$)
a	annum
AIC	Akaike's information criterion
A_max	leaf-level maximum $\mathrm{CO_2}$ assimilation rate ($\mathrm{\mu mol\,m^{-2}\,s^{-1}}$)
ASS	alternative stable state
B_U	above-ground biomass ($\mathrm{t\,ha^{-1}}$)
C_A	projected canopy area ($\mathrm{m^2}$)
$\mathrm{Ca_C}$	canopy calcium on a ground area basis ($\mathrm{mol\,m^{-2}}$)
$\mathrm{Ca_m}$	leaf calcium on a mass basis ($\mathrm{mg\,g^{-1}}$)
$\mathrm{C_m}$	leaf carbon on a mass basis ($\mathrm{mg\,g^{-1}}$)
$\mathrm{CN_s}$	soil carbon to nitrogen ratio ($\mathrm{g\,g^{-1}}$)
C_W	crown area index ($\mathrm{m^2\,m^{-2}}$)
D	diameter at breast height (m)
H	tree height (m)
H^*	upper 0.95 quantile canopy height ($d > 0.1$ m)
$\mathrm{K_C}$	canopy potassium on a ground area basis ($\mathrm{mol\,m^{-2}}$)
$\mathrm{K_m}$	leaf potassium on a mass basis ($\mathrm{mg\,g^{-1}}$)
L	leaf area index ($\mathrm{m^2\,m^{-2}}$)
m	Meter
M_a	leaf mass per unit area ($\mathrm{g\,m^{-2}}$)
$\mathrm{Mg_C}$	canopy magnesium, on a ground area basis ($\mathrm{mol\,m^{-2}}$)
$\mathrm{Mg_m}$	leaf magnesium on a mass basis ($\mathrm{mg\,g^{-1}}$)
$\mathrm{N_a}$	leaf nitrogen on an area basis ($\mathrm{mg\,g^{-1}}$)
$\mathrm{N_m}$	leaf nitrogen on a mass basis ($\mathrm{mg\,g^{-1}}$)
$\mathrm{N_m}$	leaf nitrogen on a mass basis ($\mathrm{mg\,g^{-1}}$)
OLS	ordinary least squares
P_A	mean annual precipitation ($\mathrm{m\,a^{-1}}$)
$\mathrm{P_a}$	leaf phosphorus on an area basis ($\mathrm{mg\,g^{-1}}$)
$\mathrm{P_C}$	canopy phosphorus on a ground area basis ($\mathrm{mol\,m^{-2}}$)
$\mathrm{P_m}$	leaf phosphorus on a mass basis ($\mathrm{mg\,g^{-1}}$)
SD	standard deviation
s_1, s_1,	fitted smoothing parameter
VIF	variance inflation factor
α	fitted parameter
$\delta^{13}\mathrm{C}$	leaf $^{13}\mathrm{C}/^{12}\mathrm{C}$ ratio relative to PDB (‰)
Θ	plant trait (general symbol)
θ_P	plant available soil water (m)
μ	dataset mean value
Σ_B	sum of exchangeable bases in soil ($\mathrm{mmol\,eq^+\,kg^{-1}}$)
K	leaf construction costs ($\mathrm{mg\,glucose\,g^{-1}}$)
$\mathbb{F}$	forest vegetation formation type
$\mathbb{S}$	savanna vegetation formation type
$\mathbb{V}$	vegetation formation type
$\mathbb{A}$	vegetation formation type affiliation of a species (forest or savanna)

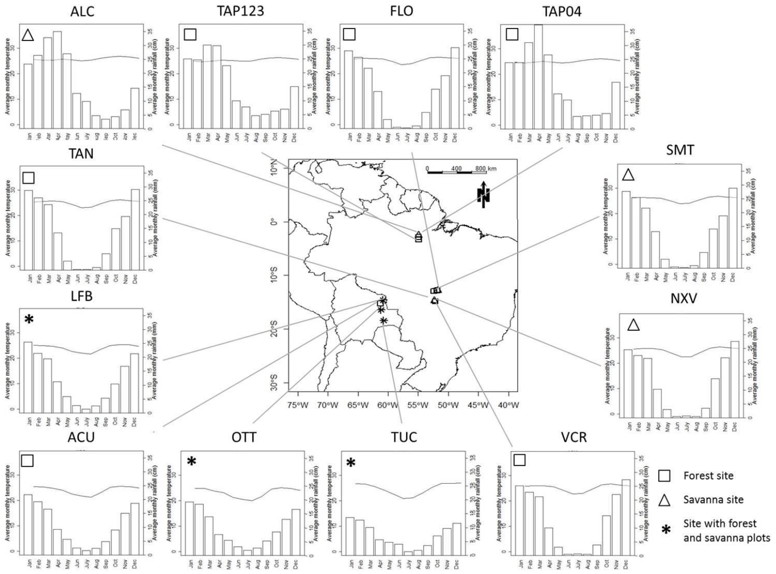

Figure 1. Map showing sampling sites and their temperature (°C) and precipitation climatologies.

Figure 2. Examples of forest (top row) and savanna (bottom row) vegetation formation types found along the precipitation gradient. **(a)** TUC-01 forest, **(b)** TUC-03 savanna (both towards the drier end of the transect); **(c)** FLO-01 forest, **(d)** SMT-02 savanna (both in the middle of the Transect); **(e)** TAP-123 forest **(f)** ALC-02 savanna (both at the moister end of the transect). Specific details of site locations, climatology and soils are given in Fig. 1 and Table S1 of the Supplement.

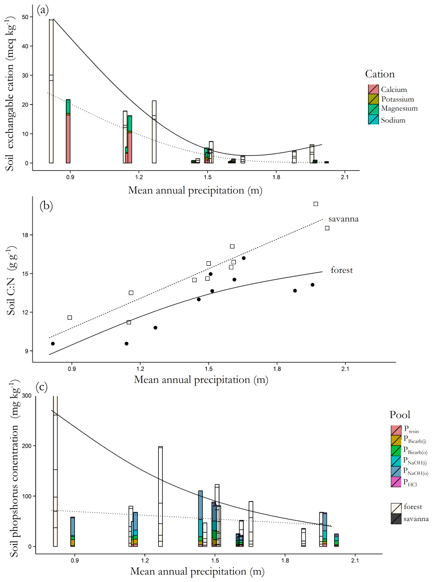

Figure 3. Variations in key soil chemcial properties (0.0–0.3 m depth) in relation to precipitation and vegetation formation type **(a)** soil exchangable cations; **(b)** soil C/N ratio; **(c)** soil phosphorus pools. For **(a)** and **(b)** forest plots are shaded more lightly than savanna with the fitted curves (solid for forest plots, dashed for savanna) representing generalised additive model fits representing for **(a)** total exchangable cations (sum of bases) and for **(c)** total extractable phosphorus. In **(c)** the phosphorus pools are as per the Hedley fractionation procedure (see Sect. 2.3.3): $[\mathrm{P}]_{\mathrm{resin}}$ – resin extractable P; $[\mathrm{P}]_{\mathrm{Bicarb(i)}}$ – bicarbonate extractable inorganic phosphorus; $[\mathrm{P}]_{\mathrm{Bicarb(o)}}$ bicarbonate extractable organic phosphorus; $[\mathrm{P}]_{\mathrm{NaOH(i)}}$ – NaOH extractable inorganic phosphorus; $[\mathrm{P}]_{\mathrm{NaOH(o)}}$ bicarbonate extractable organic phosphorus; $[\mathrm{P}]_{\mathrm{HCl}}$ – HCl extractable phosphorus.

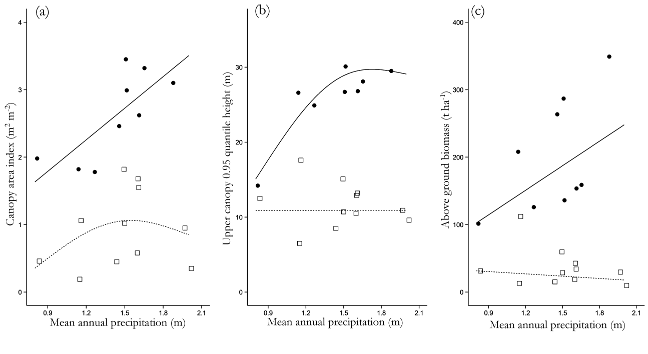

Figure 4. Variations in canopy structural properties in relation to precipitation and vegetation formation type **(a)** canopy area index; **(b)** upper 0.95 quantile height; **(c)** above ground biomass. (•) Forest plots; (□) savanna plots. Fitted curves (solid for forest plots, dashed for savanna) represent generalised additive model fits.

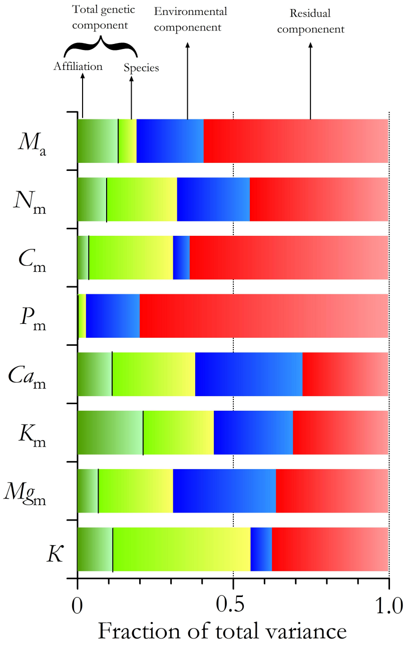

Figure 5. Partitioning of the total variance for mass-based foliar properties into genetic (green), environmental (blue) and residual (red) components with the genetic component further divided into the variations between- versus within-vegetation formation affiliation (each species having being identified as principally associated with either "forest" or "savanna"). M_a denotes mass per unit area and K represents leaf construction costs. Other symbols represent the elemental composition of the leaves on a dry mass (subscript "m") basis.

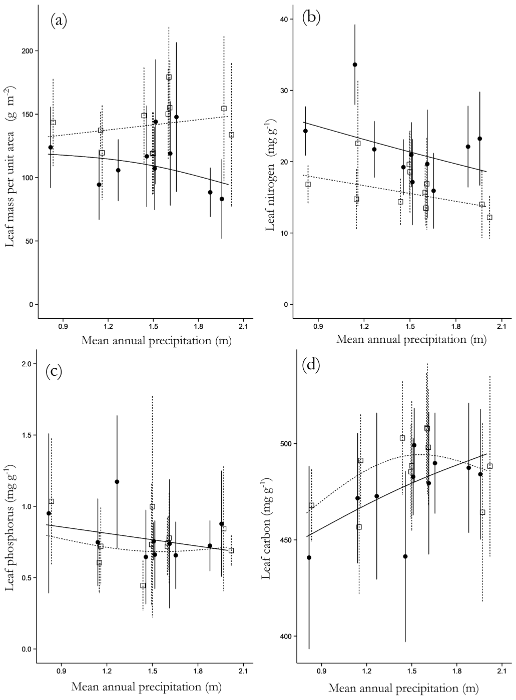

Figure 6. Variations in community-abundance-weighted mean foliar properties in relation to precipitation and vegetation formation type **(a)** leaf mass per unit area; **(b)** leaf nitrogen (dry mass basis); **(c)** leaf phosphorus (dry mass basis); **(d)** carbon (dry mass basis). (•) Forest plots; (□) savanna plots. Fitted curves (solid for forest plots, dashed for savanna) represent generalised additive model fits. Error bars represent the community-abundance weighted SD.

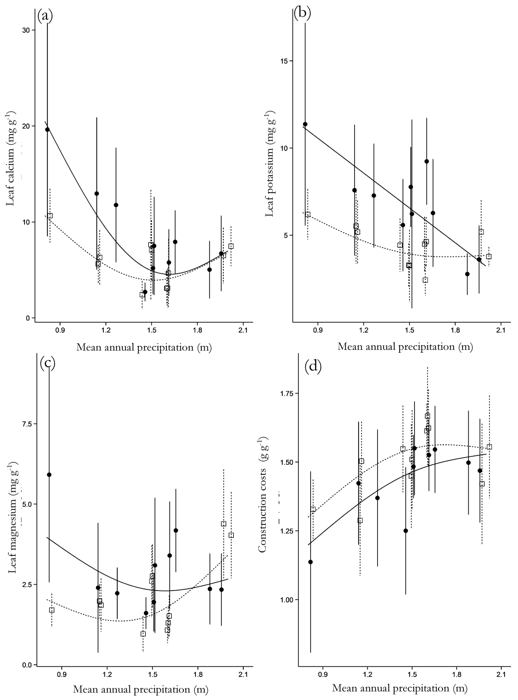

Figure 7. Variations in community-abundance-weighted mean foliar properties in relation to precipitation and vegetation formation type **(a)** leaf calcium (dry mass basis); **(b)** leaf potassium (dry mass basis); **(c)** leaf magnesium (dry mass basis); **(d)** leaf construction costs. (•) Forest plots; (☐) savanna plots. Fitted curves (solid for forest plots, dashed for savanna) represent generalised additive model fits. Error bars represent the community-abundance weighted SD.

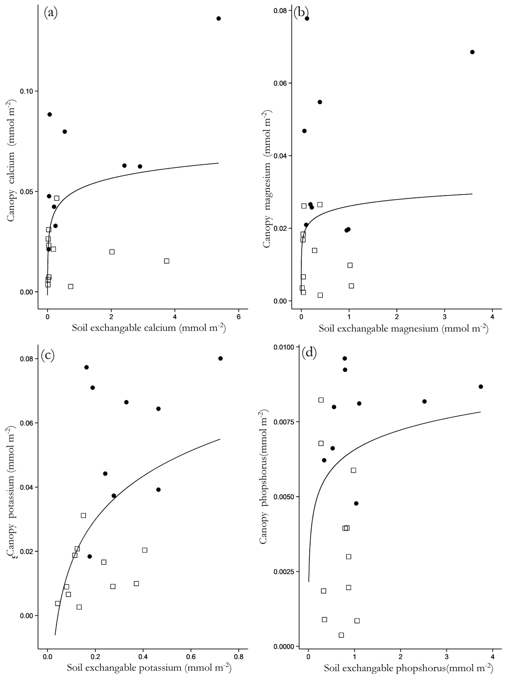

Figure 8. Relationships between soil and community-abundance-weighed foliar nutrient concentrations with both expressed on a ground area basis. **(a)** Calcium; **(b)** magnesium; **(c)** potassium **(d)** phosphorus. (•) Forest plots; (☐) savanna plots. The curves shown are log-linear viz. $y = a + b\log(x)$, fitted using a robust non-parametric procedure.

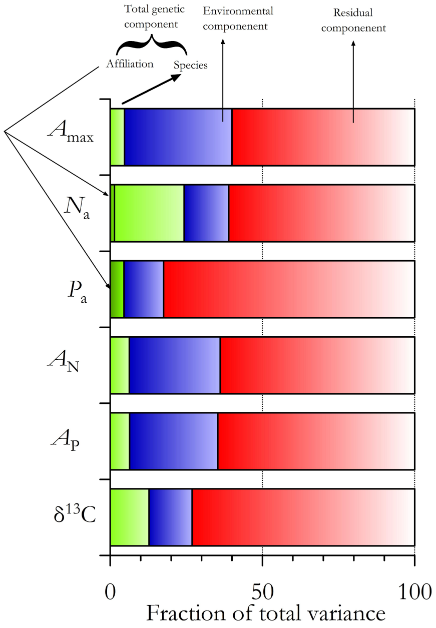

Figure 9. Partitioning of the total variance for photosynthesis-associated foliar properties into genetic (green), environmental (blue) and residual (red) components with the genetic component further divided into the variations between- versus within-vegetation formation affiliation (each species having being identified as principally associated with either "forest" or "savanna"). A_{max} denotes light and CO_2 saturated (maximum) CO_2 assimilation rate; N_a and P_a represent the nitrogen and phosphorus composition of the leaves on an area (subscript "a") basis; A_N and A_P represent the photosynthetic nitrogen and phosphorus use efficiencies (viz. A_{max}/N_a and A_{max}/P_a) with $\delta^{13}C$ a measure of the leaf $^{13}C/^{12}C$ composition.

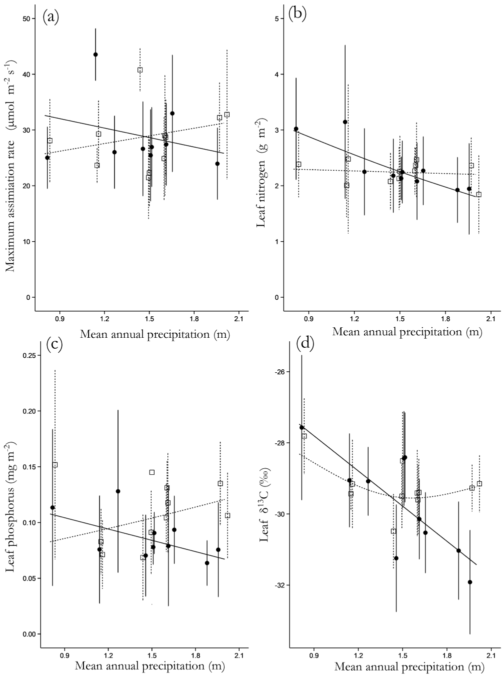

Figure 10. Variations in community-abundance-weighted mean foliar properties in relation to precipitation and vegetation formation type **(a)** light and CO_2 saturated (maximum) CO_2 assimilation rate **(b)** leaf nitrogen (area basis); **(c)** leaf phosphorus (area basis); **(d)** leaf $^{13}C/^{12}C$ composition. (•) Forest plots; (□) savanna plots. Fitted curves (solid for forest plots, dashed for savanna) represent generalised additive model fits. Error bars represent community-abundance weighted SD.

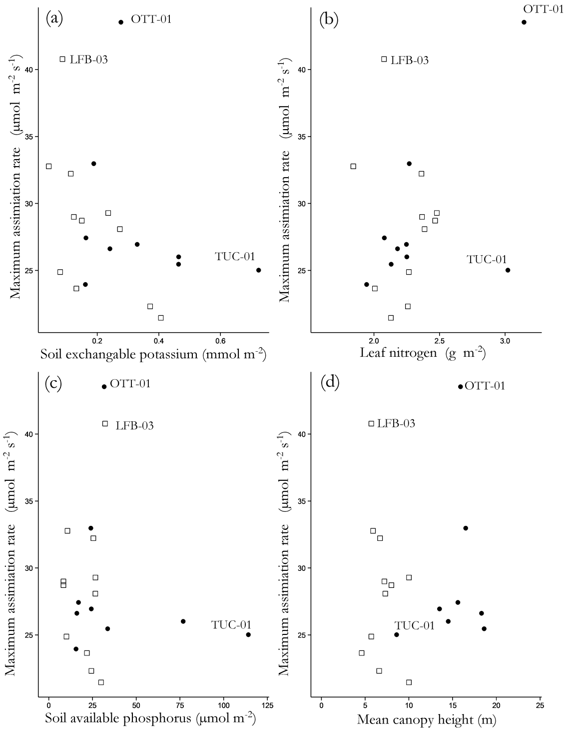

Figure 11. Relationships of community-abundance-weighted mean maximum CO_2 assimilation rates to **(a)** soil exchangeable potassium, community-abundance weighted foliar nitrogen concentrations (area basis), **(c)** soil available phosphorus and **(d)** mean canopy height. Selected plots (specifically mentioned in the text) are also shown. (●) Forest plots; (□) savanna plots.

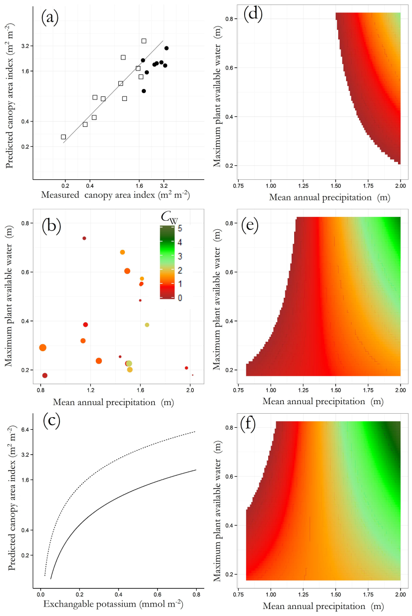

Figure 12. Modelling of canopy area index (C_W) in relation to mean precipitation (P_A), maximum plant available soil water storage (θ_p) and area-based soil potassium $[K]_{sa}$. **(a)** Modelled versus observed C_W as predicted by Model 4 of Table 3 with a 1 : 1 line also shown; **(b)** location of sample plots in terms of P_A and θ_p. Here symbol size is in proportion to $[K]_{sa}$ and with the colouring in accordance with the C_W colour scale shown; **(c)** model predictions of the relationship between C_W and $[K]_{sa}$ for $P_A = 1.0\,\mathrm{m\,a^{-1}}$ (solid line) and $P_A = 1.5\,\mathrm{m\,a^{-1}}$ (dashed line). In both cases θ_p has been held constant at 0.5 m; Model predictions of C_W in relation to P_A and θ_p for **(d)** $[K]_{sa} = 0.1\,\mathrm{mmol\,m^{-2}}$; **(e)** $0.2\,\mathrm{mmol\,m^{-2}}$; **(f)** $[K]_{sa} = 0.4\,\mathrm{mmol\,m^{-2}}$.

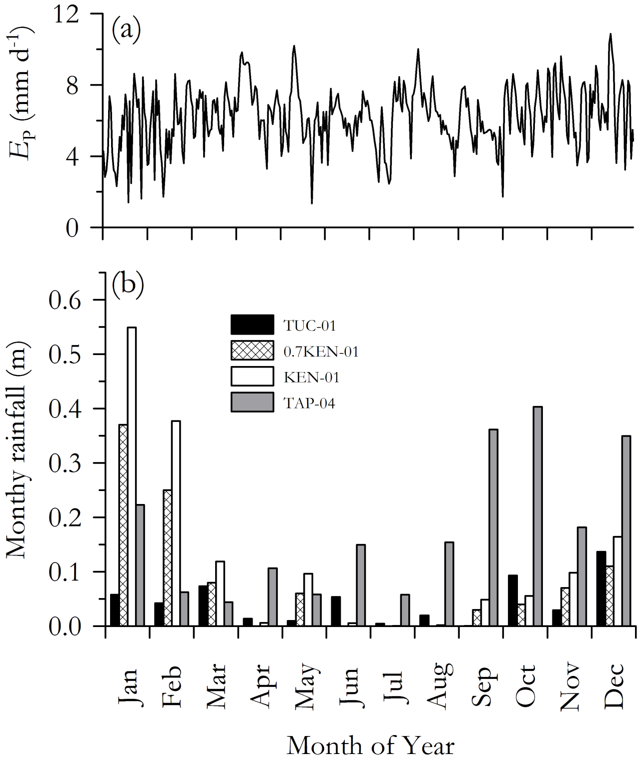

Figure A1. Key temporally varying inputs as used in the simulations **(a)** potential evapotranspiration (shown as daily totals) and **(b)** precipitation (shown as monthly sum).

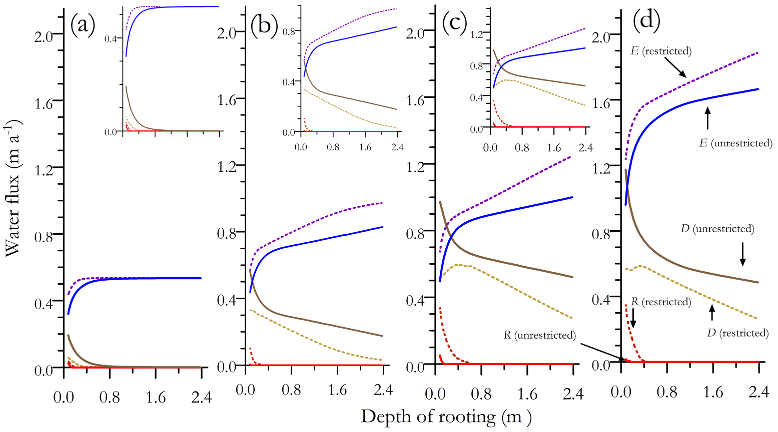

Figure A2. Simulated effects of the presence or absence or impermeable layer on soil water budgets across a range of rooting soil depths as affected by the precipitation regimes (P_A) of Fig. 1b. **(a)** P_A = TUC-01: **(b)** P_A = 0.7KEN-01 **(c)** P_A = KEN-01 **(d)** P_A = TAP-04. In all cases the main y axis has been scaled with a maximum value equal to the mean annual precipitation at TAP-04 ($P_A = 2.15\,\mathrm{m\,a^{-1}}$). Insets in **(a–c)** show same data, but with the y axis according to P_A at the site in question. Shown are model predictions for evapotranspiration (E), drainage (D) and runoff (R) as (1) a function of rooting depth where for the restricted case maximum rooting depth ($Z_{\max}$) is assumed to be restricted by an impermeable layer at the same depth ("restricted" case) and (2) where there is no imposed restriction on $Z_{\max}$ ("unrestricted" case).

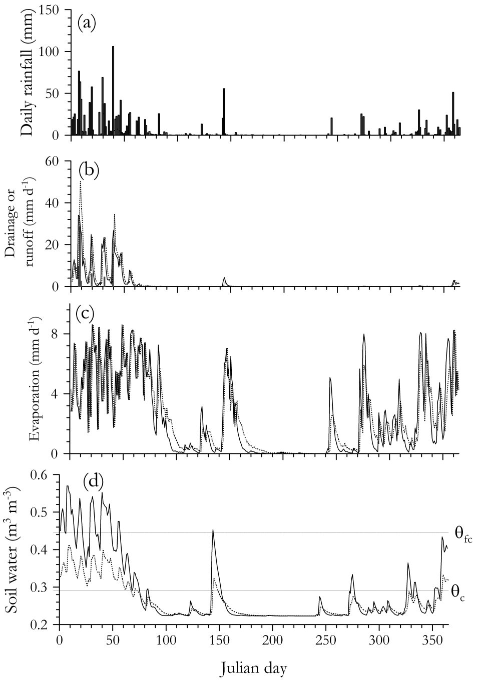

Figure A3. Simulated soil water budget components as affected by the presence of an impermeable layer at KEN-01. **(a)** Precipitation, **(b)** drainage and runoff **(c)** ecosystem transpiration, **(d)** soil water content. Solid lines: impermeable layer at 0.3 m depth. Dashed lines: with the same annual evaporation; but with no barrier to vertical water flow (rooting depth of 0.7 m). Red bar in **(b)** shows simulated daily runoff totals (impermeable layer only). Also shown in **(d)** are the prescribed minimum (critical) soil water content for plant water uptake (θ_c) and field capacity (θ_c).